Dissertation

Pathophysiology of cutaneous T-cell lymphoma: Understanding of neoplastic T-cells and non-malignant infiltrate in lesional skin

submitted by

Pablo Augusto VIEYRA GARCIA

for the Academic Degree of

Doctor of Philosophy

(PhD)

at the

Medical University of Graz

Department of Dermatology

under the Supervision of

Prof. Dr. Peter WOLF

2016

Hereby, I disclose that part of the results included in this dissertation was published in The Clinical Cancer Research journal in a paper entitled "STAT3/5-Dependent IL9 Overexpression Contributes to Neoplastic Cell Survival in Mycosis Fungoides" (Jul 1st 2016, doi: 10.1158/1078-0432.CCR-15-1784). The inclusion of such materials was done under the permission of the publisher.

I declare that this dissertation is my own original work and that I have fully acknowledged by name all of those individuals and organizations that have contributed to the research for this dissertation. Due acknowledgement has been made in the text to all other material used. Throughout this dissertation and in all related publications I followed the guidelines of "Good Scientific Practice"

January 2017.

El universo tiene un plan general, las minucias de ese plan queda a cargo de la ejecución de los actores

JL Borges reviewing "The free will controversy"
(M Davidson, 1943)

Table of Contents

Abstract (English)

In Mycosis fungoides (MF), neoplastic T-cells feed from chronic inflammation, their survival and resilience to therapy is closely tied to an abnormal pro-inflammatory microenvironment. Malignant cells produce recruitment mediators and growth factors and as disease progress, these cells accumulate mutations that enable them to better suit their environment. As skin lesions deteriorate, patients are left unable to fence off opportunistic pathogens and recurrent infections may end up with fatal consequences. Neoplastic cells are just a fraction of the infiltrating cells found in lesional MF skin. Although these cells in most cases outnumber with their predominant clonality the rest of the T-cell population, benign T-cells and other immune cell types nevertheless play an important role in the disease. This is evidenced by the fact that therapeutic strategies that induce immune tolerance and apoptosis like psoralen + UVA (PUVA) and extracorporeal photopheresis have a high degree of efficiency; nonetheless, the mechanistic effect of immune modulation has remained elusive.

In this work, the effects of PUVA on neoplastic cells, benign T-cells, and other immune cells that infiltrate skin lesions of MF patients were investigated. Transcriptional analyses of lesional skin showed enriched expression of T-cell activation-related, antigen processing-presentation and JAK-STAT signalling genes. After PUVA therapy, the expression of many of these genes was partially normalized.

Lesional skin had a high number of neoplastic and benign T-cells producing IL-9. In vitro studies indicated that the production of this cytokine was regulated by STAT3/5 and IRF4. High throughput sequencing (HTS) of the T-cell receptor (TCR) was used to look at the T-cell repertoire and identified malignant clones in skin biopsies from patients. Although patients had a significant clinical improvement to PUVA, remaining malignant clones were found in biopsies after treatment and clinical response correlated with benign T-cell turnover. Multicolour immunofluorescence was used to look at the composition of the cell

infiltrate in lesional skin and a decrease of Langerhans cells and skin resident T-cells was observed after PUVA.

These results emphasize the importance of inflammatory mediators like IL-9 and its regulators as well as the non-malignant immune cell infiltrate in the pathophysiology of MF. The mouse in vivo studies of this work in which the administration of an IL-9 blocking antibody delayed tumour growth and prolonged survival of animals, suggested that such anti-inflammatory treatment strategy could be beneficial to MF patients. Further efforts are needed to explore the targeting of neoplastic cells like the ones here presented with IL-9 as one of the key molecules in the onset of MF.

Abstract (Deutsch)

Mycosis fungoides (MF) ist charakterisiert durch neoplastische T-Zellen, die von chronischer Entzündung zehren. Das Überleben dieser Zellen und ihre Widerstandsfähigkeit gegen Therapien ist eng mit Abnormitäten der pro-inflammatorischen Mikroumgebung vergesellschaftet. Maligne Zellen produzieren Wachstumsfaktoren sowie Mediatoren zur weiteren Zellrekrutierung und mit fortschreitender Erkrankung sammeln sich Mutationen an, die den malignen Zellen bessere Anpassung an ihre Umgebung erlauben. Mit Verschlechterung der Hautveränderungen wird es Patienten unmöglich, opportunistische Pathogene abzuwehren, sodass wiederkehrende Infektionen fatal enden können. Neoplastische Zellen sind jedoch nur ein Teil der Zellen, die läsionale Haut von MF Patienten infiltrieren. Obwohl diese Zellen in den meisten Fällen mit ihrer prädominanten Klonalität die restliche T-Zell Population an Zahl übertreffen, so spielen benigne T-Zellen und andere Immunzelltypen dennoch eine wichtige Rolle in der Erkrankung. Dies ist bewiesen durch die Tatsache, dass therapeutische Strategien welche Immuntoleranz und Apoptose induzieren, so wie etwa Psoralen + UVA (PUVA) und Extrakorporale Photopherese, ein hohes Maß an Effizienz aufweisen; dennoch, der Mechanismus der Immunmodulation blieb bisher verschleiert.

In dieser Arbeit wurden die Effekte von PUVA auf neoplastische Zellen, benigne T-Zellen und andere Immunzellen, welche die Hautläsionen von MF Patienten infiltrieren, untersucht. Transkriptionsanalysen von läsionaler Haut zeigten gehäufte Expression von Genen der T-Zellaktivierung, der Antigenprozessierung und -präsentation, sowie des JAK-STAT Signalweges. Nach PUVA-Therapie war die Expression vieler dieser Gene teilweise normalisiert.

Hautläsionen wiesen eine große Anzahl an IL-9-produzierenden neoplastischen und benignen T-Zellen vor. In vitro Studien zeigten, dass die Produktion dieses Zytokins durch STAT3/5 und IRF4 reguliert ist. High-Throughput-Sequenzierung (HTS) des T-Zell Rezeptors (TCR) wurde angewendet um das T-Zell Repertoire zu untersuchen und maligne Klone in

Hautbiopsien von Patienten zu identifizieren. Obwohl Patienten klinisch signifikante Besserung nach PUVA zeigten, konnten auch in Biopsien nach Therapie verbleibende maligne Klone gefunden werden. Die klinische Besserung korrelierte mit Umsatz benigner T-Zellen. Mithilfe von Multicolor-Immunfloreszenz konnte die Komposition der Zellinfiltrate in Hautläsionen untersucht und eine Abnahme von Langerhans-Zellen und Haut sesshaften T-Zellen beobachtet werden.

Diese Ergebnisse unterstreichen die Bedeutung inflammatorischer Mediatoren wie IL-9 und deren Regulatoren ebenso wie die der nicht-malignen Zellinfiltrate in der Pathophysiologie der MF. Die In-vivo-Studien im Mausmodell dieser Arbeit, bei welchen die Verabreichung eines IL-9-blockierenden Antikörpers das Tumorwachstum verlangsamte und das Überleben der Tiere verlängerte, deuten darauf hin, dass eine solche anti-inflammatorische Behandlungsstrategie bei MF Patienten wirksam sein könnte. Es bedarf weiterer Anstrengungen das Targeting maligner Zellen wie in dieser Arbeit mit IL-9 als einem der Schlüsselmoleküle in der Anfangsphase von MF zu untersuchen.

Introduction

Biologic understanding of cancer is fundamental to improve and save the lives of the thousands of people suffering from it. Although lymphomas account for only a small proportion of the total number of malignancies diagnosed every year, they are a general challenge in diagnosis and treatment. Just in the United States there are approximately 750 new diagnoses of cutaneous lymphomas every year (Bradford et al., 2009) and over 70% of them are cutaneous T-cell lymphomas (CTCL). This is the leading type of lymphocytic malignancy observed in the skin and yet many aspects about the aetiology of this disease remain elusive. Skin lesions expand slowly but steadily and the majority of patients in remission end up relapsing, sometimes after years of treatment (Wilcox, 2016).

Cutaneous T-cell lymphoma

CTCL is a heterogeneous group of lymphoproliferative diseases characterized by the accumulation of CD3 lymphocytes in the skin. CTCL has two major forms; mycosis fungoides (MF), is the form of this disease limited to the skin and Sèzary syndrome (SS) or leukemic-CTCL (L-CTCL), a condition where the neoplastic cells not only harbour in the skin but also circulate in blood and invade lymphoid tissue (Willemze et al., 2005). Together they account for two thirds of the total number of CTCL cases reported per year in the United States (Criscione and Weinstock, 2007). The incidence of these malignancies increases every year. By 2015, about 6.4 million CTCL patients were affected according to the Surveillance, Epidemiology, and End Results (SEER) registry data (Wilcox, 2016). In the region of lower Austria in St. Pölten, between 2006 and 2013, 86 primary cutaneous lymphoma patients were diagnosed. 83% of these cases were CTCL from whom 47 patients were classified as MF (Eder et al., 2015). The numbers in other parts of Austria are very similar. Globally, the demographics of CTCL indicate a higher occurrence in males with African-American people being more frequently affected (Bradford et al., 2009). The mean age of CTCL occurrence is between 50 to 60 years and the risk grows higher with age. The risk of developing CTCL in over 70 year-olds is four times higher to the younger population (Agar et al., 2010).

The causes of CTCL remain controversial. No epidemiological study has shown a consistent environmentally or virally associated cause for CTCL. However, infection with human T-lymphotropic virus 1 (HTLV-1) leads to adult T-cell leukemia (Whittemore et al., 1989). More recently an association of MF with hydrochlorothiazide was found in a set of patients with early stage MF. However, the MF-like lesions in these patients did not show TCR monoclonality (Jahan-Tigh et al., 2013). Nevertheless, this observation indicates that certain drugs may play a role in initiation and the promotion of the disease.

A good assessment of clinical signs, extent of affected skin and extra-cutaneous involvement as well as precise staging is fundamental to establish an accurate prognosis for these patients (Arulogun et al., 2008). The management of the disease benefits from the search for surface cell biomarkers such as CD26 and CD7 (Pierson et al., 2008) that help to estimate malignant T-cell burden and distinguish the phenotype of neoplastic cells from benign T-cells.

Mycosis fungoides

MF is the most common type of CTCL with a yearly rate of 54% of primary skin T-cell lymphomas (Weinstock and Gardstein, 1999). Under the microscope, neoplastic cells have a characteristic cerebriform nucleus and vary in size from small to medium (Willemze et al., 2005). An epidermotropic band-like infiltrate is formed involving papillary dermis accompanied by substantial epidermal spongiosis. In many cases, malignant cells harbour in epidermal compartments named Pautrier's micro-abscesses (Girardi et al., 2004). Definitive diagnosis of MF is challenging as many of the clinical and pathologic features are not specific and many of them are shared with eczema and parapsoriasis. Therefore, patients are monitored sometimes even for years before a definitive diagnosis is made (Arulogun et al., 2008). Lesional skin usually evolves through several phases, in which most affected individuals start with lesions classified as patches; flat, scaly pink-reddish pigmented areas sometimes accompanied by pruritus. Patches form on the lower abdomen, upper thighs, buttocks and breasts. In most individuals some or all patches progress to plaques, i.e. raised

lesions with often a more severe hyperpigmentation and itch. Usually these lesions are in the same location of the initial patch or arise independently at a different location and the patient can present both kinds of lesions. Patches and plaques can remain stable for years or may advance into tumour stage early on. MF tumours have a substantially increased cellularity. Their raised skin is even more pronounced and the infiltrate goes deeper into the tissue. The skin barrier function is compromised which may lead to severe, most often opportunistic infections (Yamashita et al., 2012). Up to 30% of MF patients have a concomitant infection with *S. aureus.* Many cases of MF have non-malignant clones that proliferate and secrete inflammatory mediators in response to bacterial toxins acting as super-antigens (Jackow et al., 1997).

Patients with a high ratio of CD8 positive cells (Hoppe et al., 1995) and CD1a positive Langerhans cells (Meissner et al., 1990) in skin lesions have a better prognosis, however, the role of these cells at the onset of MF is not fully understood. High serum levels of LDH, β2-microglobulin and IL-2 have been associated with higher severity of the disease and poor prognosis (Diamandidou et al., 1999). Local therapy is preferred in early stage MF while systemic treatment is often reserved for more advanced stages (Al Hothali, 2013).

SS is the second most common type of CTCL; it is an aggressive presentation of the disease that rarely is preceded by MF lesions. SS patients are affected by erythroderma, pruritus, lymphadenopathy and have the distinctive characteristic of neoplastic cells circulating in blood (Yamashita et al., 2012). Although malignant cells in MF and SS appear similar, molecular biology studies have shown how different these diseases actually are. High resolution genomic hybridization uncovered the chromosomal alterations most commonly observed in MF and highlighted the difference with those seen in SS. MF patients had duplications of chromosomes 7q21-36 and 1p36-2 and deletions in 5q13 and 9p21. In contrast, SS patients had duplications in 17q22-25 and 8q22-24 and deletions in 17p13 and 10q25. These findings were fundamental

to change the misconception of SS being a severe stage of MF and separate the diseases into two distinct entities (van Doorn et al., 2009).

Genomic instability

Altered chromosomal copy numbers are relevant for the prognosis of numerous malignancies (Zack et al., 2013). In CTCL, risk stratification based on gene expression and cytogenetic analysis is only beginning to be explored. An inverse correlation between time of survival and absolute copy number alterations has been described (Salgado et al., 2010). Patients with less than three copy number alterations have a mean survival of 93 months while patients with more than 3 alterations have a survival mean of only 67 months, a rate substantially lower than those with fewer alterations (Caprini et al., 2009). As disease progresses, patients accumulate structural and numerical chromosomal aberrations with recurrent deletions in 1p, 6q, 9p, 10q, 17p and 19p (Karenko et al., 2003, Batista et al., 2006). More than 70% of patients present a spectrum of chromosomal abnormalities (Mao et al., 2002). Microsatellite instability is a reflection of impaired DNA repair mechanisms and contributes to mutagenesis in tumour-suppression genes. It is frequently seen in MF patients and is accentuated in advanced stages (Scarisbrick et al., 2003). Three groups of genes with significant abnormalities were found in the seminal study with 62 patients of Shin et al. In this work, genes were clustered into those that maintain chronic activation of T-cell proliferation, cell adhesion or skin homing molecules (Shin et al., 2007). Additionally, genes belonging to the TNF signalling pathway have been found altered in CTCL (Litvinov et al., 2010).

Gain and loss of function mutations

One of the hallmarks of carcinogenesis is the acquisition of gain of functions through mutations; resulting in the expression of genes making neoplastic cells better suited to their environment (Hanahan and Weinberg, 2011). Such mutations may be caused by chromosomal translocations, leading to a series of gene expression abnormalities like; gene silencing, fusion proteins, up regulation through duplication of genes and chronic activation (Margolskee et al., 2016). Intriguingly, malignant cells replicate the diversity of T-cell

populations in the skin and gain of function mutations seem to magnify the phenotype from which the malignant cells arise. This has been seen in a subset of SS patients who may have a malignant clone with a regulatory T-cell (T_{reg}) like phenotype, positive for Foxp3 and a cytokine secretion profile enriched with TGF-β and IL-10 (Berger et al., 2005). Another group of SS patients develops malignant clones with a Th2-like phenotype, positive for GATA3, IL-4, IL-13 and IL-5 (Wang et al., 2014, Vowels et al., 1994). Furthermore, Th17 phenotype malignant clones resulting from JAK3 V722I activating mutations have been described in a group of CTCL patients (Ehrentraut et al., 2016). In accordance to this, animal models have shown an up regulation of IL-17F in aggressive lymphoma whereas IL-17A has been found overexpressed in MF patients (Krejsgaard et al., 2013). Furthermore, activating mutations in genes required for T-cell differentiation like in PLCG1 a trans-activator of NFAT have been reported in CTCL (Vaque et al., 2014). IRF4 is an oncogene mutated in myeloid and B-cell leukemia and it has also been found translocated reciprocally with TCR-α in CD30 positive CTCL (Pham-Ledard et al., 2010). Recent results by our group and also presented in this work have shown up-regulation of IRF4 in IL-9 producing cells in MF (Vieyra-Garcia et al., 2016). Over 90% of MF patients are positive for nuclear NFκB p65, implying that constitutive activation through mutation of this pathway is fundamental for malignant T-cell transformation. Constant activation of NFκB leads to resistance to apoptosis and chemotherapeutic agents in neoplastic T-cells (Sors et al., 2006).

Several reports describe a consensus on the relevance of the JAK/STAT signalling pathway in CTCL, showing a consistent translocation of STAT3 to the nucleus (Nielsen et al., 1997). This results in deregulation of apoptosis mediators like Bcl-2/Bax (Verma et al., 2010) and up regulation of DNMT1, a promoter of epigenetic silencing of tumour suppression genes (Zhang et al., 2006). Additionally, STAT5 induces expression of miR-21 (Lindahl et al., 2016) and miR-155 (Kopp et al., 2013), promoting cell proliferation and evading apoptosis.

CTCL neoplastic cells lose expression of Fas by a variety of mechanisms such as methylation of the promoter region (Wu and Wood, 2011), inactivating mutations (Dereure et al., 2002) and loss of the long arm of chromosome 10 (Scarisbrick et al., 2000). All of them lead to a reduced sensitivity to Fas-L mediated apoptosis (Wu et al., 2009).

Cell cycle regulators like CDKN2A and CDKN2B frequently acquire aberrant mutations in CTCL. Genetic loss of any of these two genes is associated with poor prognosis, linked to an aggressive subset of CTCL both in SS and MF (Laharanne et al., 2010a). Furthermore, up regulation of cyclin D1 and loss of its regulator RB1 lead to impaired control of cell cycle in malignant cells (Mao et al., 2006). It is believed that many of mutations in CDKN2A and CDKN2B are part of a second line of alterations, once transformation has occurred and they are by-products of the increased genomic instability. Nonetheless they potentiate the aggressiveness of the disease.

Cytokine and chemokine microenvironment

Abundant cells infiltrating the skin in MF lead to the secretion of many pro-inflammatory mediators that may exacerbate the disease of these patients (Table I). Pruritus is a common symptom of CTCL and many inflammatory diseases. It has been shown that IL-31 mediates itch in MF (Cedeno-Laurent et al., 2015) released through activation of STAT6 and NFκB (Maier et al., 2014). In vitro experiments showed that histone deacetylase inhibitors (a group of drugs used in MF) reduce secretion of IL-31. IL-7 has been shown to promote cell proliferation (Yamanaka et al., 2006b) and together with IL-15 its effect is potentiated by activation of BCL-2 and c-Myd in malignant cells (Aubry et al., 2001). IL-21 has been associated with disease progression in patients bearing MEKK4 positive cells (Fredholm et al., 2016). This cytokine is involved in the constitutive activation of STAT3 in SS patients (van der Fits et al., 2012a). IL-4, a common gamma chain cytokine, together with IL-13 are the main interleukins produced by Th2 polarized cells. These cytokines are thought to be crucial in CTCL, as most patients have a predominant Th2 phenotype (Geskin et al., 2015) and its expression correlates with advanced stages of skin

involvement (Vowels et al., 1994). Most alterations in cytokine secretion have been described locally. Only a few mediators are known to be altered systemically. Nonetheless, a subset of patients has shown a substantial systemic increase of IL-18 and IgE together with caspase 1, the protease responsible for IL-18 activation (Yamanaka et al., 2006a). Furthermore, eosinophilia and high levels of IgE correlate with an increased bacterial infection incidence in CTCL patients (Nielsen et al., 2002). Many patients express one or many subunits of TNFr (Dulmage and Geskin, 2013) and it is thought that together with IFNγ signalling they mediate epidermotropism of malignant cells (Daliani et al., 1998). Evidence suggests that keratinocytes in lesional skin are the source of many cytokines that drive cell recruitment in CTCL (Celerier et al., 1997). Neoplastic T-cell survival is closely linked to alterations in the cytokine microenvironment. Several unsuccessful attempts to grow malignant cells have shown how challenging the generation of stable cell lines is without the right microenvironment. The addition of pro-inflammatory mediators in vitro is crucial to expand malignant cells and only a few cell lines have been established. The relevance of an active microenvironment that provides the cytokines needed by the neoplastic T-cells comes from a study where staphylococcal enterotoxin A was seen to activate STAT3 promoting IL-17 secretion by malignant cells only in the presence of non-malignant T-cells (Willerslev-Olsen et al., 2016). The majority of malignant cells expressed IL-17r (Krejsgaard et al., 2013) that made them responsive to IL-17 stimulation with augmented proliferation (Krejsgaard et al., 2011), constituting an autocrine circuit that potentiated malignancy.

Table I: Selection of inflammatory mediators described in CTCL

Molecule	Function	Reference
IL-2	T-cell activation by STAT5 phosphorylation	(Marzec et al., 2008)
IL-4	Increased production in neoplastic cells implicated in neoplastic cells dissemination	(Hsi et al., 2015)
IL-5	Produced by Th2-polarized malignant cells, recruitment of inflammatory cells	(Rook et al., 1997)
IL-7	Autocrine induction of neoplastic cell proliferation	(Dalloul et al., 1992)
IL-9	Neoplastic cell growth factor overproduced by STAT3/5 IRF4 pathway	(Vieyra-Garcia et al., 2016)
IL-10	Suppression of non-malignant T-cells by neoplastic cells	(Krejsgaard et al., 2008) (Kasprzycka et al., 2008)
IL-13	Synergistic effect with IL-4 to promote neoplastic cell proliferation	(Geskin et al., 2015)
IL-15	Autocrine growth factor of neoplastic cells	(Dobbeling et al., 1998)
IL-17	Malignant cell growth factor, up regulated in response to *S. Aureus* toxin	(Willerslev-Olsen et al., 2016)
IL-18	High levels in lesional skin and plasma. Promotion of TNF production	(Yamanaka et al., 2006a)
IL-21	Autocrine triggering factor of STAT3	(van der Fits et al., 2012a)
IL-31	Involved in severity of pruritus.	(Nattkemper et al., 2016)
IFNγ	Epidermotropism factor mediated by IP-10 activation	(Daliani et al., 1998)
MEKK4	Together with p38 promotes IL-21 production	(Fredholm et al., 2016)
STAT3	Apoptosis inhibition, cytokine production and T-cell polarization	(Willerslev-Olsen et al., 2016)
STAT5	Induction of miR-21 and apoptosis evasion	(Lindahl et al., 2016)
STAT6	Promotion of Th2 cytokine production in malignant cells	(Litvinov et al., 2014)
TGF-β	Suppression of non-malignant T-cell activation	(Krejsgaard et al., 2008)
TNF	Non-canonical NFκB activation and apoptosis evasion	(Ungewickell et al., 2015)

Cell of origin

Although the classification of CTCL provided by the EORTC correlates well with prognosis and survival (Campo et al., 2011), it does not consider genetic alterations and does not provide means to identify patients with high risk of progressive disease. Among the numerous efforts to understand the aberrant genetic phenotype in CTCL, a study published in 2010 led to the discovery that the majority of CTCL cases fall in the following categories: a) epidermotropic-CTCL including anaplastic large-cell lymphoma, b) leukemic-CTCL or SS and c) a hybrid category of primary MF and transformed MF of a secondary episode and blood involvement (Laharanne et al., 2010b). The authors proposed that on top of the consensus classification in CTCL and the clustering of patients in these three groups, comorbidities and histological criteria could provide a more assertive diagnosis, which in turn helps to select a more efficient treatment.

T-cells allocated in the skin express cutaneous lymphocytic antigen (CLA) (Clark et al., 2006) and skin trafficking chemokine receptors like CCR4, CCR8 and CCR10 (Reiss et al., 2001). In CTCL, neoplastic T-cells share the expression of these markers and regardless of their presence in the skin or blood, they lack CD26 and CD7 expression (Jones et al., 2001). Additionally, the population of T-cells in normal and inflamed conditions is a mixture of cells with a memory and effector phenotype. There is a subset of memory cells that infiltrate extra-nodal sites but keep their ability to get into blood circulation: these cells are named central memory T-cells (T_{CM}). In contrast, cells that stay in extra-nodal sites like the skin, develop from effector memory T-cells expressing T-cell receptors of high affinity (Frost et al., 2015) which are classified as resident memory T-cells (T_{RM}). In normal conditions, T_{RM} are the main sub-population of T-cells in the skin (Watanabe et al., 2015). The phenotype of neoplastic cells in SS and MF with secondary blood involvement share markers of T_{CM} like CCR7 and L-selectin (Campbell et al., 2010). Furthermore, treatment with alemtuzumab (an anti-CD52 antibody) is an efficient therapy particularly in CTCL patients with blood involvement. The majority of MF patients remain unresponsive due to the low availability of the antibody in affected tissue (Clark et al., 2012) and their permanent residence

in the skin by the expression of T_{RM} markers like CLA and CCR4 (Campbell et al., 2010).

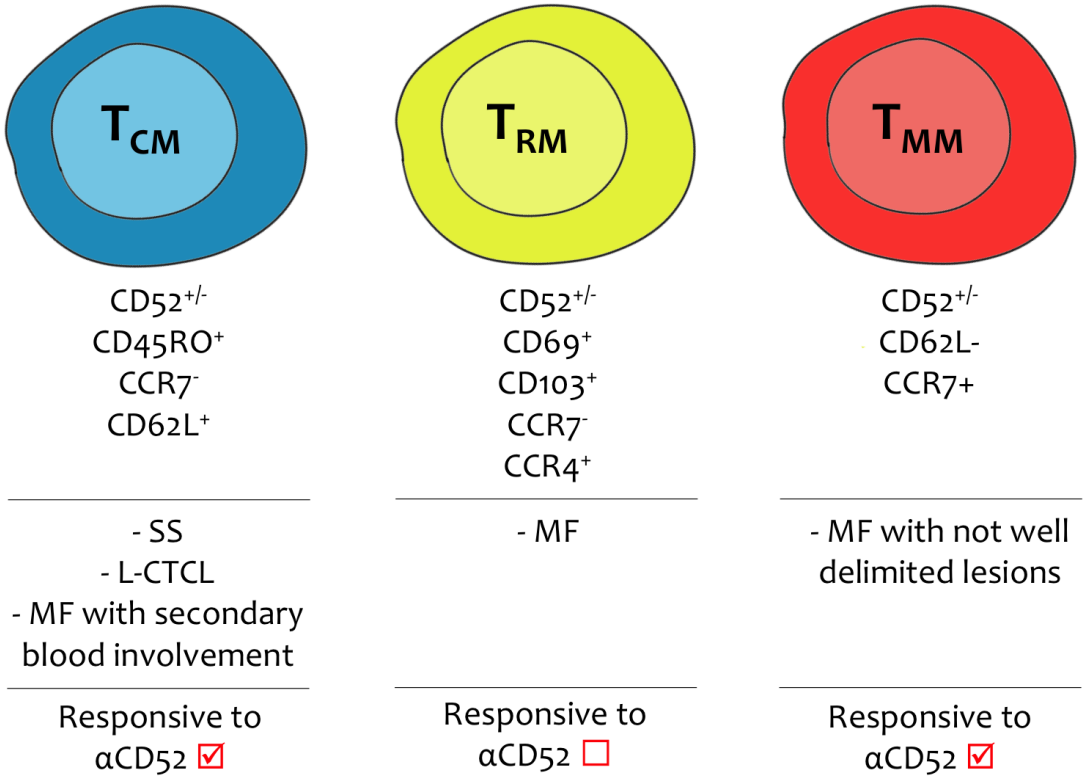

Figure I: Theoretical T-cell origin for the neoplastic cells in the main forms of CTCL. Multiple subsets of T-cells populating the skin have been described based on the expression of cell adhesion and chemokine receptors. The phenotype of the neoplastic cells in the main forms of CTCL has a high resemblance to such populations. Malignant cells in SS, L-CTCL and relapse MF with secondary blood involvement express CD45RO, CD62L and lack CCR7, as T_{CM}. Neoplastic cells in MF express CD69, CD103 and CCR4, a phenotype shared with T_{RM}. T_{MM} cells are a recently described T-cell subset with high mobility within extra nodal tissue and certain degree of blood re-circulation; these cells express CCR7, CD103 and lack CD62L. MF patients with lesions not fully delimited may carry malignant cells derived from T-cells with T_{MM} phenotype. The three cell types have expression of CD52 at different degrees however the responsiveness of patients to anti-CD52 antibody treatment may be determined by the mobility patterns of neoplastic cells.

The majority of MF patients present well-defined lesions. Generally, site and extension restriction suggests a T_{RM} origin. Moreover, some patients present poorly demarcated patches or plaques with larger extension of skin involvement. These characteristics suggest higher mobility within the tissue and possible blood recirculation. Migratory memory cells (T_{MM}) are a subpopulation of T-cells in the skin with expression of CCR7 and lack of CD62L. These cells are thought to have these mobility patterns; hence the malignant clone may arise from T_{MM} in those patients (Watanabe et al., 2015).

High throughput TCR sequencing

To date, CTCL diagnosis relays on clinical presentation, demographic risk factors and suggestive histopathology. Molecular biology techniques like flow cytometry looking at the expression of CD7 and CD26 (Hristov et al., 2011) or clonal rearrangement by qPCR (Xu et al., 2011) are currently used as tools in the differential diagnosis of CTCL. Nevertheless, these techniques are limited by their sensitivity to detect malignant cells with low frequency in lesional skin. In MF, this is particularly accentuated since the malignant cells constitute a minority of the T-cell population (Fivenson et al., 1994). This highlights the need for techniques with higher resolution to identify malignant clones and improve diagnosis. Studies addressing the clonality in CTCL indicate that even at early stages, most cases have a predominant clone with a complex chromosomal aberration (Marcus Muche et al., 2004). Finding the malignant clone is the first step to look into the mutations these cells have acquired. Multiplex/HD PCR on PAGE is routinely used in CTCL. However, its sensitivity is not ideal; for instance one study showed that was only 76% in T1 stage MF and it required the combination with other techniques like capillary electrophoresis with GeneScan to increase its sensitivity (Ponti et al., 2008). The impact of these limitations is evident by the fact that in average definitive diagnosis of MF may take up to 6 years (van Doorn et al., 2000). In the worst-case scenario, patients may get unsuitable treatment that may let malignant cells progress and become more aggressive.

The rapid evolvement of high throughput sequencing (HTS) of DNA has found application in many fields. T-cell biology has gained an instrument that allows a profound exploration of the T-cell repertoire by analysing millions of short sequences in parallel. Deep sequencing of the CDR3 region of the TCR is performed by generating a library of template molecules that are amplified with a universal polymerase chain reaction set of primers in both ends. Each template is immobilized in a solid surface resulting in groups of template clusters. The nucleotide sequence of each rearranged beta chain of any number of T-cells is identified. Quantitative studies on the frequency of every clone and the total number of distinct clonotypes are assessed (Robins et al., 2009). The estimated diversity of the entire αβ T-cell repertoire is theoretically assessed in as much as 10^{16} different possible rearrangements (Arstila et al., 1999). By just looking at the β chain with this technique, the actual number of distinct clonotypes was 4 times higher than the original estimate, presumably related to the higher resolution of single-molecule DNA sequencing that provide sufficient depth to accurately assess diversity (Robins et al., 2009).

HTS of the TCR has been used to identify malignant clones in CTCL and has successfully identified the malignant clone in all of the 46 patients analysed in a recent study (Kirsch et al., 2015). Additionally, this study shed light to the putative origin of malignant cells and brought evidence to discard the hypothesis on a precursor cell background of neoplastic T-cells, acquiring T-cell markers during transformation process. It was shown that malignant cells had 1.8 rearrangements in the gamma chain in average, similar to that one commonly observed in mature peripheral blood αβ T-cells (Sherwood et al., 2011).

Non-malignant infiltrating immune cells

Despite the accumulation of many cell growth driving mutations in MF, that silence tumour suppression genes and enhance activation of oncogenes, it is unlikely that malignant T-cells can sustain their growth on their own. Growing neoplastic T-cells in vitro usually requires the addition of cytokines like IL-7 (Dalloul et al., 1992) or immature dendritic cells (Berger et al., 2002). Moreover,

animal models such as RAG knockout mice have a low rate of successful tumour engraftment and do require the “humanization” of mice (van der Fits et al., 2012b), indicating the relevance of an appropriate microenvironment to foster neoplastic cells. In SS, CD40L, a key molecule for T-cell activation is missing (French et al., 2005). Thus, in vitro expansion of neoplastic SS cell requires the addition of co-stimulatory mediators like CD28, demonstrating the crucial role of co-stimulatory signals provided by external sources in CTCL (McCusker et al., 1997).

The phenotype of macrophages infiltrating tumours such as in follicular lymphoma and classic Hodgkin lymphoma has a prediction value for the survival of patients (Dave et al., 2004, Steidl et al., 2010). In CTCL, it has been described that lesional skin accumulates high numbers of DC-SIGN positive dendritic cells (Schlapbach et al., 2010) with an immature phenotype, possibly contributing to immune escape of the proliferating malignant clones. In vitro addition of immature DCs has extended malignant cell survival for up to 3 months (Berger et al., 2002). Monocyte-derived cells have also been found accumulated in lymphoproliferative disorders. These cells are recruited by tumour-produced CCL5 and in turn provide resistance to apoptosis and promote engraftment of malignant cells in non-obese diabetic mouse models (Wilcox et al., 2009). Malignant cells may also alter the phenotype of DC by producing IL-10, keeping these cells from activating anti-tumour immunity, thus, making them more suitable to their microenvironment (Wilcox, 2010).

Local therapy for MF

Early stage MF frequently has low or no systemic involvement and detection of blood circulating malignant cells requires techniques with high sensitivity. Malignant cells accumulate in lesional skin, a feature that makes local therapies the first option to manage these patients. The majority of early MF patients (60-80%) has a good response to such therapies (Lansigan and Foss, 2010), which aim to control the inflammation and induce apoptosis of neoplastic cells. The main local therapies for CTCL are narrow band UVB, psoralen plus UVA

(PUVA), topic steroids, retinoids, nitrogen mustard and total skin electron-beam radiation (Querfeld et al., 2005).

Corticoid steroids have a success rate of 90% in T1 stage patients that drops to 25% in T2 stage (Zackheim et al., 1998). These drugs have minor side effects and are preferred as first line therapy for early stage patients in the United States (Zackheim, 2003). Retinoids are drugs commonly used in combination regimes. They pass through the cell membrane by endocytosis and are transferred to the nucleus by cellular retinoic acid-binding proteins (CRABPs). Their biological effect is mediated by a group of retinoic acid receptors, members of a nuclear hormone receptor family. Retinoids form hetero-complexes that bind to specific DNA sequences, activating the transcription of retinoid response elements, leading to apoptosis (Zackheim, 1999).

Due to its favourable safety profile, narrow band UVB is recommended nowadays as first treatment choice for MF patients with superficial plaques and patches (Trautinger, 2011). For instance, the complete response rate of MF patients treated with narrow band UVB was 76% and no major side effects were observed in the study by Abdallat et al (Abdallat et al., 2014). PUVA is advised in patients who do not respond to narrow band UVB and those with folliculotropic MF (Trautinger et al., 2006). PUVA combines orally given 8-methoxypsoralen followed by the exposure of the affected skin to UVA light. Patients are commonly treated two to three times per week with increasing light exposure dosages. PUVA is also used in combination with bexarotene, or type I interferons in cases with poor response or with low tolerance to light irradiation alone. Combination regimes are used to decrease light doses and the number of therapy sessions (Li et al., 2012). In average, MF patients have been shown having a stratified response to PUVA with 90% complete response in stage IA patients, 76% in stage IB, 78% in stage IIA and 59% in stage IIB (Herrmann et al., 1995a). In most clinical settings, PUVA is used as a second line of treatment due to its high efficacy but an associated risk of ultraviolet related secondary malignancies (Trautinger et al., 2006).

Extracorporeal photopheresis (ECP) is a variant of PUVA developed for the treatment of systemic involvement in CTCL like in erythrodermic MF or SS. In ECP, blood leukocytes are irradiated *ex vivo* and re-infused into the patient. Despite that only 2% of the total blood circulating cells are irradiated, ECP treated patients have a good clinical response, possibly related to immune tolerance induction that synergises with the depletion of malignant cells (McKenna et al., 2006).

Total skin electron beam is an aggressive therapy used as last resort in patients unresponsive to previous therapies. It has a complete response in approximately 60% of cases in average. This treatment is an alternative for patients difficult to manage, who often develop moderate to severe cosmetic effects (Navi et al., 2011).

Histone deacetylase inhibitors are an emerging group of drugs in the treatment for many lymphocytic malignancies. By keeping an open state chromatin, the transcription of cell cycle regulators and pro-apoptotic genes is increased, leading to malignant cell depletion (Johnstone, 2002). In phase II studies, patients treated with the histone deacetylase inhibitor Vorinostat achieved an overall response of 30% within approximately 10 weeks (Kavanaugh et al., 2010), whereas Romidepsin (another histone deacetylase inhibitor) had a 34% response rate (Whittaker et al., 2010). However, both studies had a low number of patients with complete response after treatment with either of these drugs.

The growing understanding of tumour biology is making its way into translational medicine and many immunology-based treatments are under investigation. Alemtuzumab had an overall response rate of 55% with 32% of patients in remission in a study by Lundin et al (Lundin et al., 2003). The results of a study testing Mogaluzimab, an anti CCR4 antibody targeting skin-homing T-cells, showed an overall response rate of 37% with minor side effects in treated patients, which led to a phase III clinical study (Duvic et al., 2015a).

CD30 is expressed in a large proportion of CTCL cases and is considered a good prognostic indicator. Brentuximab vedotin is a conjugate antibody

targeting CD30 bound to the cytotoxic tubulin agent monomethyl auristatin. Patients treated with this antibody had an overall response of 70%, with a 73% reduction of modified Severity Weight Assessment Tool (mSWAT). CD30 positive patients were the best responders to this treatment (Kim et al., 2015, Duvic et al., 2015b). Although, treatment with biologic drugs has the disadvantage of being yet expensive and requiring long periods of treatment, they constitute a solid step towards personalized medicine, powered by a profound understanding of this malignancy.

Research problem statement

The accumulating knowledge about the biology of CTCL and more precisely, the targeting of molecules expressed by malignant cells has started a revolution in the care of these patients. Antibodies designed to recognize CD52, CD25 and CCR4 are currently under evaluation or have been used to stimulate the immune system to eliminate malignant clones. In different degrees, these approaches have been successful. However, none of them addresses the inflammatory microenvironment where the malignant cells reside. Until very recently, there has been a lack of tools to study the non-malignant inflammatory cell composition and its role on the pathophysiology of the disease in response to treatment.

The literature suggests, that benign T-cell may play an important role in CTCL. An oligoclonal T-cell response to a toxin from *S. aureus* may cause severe inflammation that may support the growth of the malignant clone (Jackow et al., 1997), worsening the disease of CTCL patients. The frequency of this phenomenon hasn't been investigated but in a cohort of 42 patients, 76% had *S. aureus* carrying genes coding for the toxin. Therapies that induce immune tolerance like ECP lead to a significant improvement in SS patients. The therapeutic effect of ECP does not necessarily involve the direct irradiation of the malignant cells given that only 2% of the total cells in circulation are exposed to the treatment and yet it is still effective. Malignant cells also have the potential to polarize benign T-cells into cells producing Th2 cytokines (Guenova et al., 2013), implying a favourable microenvironment for their survival.

This work aims to address the role of inflammatory mediators in early stage MF. Patients in this stage are often difficult to diagnose by the low frequency of neoplastic cells. Moreover, not much literature is available on the mechanistic effect of therapies like PUVA, the transcriptional profile of lesional skin and the changes in the T-cell repertoire throughout treatment.

Results

Transcriptional profile of early MF

Lesional skin in MF presents an increased number of T-cells infiltrating the skin associated to a chronic inflammatory state. To understand the feedback of inflammatory signals a characterization of the transcription profile of lesional skin was performed. RNA isolated from biopsies taken at baseline were compared with RNA obtained from normal skin took from individuals undergoing surgical procedures. The PanCancer Immune Profiling Panel from Nanostring was selected due to the following advantages: this is an assay capable to analyse the expression of up to 770 genes in a relatively small sample using only 100ng of RNA without requirement of amplification by polymerase chain reaction. With this assay, the expression of genes related to humoral responses, cancer, adaptive and innate immunity markers were examined. This technology also includes a set of 40 housekeeping genes to get a thorough normalization of gene expression and comes with an easy to use analysis tool. To identify genes differentially expressed in lesional skin compared to normal tissue, threshold values were established in which only genes that had a difference in mean expression with a p-value under 0.05 and a false discovery rate (FDR. Based on correction of p-value for multiple testing (Noble, 2009) under 0.5 were considered. The resulting genes were graphed in a volcano plot to visualize positive/negative fold change values as well as their statistic evaluations (p-value, FDR) (Fig. 1). A total of 221 differentially expressed genes were found. Among these, 130 genes were up regulated and 91 genes were down regulated in lesional skin compared to normal skin. Among the genes with the highest degree of differential expression, markers of antigen processing (HLA-G, HLA-DPA1, TAP1), lysosome formation (CTSH), T-cell co-stimulatory signals (CD40), cytokine signalling (RELA, MAPK1, MAP2K1) and adhesion molecules (CD47, ITGAE) (Fig. 2) were found. Up regulation of T-cell markers was expected, however T-cell markers were accompanied by a high degree of B-cell (CD20) and innate immunity related molecules (MRC1, CD163 and CD209).

To have a better understanding of critical pathways altered in lesional skin, the

KEGG database was used to integrate our nanostring results into signalling maps that incorporate gene-to-gene interactions. The KEGG database is a platform from the Kyoto University with a vast collection of drawings on various cell functions, able to elucidate biological systems out of sequencing data, microarray, nanostring, etc. A map on T-cell receptor signalling is presented (Fig. 3). The higher expression of several elements of the TCR (in red) correlates with higher expression of downstream molecules like ZAP70 and NFκB regulatory elements. Higher expression of T helper (CD4) and cytotoxic (CD8) cells as well as protein tyrosine phosphatase receptor type C (CD45) and its downstream molecule LCK were found. The NFAT pathway seems to be reduced in lesional skin (in green) and a significant activation of NFκB and down regulation of some of its negative regulatory elements like IKK proteins were observed. An up regulation of phosphatidylinositol-4,5-biphosphate 3-kinase (PI3K) was found. The map did not show the triggering of PI3K by JAK proteins, however an up regulation of JAK/STAT and Src signalling was found. Furthermore, increased expression of B-cell activation (Fig. 4) like CD20, Igα (CD79) and the tyrosine kinase LYN a downstream molecule of BCR signalling was found. Controversially, a higher expression of the BCR signalling inhibitor SHIP and the IFN element response LEU13 that belongs to the CD19-21 activation complex was found. This analysis was particularly aimed to look into the cytokine microenvironment of diseased skin since the finding of key mediators of the constant inflammatory process is a promising target for novel therapies. A map of cytokine and chemokines with their described receptors was drawn (Fig. 6). Chemokines like CXCL2, CXCL5, CCL25, CCL3, CCL16, and CCL15 were down regulated together with the chemokine receptors CCR9, and CCR3. This profile contrasted with the up regulation of CXCL9, CXCL10, CXCL16, CCL13, CCL5 and CCL18. The expression of chemokine receptors correlates with the profile on the chemokines found; CXCR3 (receptor of CXCL9/10), CXCR1, CCR2 (receptor of CCL13), CCR5 and CCR1 (both receptors of CCL5) were up regulated. Furthermore, several cytokines down regulated on lesional skin were found: IL-1, IL-6, IL-11, IL-4, IL-3, IL-24, IL-28, IL-17B/E and type I IFN. A high expression of IL-10 receptor alpha and the gamma (IL-2r-gamma) chain of the IL-2 receptor were found. IL-2r-gamma is

molecule involved in the signalling of a wide number of cytokines (IL-2, IL-4, IL-7, IL-9, IL-15 and IL-21). However, these analyses did not detect an up regulation on any of these cytokines. An up regulation of many genes of the TNF family was found: TNF, TNFSF10, TNFSF14, TNFSF13B and TNFSF8. The receptors SF14, SF7 and CD40 (a co-stimulatory signal member of the TNF receptor family) were up regulated. Furthermore, a close look into TNF signalling (Fig. 5) found that TRAF2 and TRAF5 downstream mediators of TNF were also up regulated.

A visualization of these results in the context of T cell populations and other cell types provides a better overview of what specific signature was enriched in lesional skin. Many specific T cell markers were represented (Fig. 7A), from surface antigens to intracellular molecules like ITK (a tyrosine kinase expressed in response to IL-2), NFATC3 (expressed on activated T-cells) and LCP1 (a cytosolic protein expressed in lymphocytes). Taking total RNA from non-dissected tissue makes it challenging to attribute results of markers to specific cell populations. The markers CCL5 and CCR5 linked to Th1 sub-populations were found up regulated. However, an up regulation of T-bet, the master regulator of Th1 cells, was not found. STAT3 was found up regulated which known to be associated to activation of Th17 cells; however, expression of IL-17B/E was decreased. Expression of markers associated to T_{reg} cells was altered, with a higher expression of LAG3, IDO and STAT5. These results also indicated a prominent activity of CD8 T-cells since granzyme and perforin were up regulated together with STAT1. Moreover, markers of antigen presenting cells (Fig. 7B) like co-stimulatory signals CD80 and CD86, many genes member of the MHC-I (HLA A-C) and MHC-II (HLA-DM-DR), LAMP1, CD1b and MR1 were up regulated. Together these results indicate that lesional skin in MF has profound diversity of cells with the secretion of many pro inflammatory markers when compared to lesional skin.

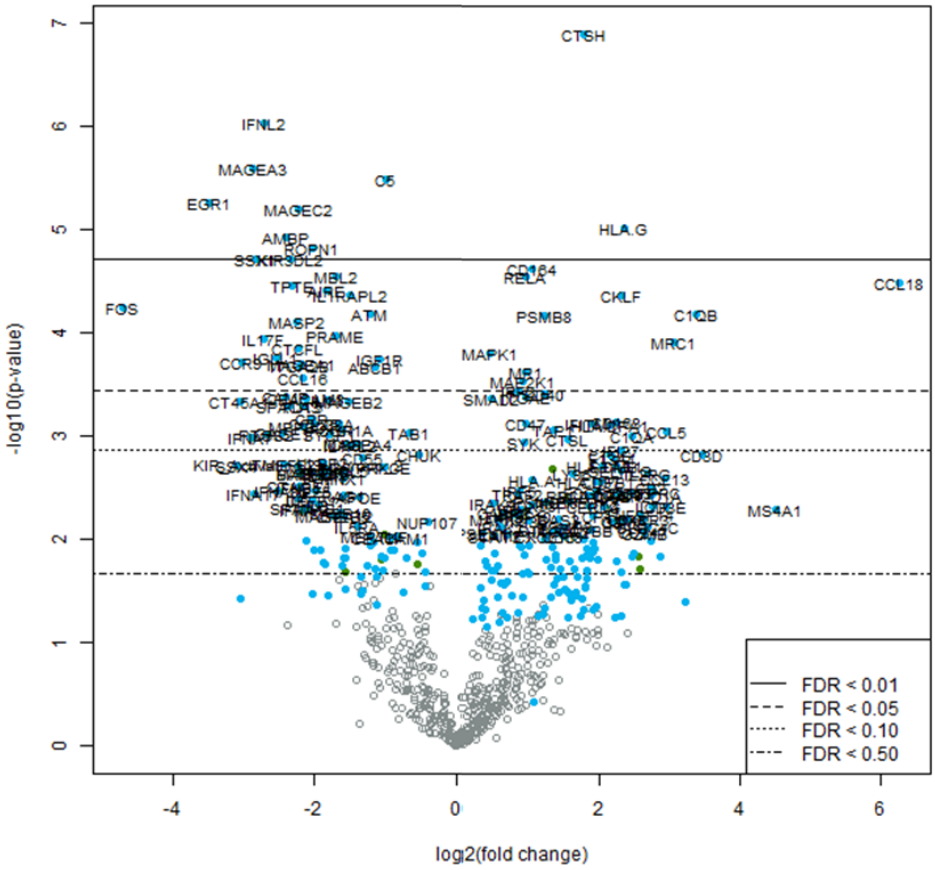

Figure 1: Deregulated inflammatory gene expression in early stage MF. Volcano plot showing gene expression data from nanostring analyses. Skin biopsies from lesional MF skin were taken at baseline and compared to normal tissue. Fold-change is shown in the X-axis, statistical significance is plotted in the y-axis. Genes with high statistical value are annotated. False discovery rate (FDR) thresholds (for different p-value levels ranging from <0.01 to <0.5, after correction for multiple testing) are indicated with dotted, dashed and solid lines.

Gene	p-value	FDR	Biologic classification/function
CTSH	7,01E-08	0,000367	Lysosome
CD164	9,51E-06	0,0166	endolyn
HLA.G	1,68E-05	0,022	MHC I
RELA	2,47E-05	0,0259	NFkB p65
CKLF	3,36E-05	0,0283	Chemokine like factor
PSMB8	3,78E-05	0,0283	Proteasome subunit
CCL18	4,46E-05	0,0292	Chemokine
MAPK1	0,000154	0,0466	Cytokine signaling
MRC1	0,00016	0,0466	Macrophages
C1QB	0,000174	0,047	Complement
SMAD2	0,000179	0,047	Antiapoptotic protein
ITGAE	0,000274	0,0683	Integrin
CD40	0,000327	0,0771	Costimulatory
MAP2K1	0,000354	0,0771	Cytokine signaling
CD47	0,000376	0,0787	Integrin associated
TAP1	0,000509	0,0952	Antigen processing
CCL5	0,000654	0,103	Chemokine
CTSL	0,000636	0,103	Cysteine protease
CD225	0,000668	0,103	Antiviral IFN responsive element
HLA-DPA1	0,000719	0,104	MHC II

Figure 2: Top 20 up regulated genes in early stage MF. List of the top 20 up regulated genes in lesional MF skin. A cut off was applied of p-value of 0.001 and a threshold for false discovery rate (FDR) of 0.2. A biological context of the genes is given under “biologic classification/function”.

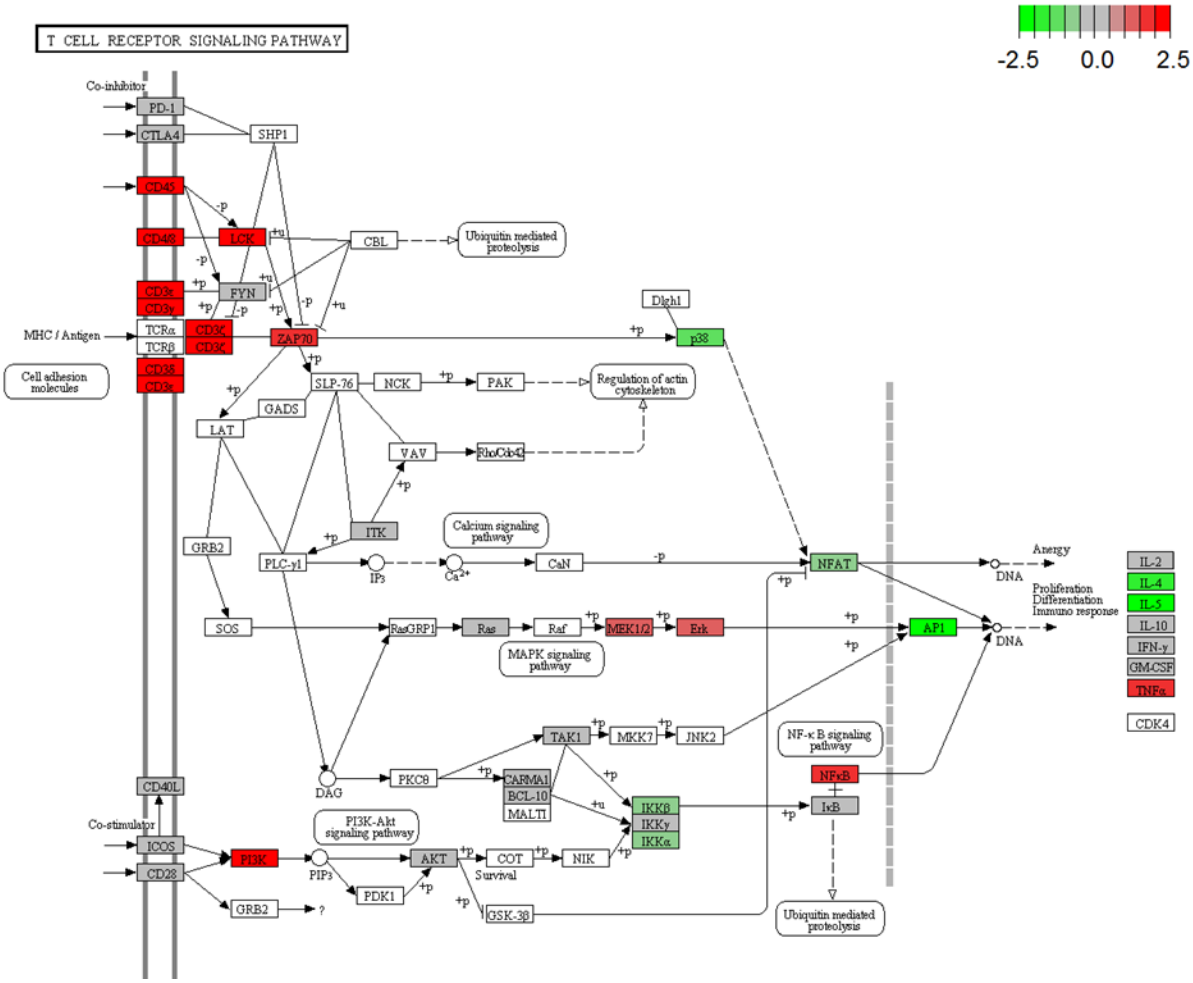

Figure 3: T-cell signalling alterations in early stage MF. Based on gene expression results, altered genes that play a role in T-cell signalling are visualised on a KEGG map generated with Pathview. Genes with higher expression in lesional skin compared to normal skin are shown in red, genes with lower expression in lesional skin are shown in green. Subunits of the TCR, ZAP70 and co-stimulatory signals were up regulated. AP1, p38, and Th2 cytokines were down regulated. The use of this map is licenced by its developer Kyoto Encyclopaedia of Genes and Genomes (KEGG) with Pathway Solutions Inc.

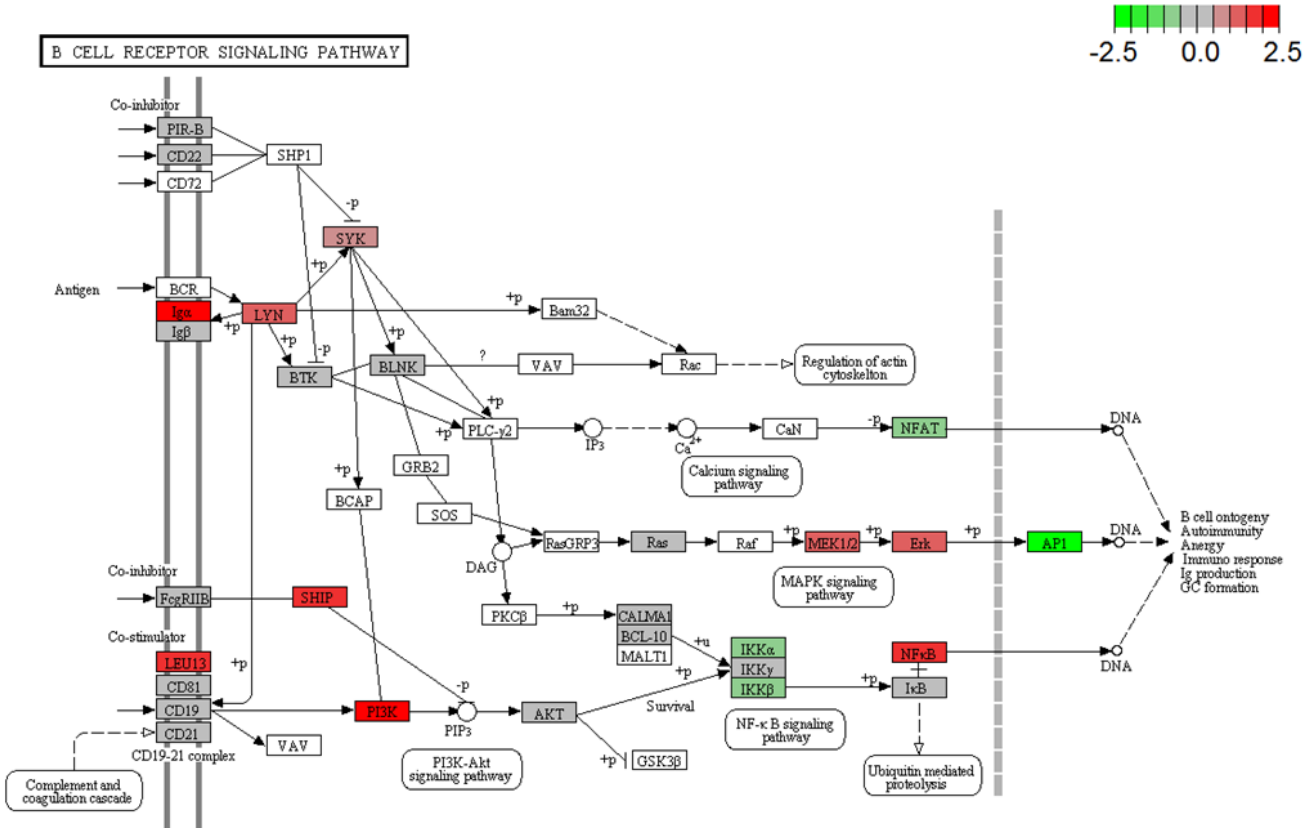

Figure 4: B-cell signalling alterations in early stage MF. Based on gene expression results, altered genes that play a role in B-cell signalling are visualised on a KEGG map generated with Pathview. Genes with higher expression in lesional skin compared to normal skin are shown in red, genes with lower expression in lesional skin are shown in green. Alpha globulin, CD225 and PI3K were up regulated. NFκB suppressors IKKα and IKKβ were down regulated. The use of this map is licenced by its developer Kyoto Encyclopaedia of Genes and Genomes (KEGG) with Pathway Solutions Inc.

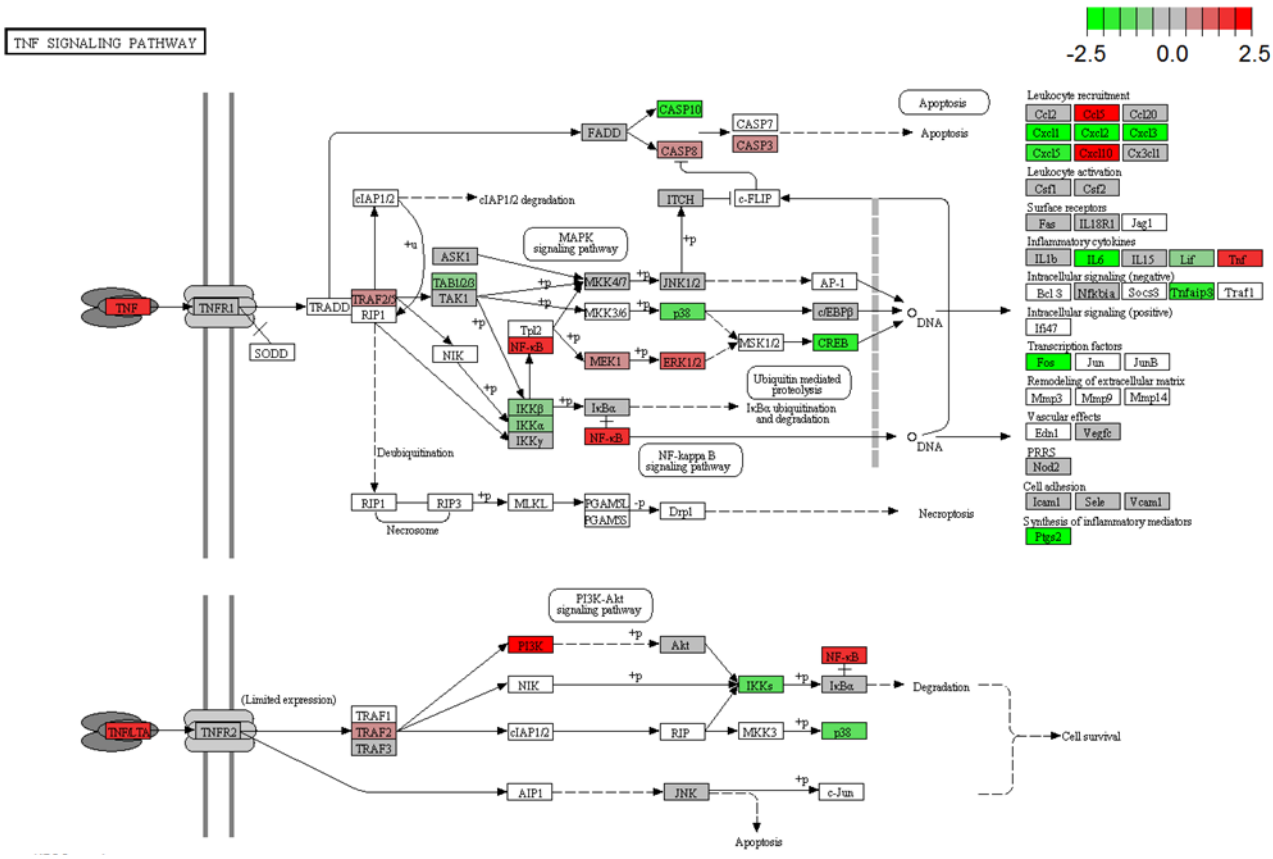

Figure 5: TNF signalling alterations in early stage MF. Based on gene expression results, altered genes that play a role in TNF signalling are visualised on a KEGG map generated with Pathview. Genes with higher expression in lesional skin compared to normal skin are shown in red, genes with lower expression in lesional skin are shown in green. TNF, NFκB, ERK and LTA were up regulated. CASP10, IL-6, Fos and CREB were down regulated. The use of this map is licenced by its developer Kyoto Encyclopaedia of Genes and Genomes (KEGG) with Pathway Solutions Inc.

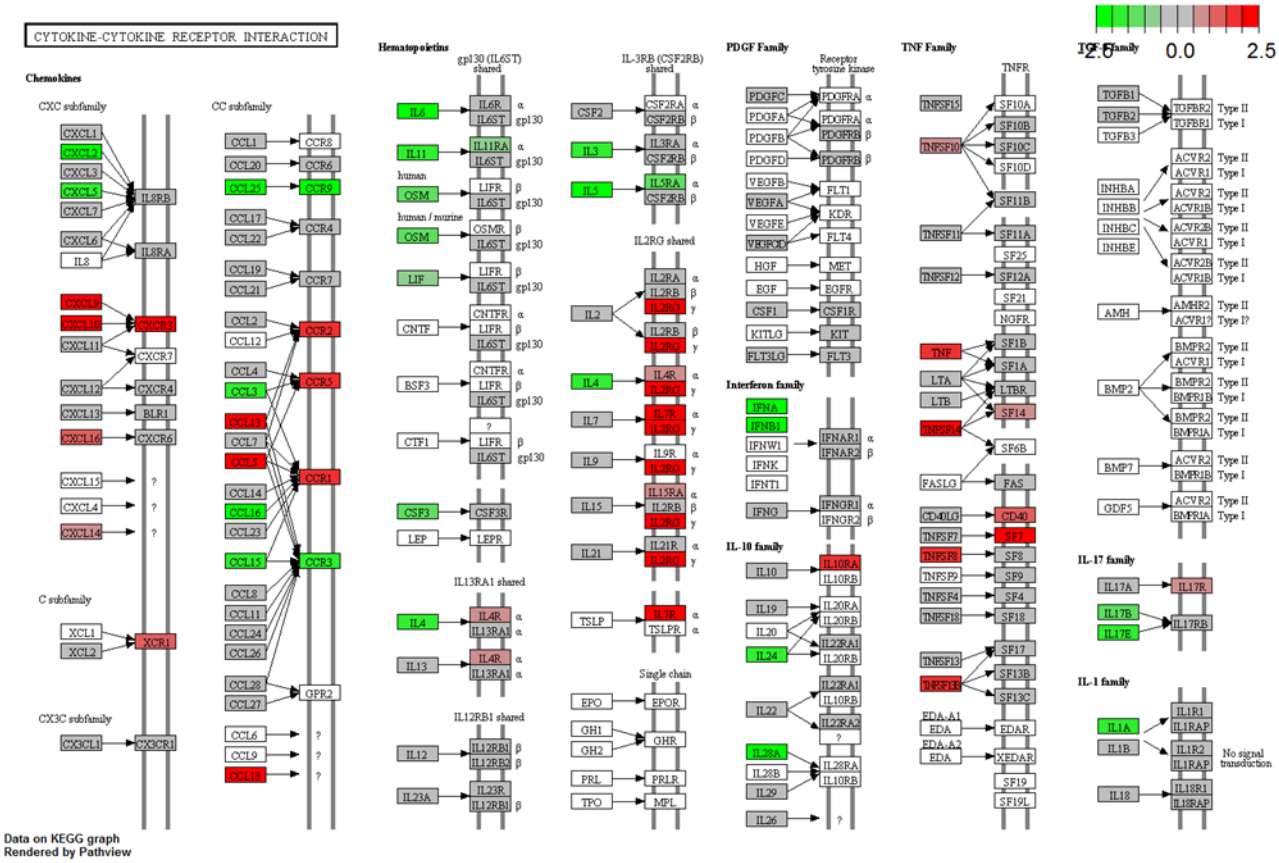

Figure 6: Cytokine to cytokine receptor alterations in early stage MF. Based on gene expression results, cytokines and their receptors are visualised on a KEGG map generated with Pathview. Genes with higher expression in lesional skin compared to normal skin are shown in red, genes with lower expression in lesional skin are shown in green. CXCL9/10, CCL5/13 CCL18 and their corresponding receptors CXCR3, CCR1/5 and the common gamma receptor were up regulated. CXCL2/5, CCL25/3/16/15, the receptors CCR9/3, IL24 and type I IFN were down regulated. The use of this map is licenced by its developer Kyoto Encyclopaedia of Genes and Genomes (KEGG) with Pathway Solutions Inc.

A

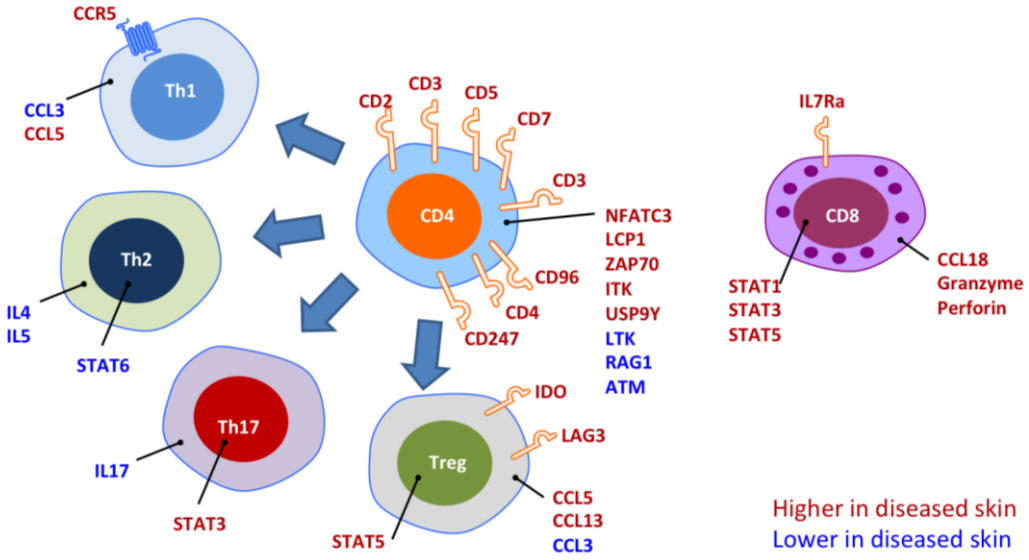

B

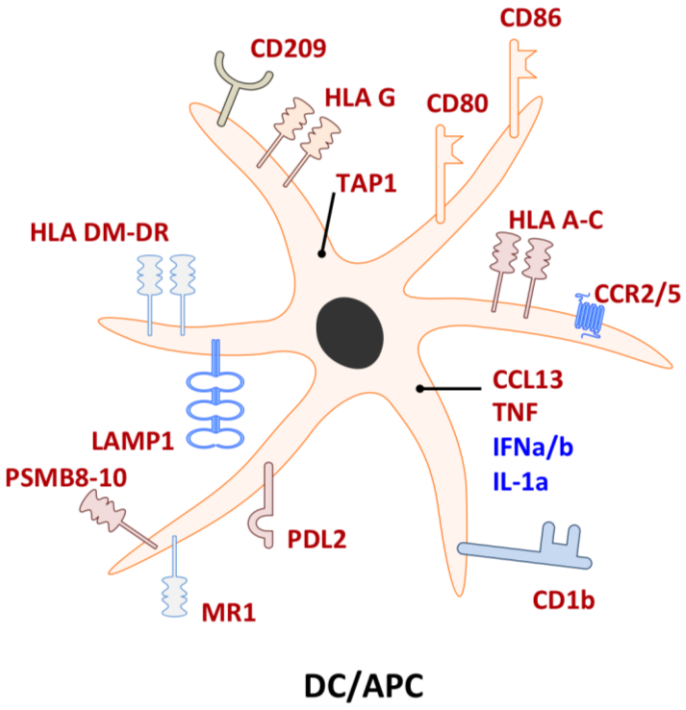

Figure 7: T-cell subsets and antigen presenting cells in early stage MF. A) Based on gene expression results of lesional skin compared to normal skin, genes associated to the main T-cell subsets were grouped: Th1, Th2, Th17, T_{reg} and cytotoxic T-cells. Up regulated genes are shown in red, down regulated genes are shown in blue. Th2 associated cytokines and STAT6 were down regulated. STAT3 and STAT5, cytotoxic molecules and immunosuppressive IDO and LAG3 were up regulated. **B)** Genes associated to antigen presenting cells, antigen processing or T-cell co-stimulatory molecules are depicted.

Inflammatory signals on CTCL cell lines

CTCL cell lines from MF and SS patients were established in the middle 70's and have been widely accepted as in vitro models to explore metabolism, expression biomarkers and to test new target molecules to treat patients. The cell lines, Hut78 and SeAx derived from an SS patient and MyLa2000 derived from an MF patient were used. Given the nature of cutaneous T-cell lymphoma; epidermotropic T-cells with deregulated cell cycle and cytokine production, the expression of transcription factors that govern T-cell polarization was analysed. Flow cytometry was used to determine the positivity of T-Bet, RORγT, Foxp3 and PU.1 (Fig. 8) and observed a differential expression pattern. Hut78 cells had a low expression of Foxp3 and lacked expression of t-Bet, RORγT and PU.1. MyLa2000 cells had a high expression of the four transcription factors. SeAx cells lacked expression of t-Bet, RORγT and PU.1 but had a high expression of Foxp3. MyLa2000 cells had the most diverse transcriptional profile and were positive for all transcription factors; this may reflect an elevated secretion of different cytokines.

To assess the secretory potential of MyLa2000 cells as a model of malignant cells in tissue, analysing secretion of IL-9 was initiated since MyLa2000 was the only cell line with expression of PU.1. Furthermore, it has been reported that memory T cells in the skin have a large production of IL-9 and a remarkable role in immunity and disease (12). ELISA was used to determine the production of IL-9 in the supernatants of Hut78, SeAx and MyLa2000 cells after 2 and 4 days of culture (Fig. 9A). Hut78 and SeAx did not produce detectable levels of IL-9, whereas MyLa2000 cells had a high production of this cytokine sustained for up to 4 days. This result indicated that MyLa2000 cells were the most active cells among the cells tested in terms of cytokine production. A particular interest in this cytokine came across since it has been described that IL-9 and its downstream molecules are important targets in immune therapies for other lymphomas (Chen and Wang, 2014). The expression of IRF4 was determined to test for the polarization to a Th9 population (Fig. 9B) of MyLa2000 cells and compared them to Hut78 cells (negative for IL-9 production). In consistence with these results, MyLa2000 cells were positive for IRF4 while Hut78 cells were negative.

IL-9 secretion in the skin has been suggested to be a driving force of vascularization (Singh et al., 2013). IL-9 is highly produced in psoriatic lesions and has paracrine functions among T-cells and other cell types (Schlapbach et al., 2014). To assess if the cytokines produced by MyLa2000 cells can indeed function as growth factors, supernatant from MyLa2000 cells in culture for up to 96h was collected. A mixture of this supernatant with fresh medium was used to culture SeAx and HaCat cells to determine proliferation by ^{3}H-thymidine incorporation (Fig. 10). HaCat cells were used since it is known that IL-9 can support their growth (Sismanopoulos et al., 2012). The supernatant from Hut78 cells was used as negative control. Both cell lines cultured with 10% of supernatant from MyLa2000 had higher proliferation rate than the ones cultured with Hut78 supernatant. SeAx cells had even a more drastic boost of proliferation with 30% of MyLa2000 supernatant while supernatant at 50% reduced their proliferation. In contrast to SeAx cells, HaCat cells did not further increase proliferation response with the mixture of Hut78 or Myla2000 at both concentrations 30% and 50%. Additionally the direct effect of IL-9 on cell proliferation of HaCat (as a model for keratinocytes) and SS cell lines Hut78 and SeAx cells was determined. These cells were stimulated with increasing amounts of recombinant IL-9 (Fig. 11). A tendency of higher cell growth in HaCat cells at 96h in an IL-9 concentration dependent manner was observed. Hut78 and SeAx cells also exhibited an IL-9 dependent cell growth as early as 48h of culture. These results provide insight into the role of IL-9 as a mediator of malignant cell growth in MF.

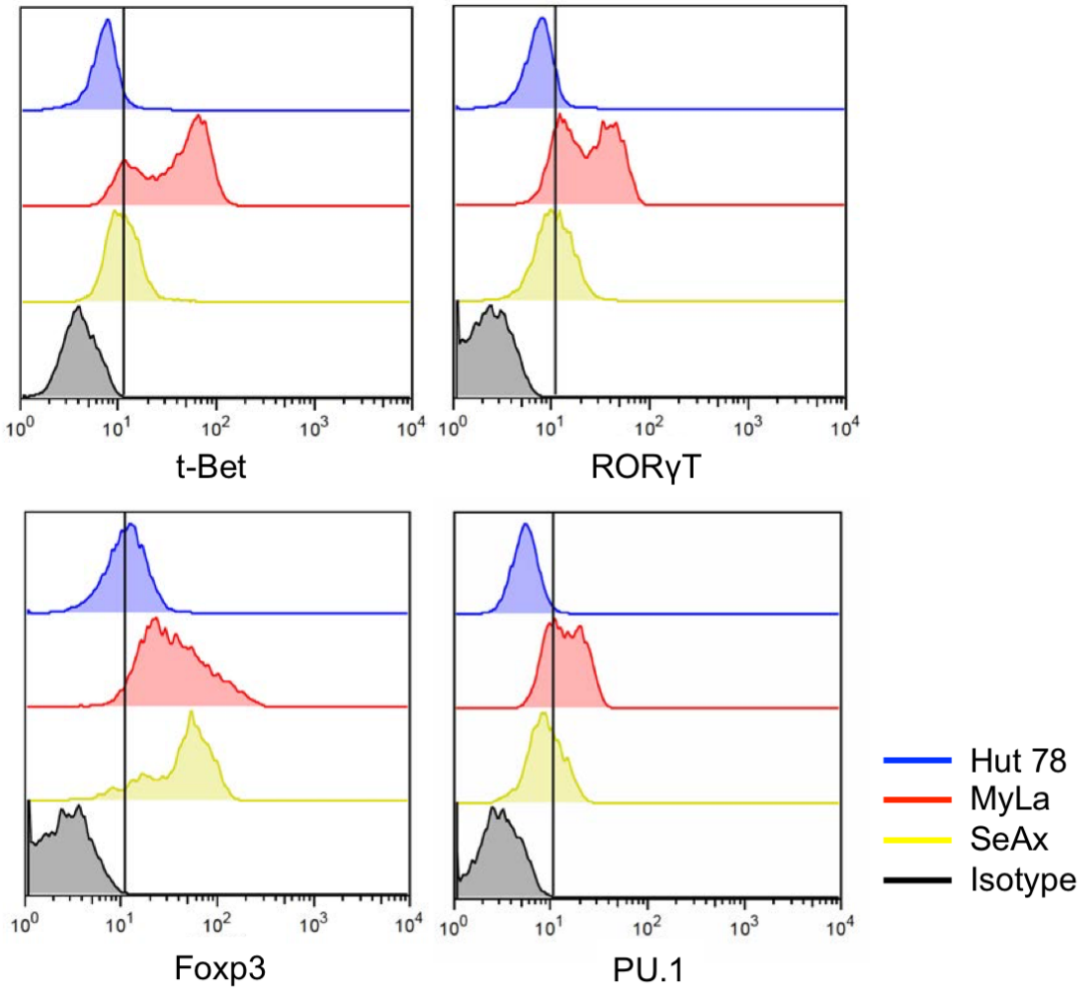

Figure 8: Expression of polarization related transcription factors in CTCL cells. Intracellular stain of t-Bet, RORγT, Foxp3 and PU.1 on Hut78, MyLa2000 and SeAx performed in cell cultured for 48h.

A

Standard Curve	
IL-9 (pg/ml)	Abs
100	3.19
50	2.00
25	1.12
12.5	0.65
6.25	0.36
3.13	0.22
1.56	0.14
0.78	0.10

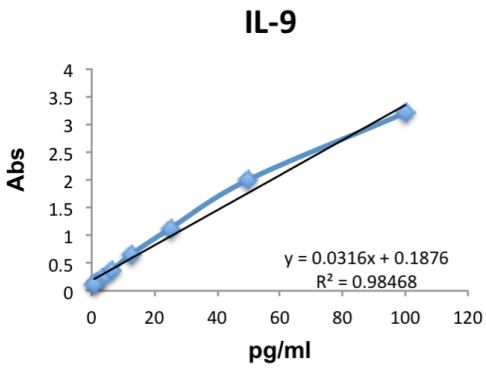

Sample	Time culture	Abs	IL-9 (pg/ml)
Negative CTRL	-	0.091	0.00
Positive CTRL (1ng/ml)	-	4.000	120.65
Hut78	48h	0.082	0.00
Hut78	96h	0.080	0.00
MyLa2000	48h	3.510	105.14
MyLa2000	96h	4.000	120.65
SeAx	48h	0.075	0.00
SeAx	96h	0.161	0.00

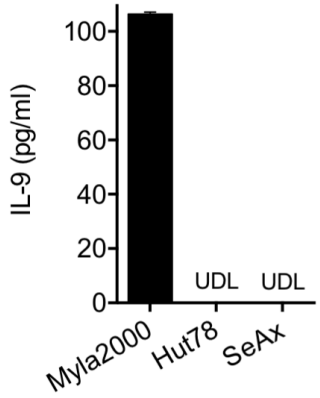

B

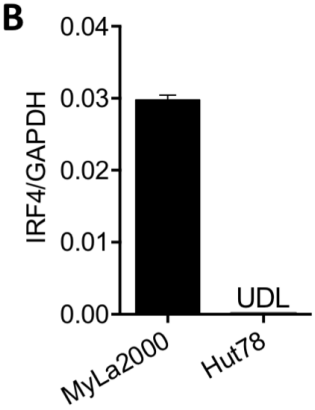

Figure 9: Spontaneous secretion of IL-9 in MyLa2000 cells: A) CTCL cell lines Hut78, SeAx and MyLa2000 were cultured for up to 96 hours. Supernatant was taken at indicated time points to quantify IL-9 by ELISA. IL-9 concentration at 48h of culture is shown in bottom panel. Standard curve is shown in the top panel. **B)** Expression of IRF4 was assessed by qPCR after 48h of cell culture.

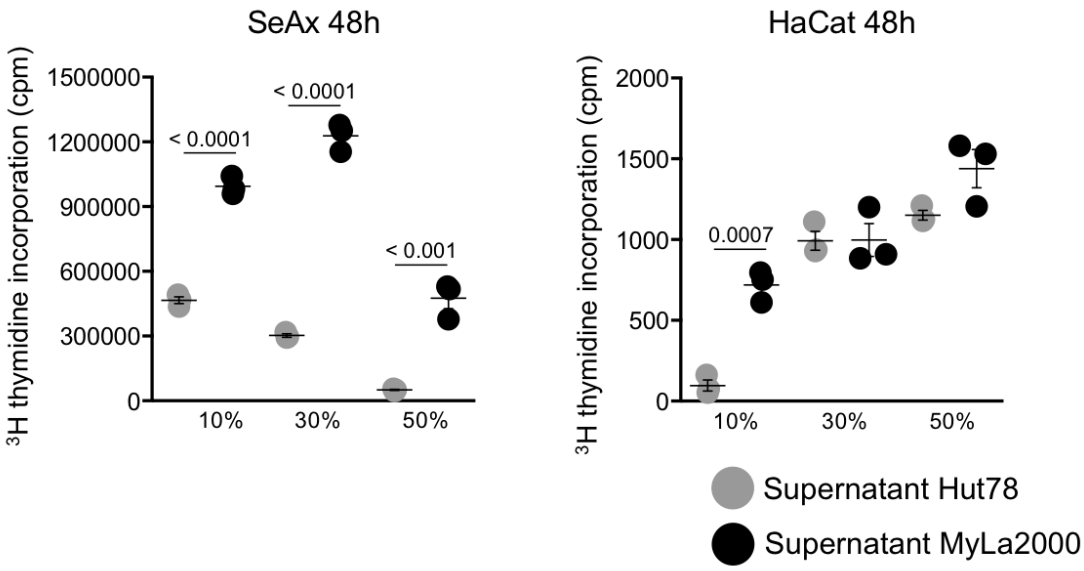

Figure 10: MyLa2000 supernatant increase cell proliferation of CTCL and keratinocyte cell lines. SeAx and HaCat cells were cultured on media supplemented with supernatant of 96h culture of MyLa2000 (black dots) cells or Hut78 (used as control, grey dots). After 48h of culture cells were harvested to determine cell proliferation by thymidine incorporation. Counts per minute are shown. Statistical significance was assessed by student t-test. p values are shown

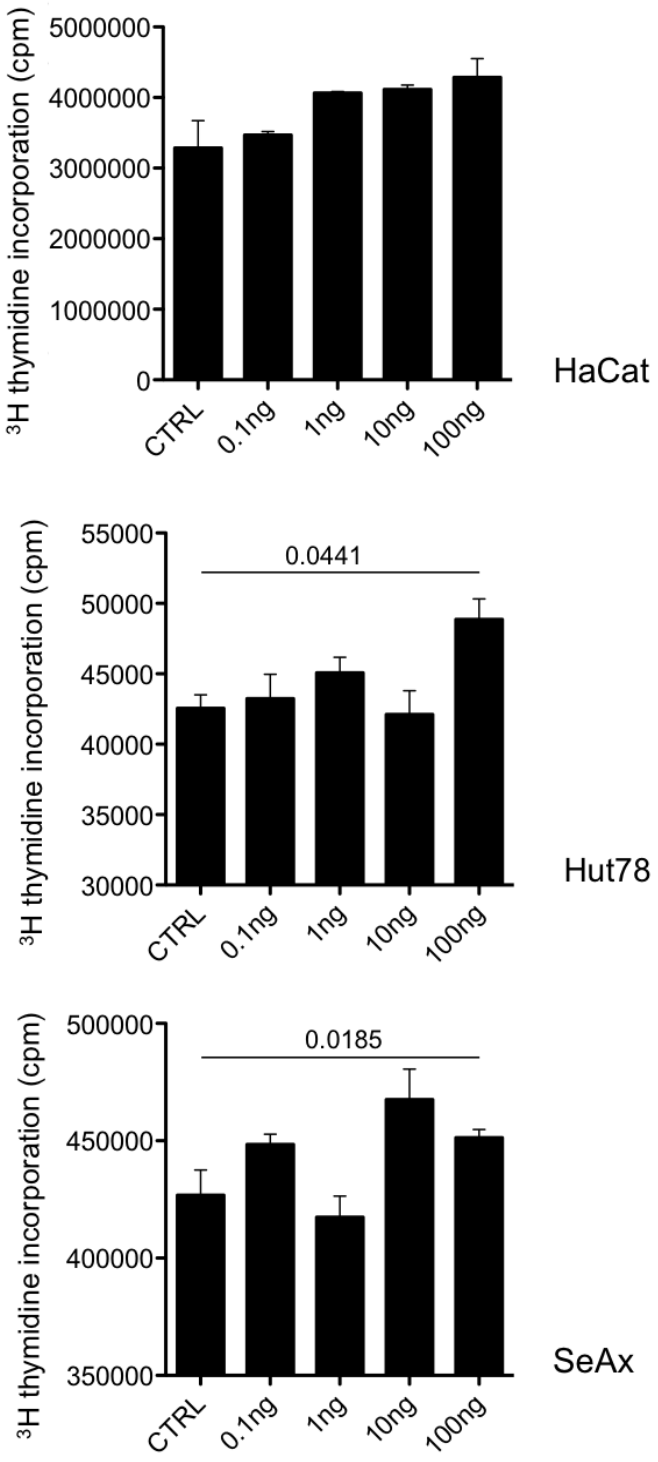

Figure 11: IL-9 increases proliferation in keratinocyte and CTCL cell lines. HaCat, Hut78 and SeAx cells were cultured in medium supplemented with increasing concentrations of recombinant IL-9 (0.1ng – 100ng/ml). After 48h of culture cells were harvested to determine cell proliferation by thymidine incorporation. Counts per minute are shown. Statistical significance was assessed by Dunnet post-test. p values are shown.

Targeting inflammatory signals limits malignant cell development/activity

The fact that in CTCL cell lines and HaCat cells IL-9 serves as growth factor prompted the possibility to target this cytokine as a therapeutic approach. The blockade of IL-9 was evaluated to reduce on cells by seeding HaCat and SeAx cells in medium supplemented with IL-9 and adding increasing amounts of anti-IL-9 antibody (Fig. 12). HaCat cells had a dose dependent reduction of proliferation at 48h of culture, SeAx cells did not show inhibition with 100ng/ml but a significant decreased proliferation with 200ng/ml and 500ng/ml of anti-IL-9 antibody. This set of experiments was carried out in MyLa2000 cells without IL-9 supplement but did not observe a reduction in cell growth.

Furthermore, given the fact that the therapeutic potency of PUVA in MF patients improves when patients are given concomitant treatment like with steroids or recombinant type 1 interferon (Nikolaou et al., 2011), the combination of IL-9 depletion with PUVA may be another strategy to increase the therapeutic effect of treatment. Myla2000 cells with PUVA alone or in combination with an anti-IL-9 antibody were cultured for 48h to determine viability by AnnexinV and propidium iodide incorporation (Fig. 13A). Supplementation of IFNα2b was used as control based on previous findings on its capacity to increase PUVA efficacy. The combination of PUVA with IFNα2b reduced cell viability to 38% while PUVA treatment alone reduced it by 56%. PUVA/anti-IL-9 treatment exhibited a reduction in cell viability of 37%, similar to IFNα2b treated group, and the combination of PUVA/IFNa2b/anti-IL-9 reduced viability with a small additive effect down to 35%.

Having seen in vitro that targeting IL-9 can potentiate PUVA effect, downstream molecules of the IL-9 pathway were analysed. STAT5 was one of the main interests since it is one of the immediate molecules triggered by IL-9 stimulation. Silencing RNA (siRNA) ON-TARGETplus from Dharmacon was used since it is a platform that combines a set of primers that hybridize in four different sites to magnify the silencing of the gene targeted. MyLa2000 cells were transfected with siRNA specific for STAT5 or control RNA (siCTRL) 24

hours before PUVA treatment. Treated cells were kept in culture for 48h to determine cell viability (Fig 13B). A decrease of cell viability in PUVA/siSTAT5–treated cells down to 18% compared with 58% on the 8-MOP alone and 42% in PUVA/siCTRL group.

As a closer approach to therapeutic alternatives to target cytokine pathways with drugs already available in the market, the effect of ruxolitinib was analysed. This selective JAK1/2 inhibitor developed by Novartis for the treatment of myeloproliferative disorders in bone marrow (Mascarenhas and Hoffman, 2013) and is currently under examination for the treatment of plaque psoriasis (Hsu and Armstrong, 2014) and alopecia areata (Blume-Peytavi and Vogt, 2015). The kinetics of IL-9 expression by qPCR on Myla2000 cells treated with Ruxolitinib for up to 48h (Fig. 14A) was determined. The peak of IL-9 expression was reached at 8h and decreased by 48h. Treated cells exhibited a reduction of IL-9 expression at all time points investigated without a significant loss of cell viability (data not shown). Transfection of MyLa2000 cells with siRNA targeting STAT3 or STAT5, the two regulators of the IL-9 signalling pathway was done and IL-9 expression was determined for up to 48h (Fig. 14B,C). Silencing was confirmed by western blotting at 24 and 48 hours after transfection (Fig. 14D). siSTAT5-transfected cells had a high reduction of IL-9 expression at 24 hours. By 48 hours, both siSTAT3 and siSTAT5 reduced IL-9 expression significantly. Similar results were found with a reduction of IL-9 expression when IRF4 was silenced as early as at 24h and up to 96h (Fig. 14E). These data indicate that direct targeting of IL-9 or its regulators can limit the growth and transcriptional activity of malignant cells.

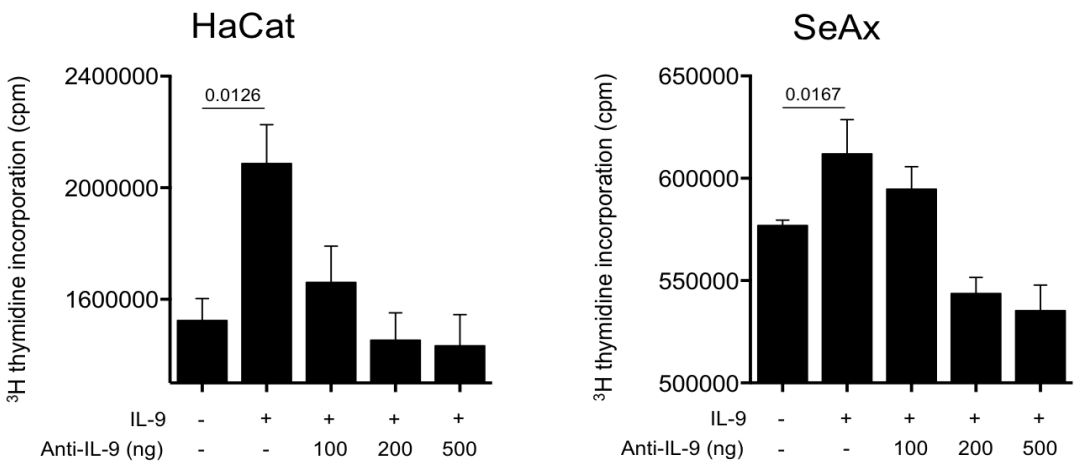

Figure 12: IL-9 blockade limits cell proliferation in keratinocyte and CTCL cell lines. HaCat and SeAx cells were cultured in low bovine serum conditions and 100ng/ml IL-9. A blocking antibody targeting IL-9 was added at increasing concentrations (100 – 500ng/ml). After 48h of culture cells were harvested to determine cell proliferation by thymidine incorporation. Counts per minute are shown. Statistical significance was assessed by Dunnet post-test. p values are shown.

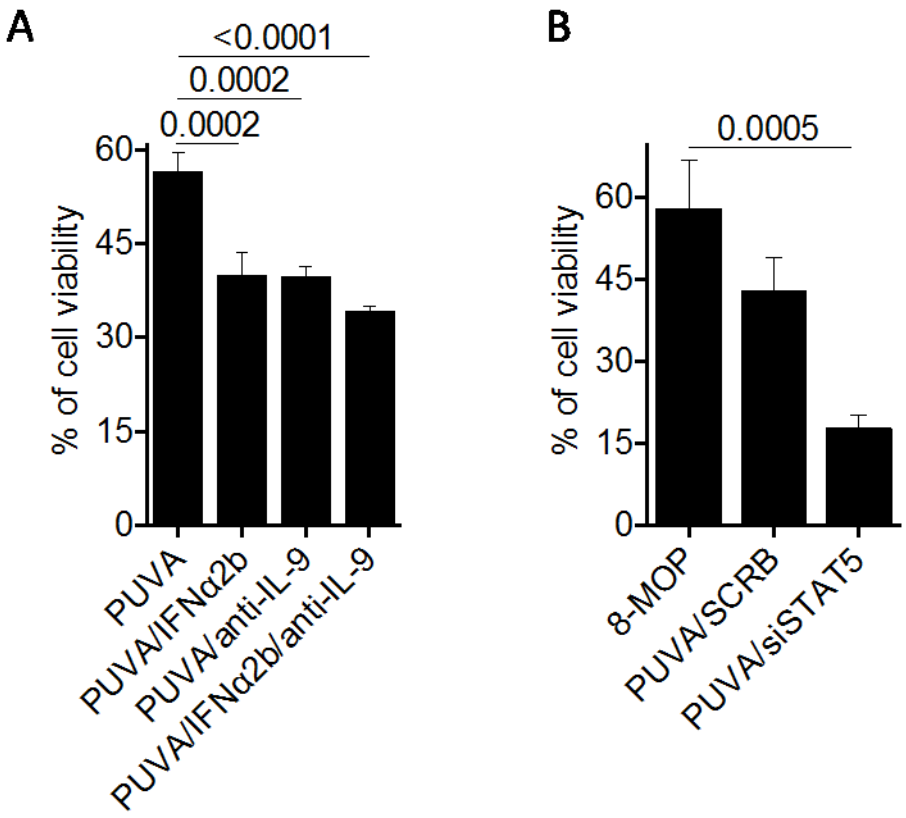

Figure 13: Targeting IL-9 and its downstream regulators potentiate the effect of PUVA. A) MyLa2000 cells were given PUVA followed by incubation in media supplemented with IFNa2b (1,500 U/mL), goat polyclonal anti-human IL-9 antibody (20 mg/mL) or the two combined. **B)** MyLa2000 cells were transfected with siSTAT5 or siCTRL 24 hours before treated with PUVA in vitro (1 mmol/L 8-MOP, 0.4 J/cm2). Viability was assessed by AnnexinV/PI incorporation after 48 hours of culture. Statistical significance was assessed by Dunnet post-test. These results are part of a recent publication (Vieyra-Garcia et al., 2016) and are included in this document under agreement with the publisher.

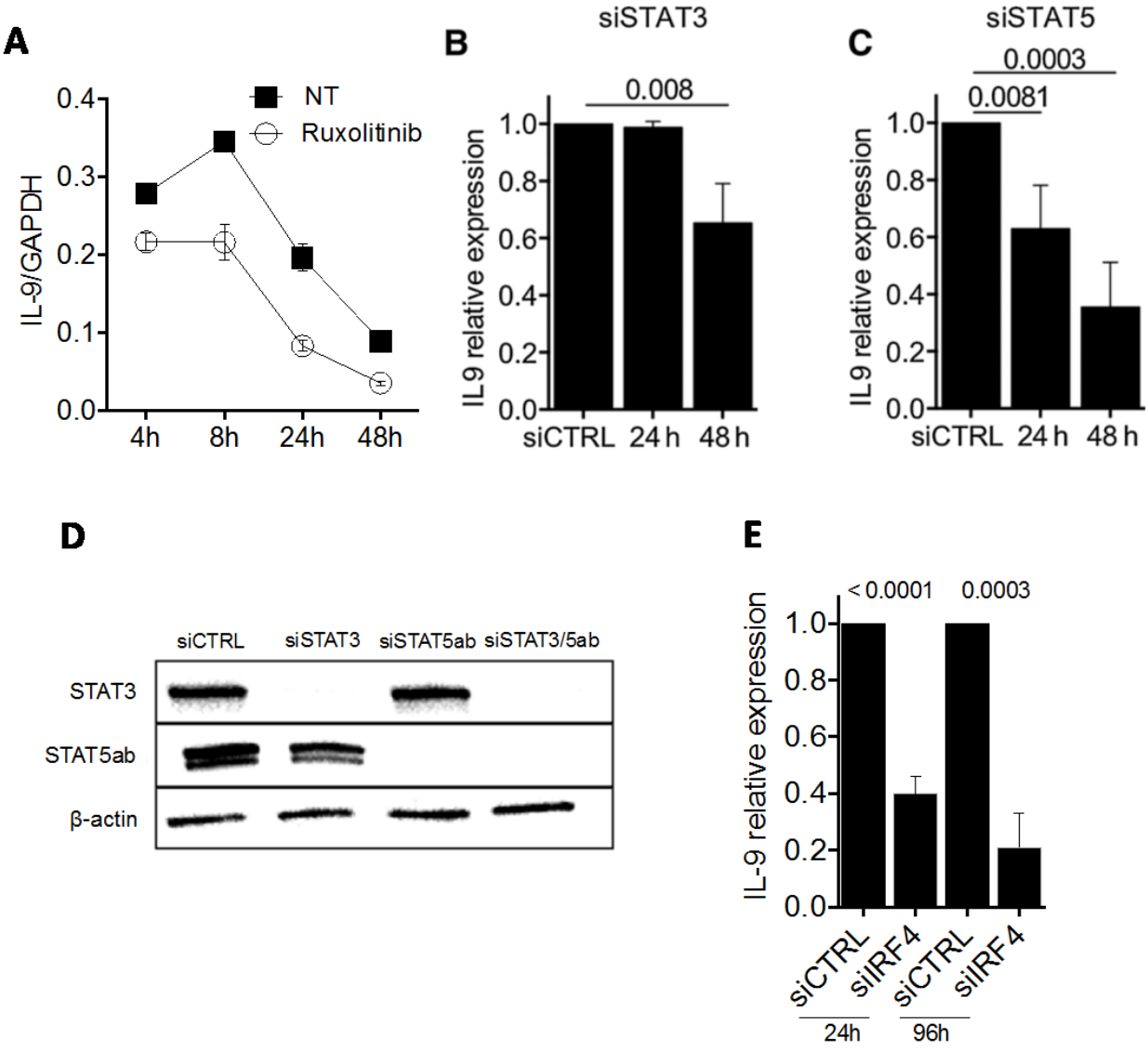

Figure 14: STAT3/5 pathway regulates IL-9 production in MyLa2000 cells. A) MyLa2000 cells were treated with 180nmol/L of ruxolitinib and cultured for up to 48h. IL-9 expression was quantified by qPCR at indicated time points; not treated (NT) cells were used as controls. **(B-C)** MyLa2000 cells were transfected with siRNA targeting STAT3 and STAT5. IL-9 expression was quantified by qPCR at indicated time points; fold change is shown normalized with unspecific siRNA-treated cells (siCTRL) as reference control. **D)** Western blot for STAT3 and STAT5 on siRNA transfected cells. **E)** siRNA was used to silence IRF4 and IL-9 expression was determined for up to 96 hours of transfection. Statistical significance was assessed by Dunnet post-test; p-values are shown. These results are part of a recent publication (Vieyra-Garcia et al., 2016) and are included in this document under agreement with the publisher.

Animal models highlight the importance of inflammatory signals

The study of new therapeutic targets such as IL-9 and mechanistic aspects of therapies like PUVA in cutaneous T-cell lymphoma require developing an animal model. The cell line EL-4 (a mouse CD4 T-cell line) was used for a syngeneic mouse model by intradermal injections in the back of C57BL/6 mice. By doing so, mice developed skin lesions that turned into tumours within 2 weeks. Using a cell line from a mouse background allowed experiments that took into account the contribution of the autologous immune system of the animals and assessed the influence to the *bona fide* of the tumours or to the protection of the host. Moreover, EL-4 cells have been used previously in lymphoma models like acute lymphoblastic leukemia (Jacoby et al., 2014) and lymphatic metastasis (Ochsenbein et al., 1999). At first this model was developed to look into therapeutic mechanisms of PUVA. After 24h of injection of the malignant cells, PUVA was initiated and given in subsequent rounds every 72h. Tumour diameter was determined to assess efficacy of PUVA, however no significant reduction of tumour growth as measured by macroscopic diameter was observed in treated mice. Nevertheless, by looking at the structure of the tumours in a H&E staining (Fig. 15A) at day 14 after cell injection, it was evident that PUVA treated mice had a reduction in the thickening of the epidermis and a band of clearance in the superficial area of the dermis. The frequency of regulatory T-cells was determined by flow cytometry in spleen and lymph nodes (Fig. 15B). A high number of T-cells with expression of Foxp3 were found in the inguinal lymph nodes and spleen in PUVA treated mice, suggesting that local therapy had an impact on systemic anti-tumour response and supporting previous findings on immunomodulation effect of PUVA.

After recognizing that MyLa2000 cells produce IL-9, and that this cytokine increased the growth of HaCat and CTCL cell lines. Experiments to examine the effect of targeting this molecule in the lymphoma animal model were carried out. First, the effect of IL-9 in the growth of EL-4 was determined in vitro. These cells were stimulated with increasing concentrations of recombinant IL-9 and cell proliferation was measured after 48h (Fig. 16A). EL-4 cells had a concentration dependent proliferation, which prompted the evaluation of the

role of IL-9 in vivo. After 6h of the injection of EL-4, anti-IL-9 antibody was administered by a series of intralesional injections every 48h (Fig. 16B). IL-9 depleted animals had a slower growth of tumour that increased the survival rate of these animals compared to isotype antibody injected mice (Fig. 16C). The frequency of regulatory T-cells and antigen experienced T-cells was evaluated as a measure of anti-tumour response in inguinal lymph nodes. It was found that IL-9 depleted animals had higher frequencies of T_{reg} cells (Fig. 16D), CD4 (Fig. 16E) and CD8 (Fig. 16F) antigen experienced cells. These results indicated that IL-9 is an important modulator of tumour development.

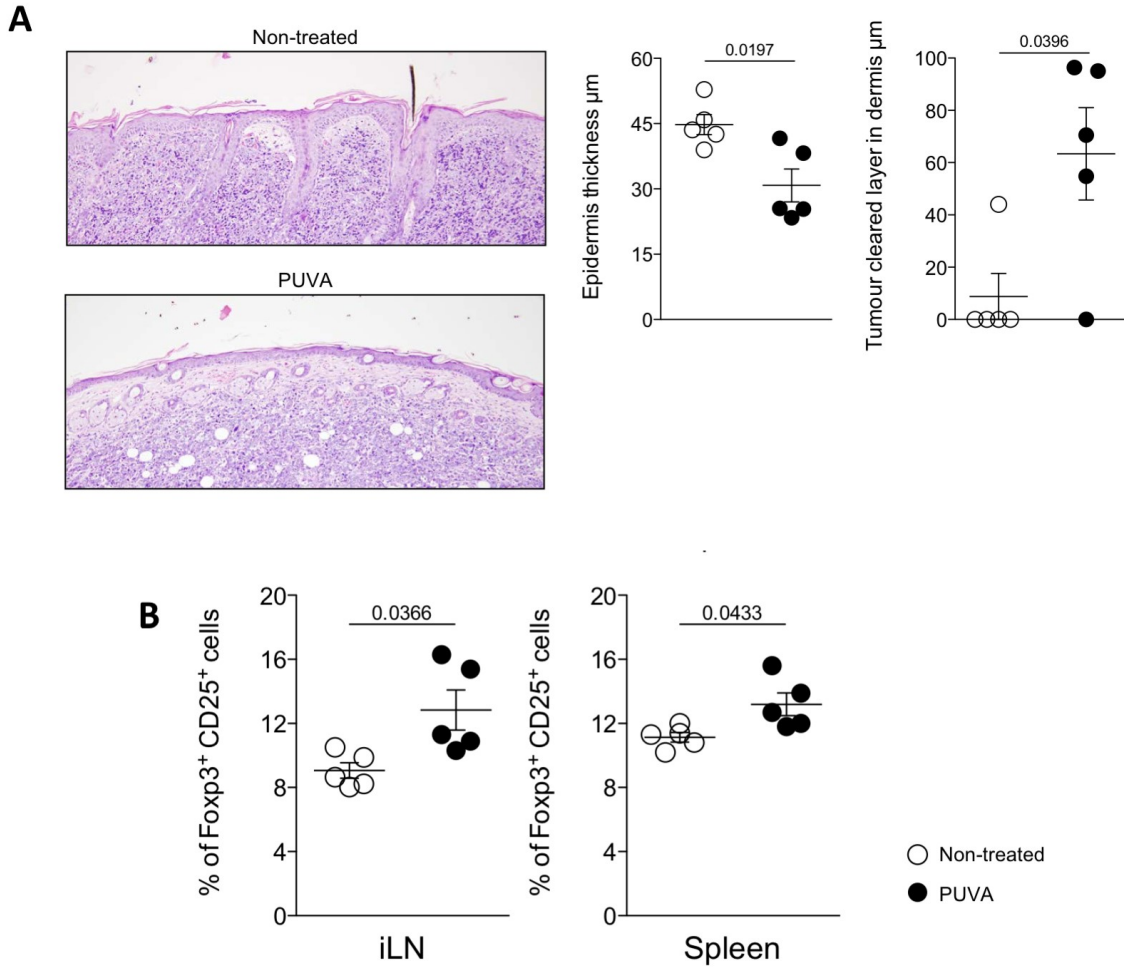

Figure 15: PUVA limits the growth of malignant cells in the superficial dermis and increases systemic number of T_{reg} cells. A) Mice were injected intradermically with 10^4 EL-4 cells in the dorsal skin (n5), PUVA treatment (filled dots) was given two times per week (8-Methoxypsoralen 1%, 1500 mJ/cm^2). Two weeks after injection mice were sacrificed and lesion skin was examined by histology. H&E staining showed thickening of epidermis and clearance of infiltrate in the superficial layer of the dermis. **B)** Inguinal lymph nodes and spleen were analysed by flow cytometry to determine T_{reg} cell frequency by expression of CD3+, CD4+ CD25+ and Foxp3+. t-test was used for statistical analysis; p value is depicted on top.

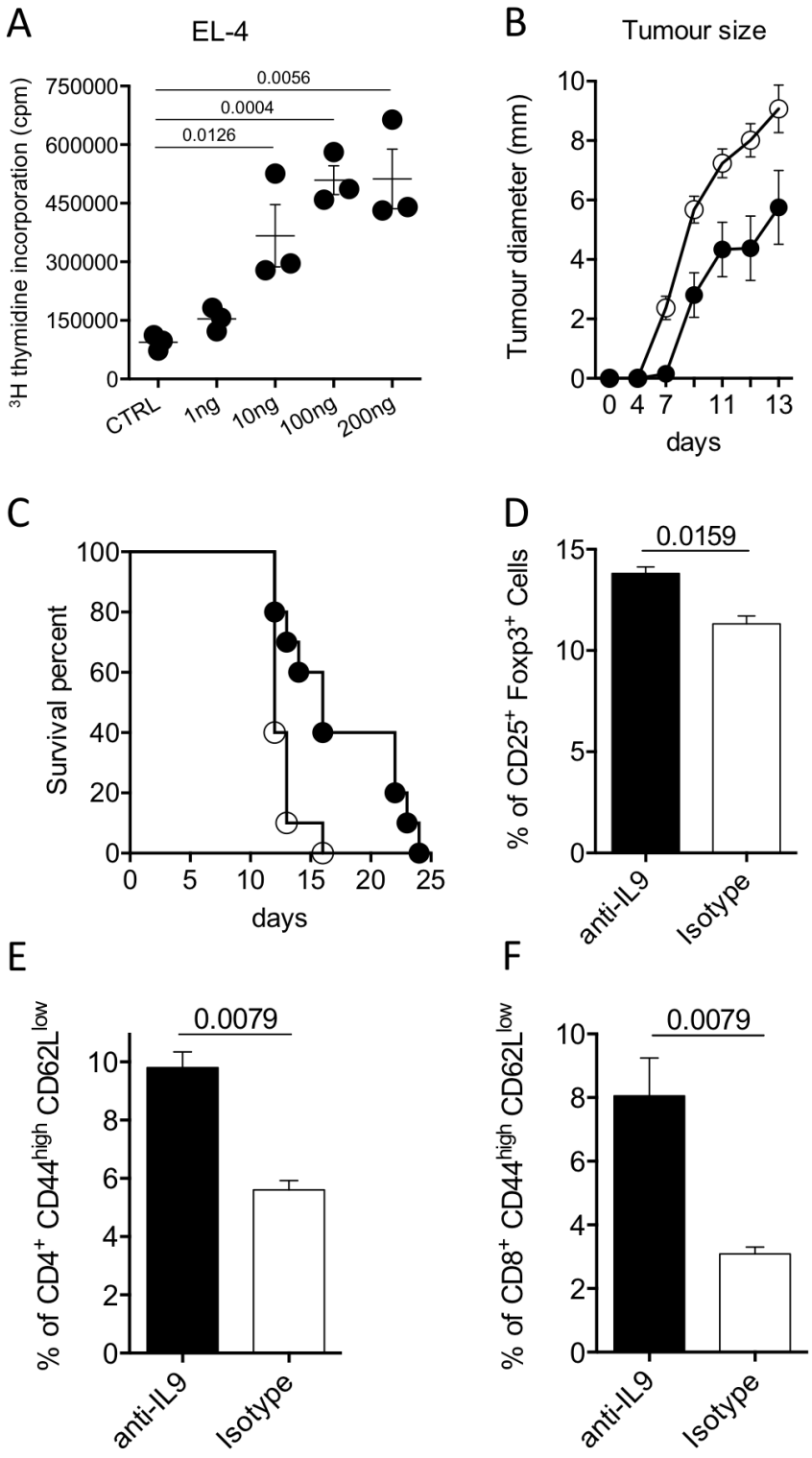

Figure 16: IL-9 increases proliferation of malignant cells in a lymphoma mouse model. A) EL-4 cells were cultured in medium supplemented with increasing concentrations of recombinant IL-9 (1ng – 200ng/ml). After 48h of culture cells were harvested to determine cell proliferation by thymidine incorporation. Counts per minute are shown. **B-E)** Mouse T-cell lymphoma cell line EL4 (10^4 cells) were injected intradermally into the backs of C57BL/6 mice. Polyclonal goat anti-IL-9 antibodies (20

μg) or isotype control was given together with the cells and repeatedly every 48 hours (n10 mice per experimental group). Tumour growth was assessed daily for 14 days using a Mitutoyo Mini-calliper, tumour diameter mean is depicted **(B)**. Mice were sacrificed when tumour size reached 1 cm of diameter; survival is shown **(C)**. Inguinal lymph nodes were taken on day 14 to analyse the frequency of T_{reg} cells **(D)** and antigen experienced (CD44high, CD62Llow) CD4 **(E)** and CD8 T-cells **(E)** by flow cytometry. Statistical analyses were done by Dunnet post-test **(A)**, Mantel Cox **(C)** and student t **(B, D-F)**. These results **(B-E)** are part of a recent publication (Vieyra-Garcia et al., 2016) and are included in this document under agreement with the publisher.

Therapies in humans like PUVA modulate inflammatory signals without complete elimination of malignant cells

A detailed analysis of the cells that infiltrate lesional skin is needed to have a better understanding of the complexity of the visible inflammation in MF patients. The first step was to analyse the landscape of T-cells that invade the skin, given the fact that lesional skin in MF not only is invaded by malignant clones but also benign T-cells. This is a challenging task due to the few molecular markers described that permit the identification of cells with aberrant phenotype within the diffuse infiltrate seen in histological preparations. Beta chain HTS of the TCR was used to study the entire T-cell repertoire to identify unique clones, look at the length of the CDR3 region, estimate the frequency of each clone within the population and classify clones by their constitutive variable (V) and joint (J) genes. 300ng of total DNA extracted from lesional skin was used to perform the sequencing in collaboration with Adaptive Biotechnologies, a Seattle (USA) based company that did the sequencing and provided an online tool analysis software; Immunoseq. Malignant clones were identified by their high frequency. In average, the frequency of any T-cell clone is not higher than 1%, in contrast, malignant T-cells had several folds higher frequency than the rest of benign T-cells that populate the skin. A three-dimensional plot is presented as representative of these findings (Fig. 17).

In this patient, a particular expanded sequence was found, outnumbering the rest of the cellular population (blue bar indicative of an expanded malignant clone). This clonotype constituted nearly 3% from all cells with functional T-cell receptors (after excluding non-functional rearrangements or fragmented sequences) and had almost 10 times higher frequency when compared with the second most frequent clone (Fig. 18A). The malignant clone carried the TCRbV02-01001 and TCRbJ01-01001 genetic fragments and with these findings, experiments were carried out to visualize the malignant clone on histological sections by using commercially available antibodies (70% of the total T-cell clonotypes are covered by monoclonal antibodies). The Vb22 antibody recognizes the annotated TCRbV02 and by using sequencing data, an estimate of 38% from all Vb22-positive cells was projected to belong to the malignant clonal population (Fig. 18A,B). Furthermore, an analysis of whether

the malignant cells were producing IL-9 in the tissue was carried out. An IL-9/CD3 double staining was performed to analyse the expression of IL-9 in the total T-cell population (Fig. 19A). It was found that IL-9 was exclusively produced by T-cells since only CD3+ cells co-stained with IL-9. Next, the assessment of whether malignant cells exclusively produced IL-9 was performed and Vb22/IL-9 double positive cells were found located at the basal epidermis and across the infiltrate of the dermis (Fig. 19B). Furthermore, IL-9-producing cells, negative for Vb22 were present, suggesting that IL-9 is produced not only by T-cells but also by benign cells together with malignant cells are the source of the IL-9. This presumably leads to an enriched microenvironment of this cytokine. To test whether malignant cells in tissue also expressed the Th9 related transcription factor IRF4 in correlation with the observations in MyLa2000 cells, a Vb22/IRF4 stain was done (Fig. 19C). Several Vb22-positive cells had expression of IRF4; in fact, IRF4 single positive cells with lymphocyte morphology were found, suggesting that IL-9 expression involves IRF4 in both malignant and benign T-cells.

After finding that the results from in vitro and the in vivo animal model correlated with expression of IL-9 in lesional skin of patients, the question of whether patients with clinical response to phototherapy also experience a decrease in IL-9-producing cells in lesional skin was addressed. Biopsies taken at baseline and after 6-45 weeks of treatment (the time when complete clinical response was achieved) were used to carry out histological examinations. These biopsies came from the archive of the Department of Dermatology. A summary of medical information about these biopsies is presented in the methodology section (M&M table 4). As shown in Fig. 19A, a significant number of IL-9-positive cells populating the dermis before the patients were treated with PUVA was observed. The biopsies taken after clinical response showed that the total infiltrate of IL-9-positive cells was reduced by 69% (from 245 to 77 cells/mm2; Fig. 20A). Additionally, a staining for IL-9 receptor was performed with the aim to estimate the potential number of cells responsive to IL-9. A substantial reduction of IL-9r-positive cells by a 64% (from 187 cells/mm^2 before treatment to 68 cells/mm^2 after treatment was observed; Fig. 20B).

Subsequent from this, a follow up of patients undergoing PUVA was set up to characterize the mechanistic effect of this therapy. A clinical study to recruit early stage MF patients was initiated. After signature of an inform consent, the patients were treated with PUVA two times per week. Scheduled data collection visits with the patients were programed to evaluate clinical response and to take biopsies from lesional skin. Two reference tools to assess the degree of clinical improvement were used: The mSWAT score, a grade system that weights the overall involvement of body surface and CAILS, a score for a particular index lesion. In order to keep track of clinical response, a defined (marker) lesion was selected on the first visit to take a baseline biopsy and subsequent biopsies from a site in close proximity whenever possible. The clinical scoring after 12-16 weeks of PUVA is presented (Fig. 21). The patients had a mean improvement of 88% in the mSWAT score, as well as 81% in CAILS, meaning that all patients had significant response to the treatment both in overall and at the site of marker lesion.

Next, an examination of the total number of T-cells in the skin was done by high throughput sequencing of the TCR and making an estimation of number of sequences per 100ng of DNA (Fig. 22). A decrease of nearly 50% of the total T cells after treatment was observed. Furthermore, the frequency of the malignant clone was examined. At baseline, a clone outnumbering by several orders of magnitude the rest of the population was found in all patients. These cells were considered as malignant clones. Surprisingly, after an evident clinical response, malignant cells were still found at high frequency in the majority of cases (Fig. 23), at least in the early phase of treatment with 12-16 weeks of exposure to PUVA. After a careful analysis of the sequencing data at baseline, it was clear that patients fell into two categories; patients with a high burden (n5) of malignant cells and patients with low burden of malignant clones (n3). Despite having patients with two degrees of malignant T-cell burden, no significant differences were found in the improvement of mSWAT and CAILS scores (Fig. 24) when the two groups were compared.

After treatment, only one patient of the high burden group had a lower percentage of the malignant clone. Two patients had similar percentages of malignant cells and 2 patients had even higher percentages of malignant cells

than at baseline. Patients of the low burden group all had a significant reduction of the malignant clone. The benign T-cells for each patient at baseline compared to after PUVA were classified into four groups (Fig. 25): Malignant cells (red), persistent benign T-cells found at baseline and after PUVA (blue), benign T-cells not found (or eliminated) after PUVA (light green) and benign T-cells newly recruited after PUVA (dark green). In the majority of cases (6 out of 8) a considerable percentage of malignant cells at baseline and after PUVA were found. A relatively low number of benign T-cells that remained in tissue after therapy was observed, however, a sizable proportion of benign T-cells left the skin after therapy, which meant that the majority of benign T-cells found after PUVA was newly recruited. Furthermore, a possible association between the significant improvement after treatment with PUVA and the redistribution of the T-cell repertoire was examined. A linear regression analysis was carried out to look for a correlation of mSWAT reduction (due to its indicative significance of systemic improvement) with alterations in T-cell populations. mSWAT improvement did not correlate with changes in the percentage of malignant cells. However, a significant correlation between benign T-cell elimination and clinical response was found (Fig. 26). In fact, in all patients there was a significant turnover of benign T-cells after PUVA (Fig. 27).

Moreover, nanostring analyses were done on biopsies of these patients to examine possible treatment-induced changes on the MF transcriptional profile (comparing baseline to after-treatment biopsies). The signature of MF that is described in figures 1-7 was partially normalized after treatment. Although clustering of groups before and after treatment wasn’t found, genes involved in T cell responses, antigen processing, chemokine signalling, macrophages and dendritic cells were down regulated after PUVA therapy, suggesting that immunomodulation by PUVA is a significant element of its therapeutic mechanism (Fig. 28A). From the top genes (many of them related to immune regulation) with lower expression found at baseline, only four genes lost significance, suggesting that the restoring of homeostasis does not primarily depend on compensatory immune responses. In contrast, the majority of genes with higher expression at baseline lost significance in patients with clinical response (Fig. 28B), indicating the relevance of down regulated genes that

diminish visible inflammation as an effective approach on limiting the severity of this disease.

Previous reports suggest that MF lesional skin infiltrate is composed by a high diversity of cell types. However, so far there hasn't been a quantitative analysis of the cell infiltrate composition, partially due to the lack of analytical tools in microscopy that can carry out systematic quantification of cells in histological sections. To gain an insight in of which cells and in which proportion such cells populate lesional skin, tyramide signal amplification (TSA) based immunofluorescence was performed. This assay allowed us to use up to 5 primary antibodies on a single slide. The principle of this technique is that after binding of a primary antibody, a biotinylated secondary antibody is applied followed by streptavidin-HRP. This constitutes a signal amplification complex that when tyramide bound fluorophores are added, fluorescent molecules form stable covalent bonds deposit as fluorescent dyes. By applying heat to the sample, the whole complex is destabilised and the slide keeps the fluorescence deposited. A new primary antibody with different specificity can be added to have a second signal, and this can be expanded with as many fluorescent dyes available in the detection spectrum of an instrument. PerkinElmer's imaging system Mantra and the analysis tool inForm with a trainable algorithm to assign phenotypes on cells with a specific fluorescent dye were used to quantify immune fluorescence. Three different panels of antibodies were employed to quantify adaptive immune cells (Fig. 29), innate immune cells (Fig. 30) and certain specific subpopulations of T cells (Fig. 31). In this methodology, an image of the immunofluorescence is composed by a series of pictures taken at different wavelengths stacked into one file. The software identifies the peak emission of each fluorescent dye and generates layers of individual stains used for analyses and training of the algorithm (refined by the user criteria). After training, the program generates a composite image of the phenotype of each cell based on the training. Biopsies taken at baseline and after treatment were analysed to make a comparison of the infiltrate composition.

In the adaptive immune cell panel, stains for CD4, CD8, CD20 and the residence marker for T-cells CD103 (Mackay et al., 2013) were done (Fig. 29).

A decrease of 50% on the number of CD4 positive cells per square millimetre was found. This result correlated with our findings by TCR HTS. A decrease in the number of B-cells, and CD103 cells (summing cells positive for either CD4 or CD8) was found, whereas the number of CD8 positive cells had only a minor decrease after PUVA (Fig 32A, 33A). In the innate immune cell panel (Fig. 30), the marker for Langerhans cells CD1a, the marker for conventional dendritic cells CD11c, and two markers for macrophages CD68 and CD163 were used. A significant decrease of CD1a positive cells, mainly located in the epidermis and superficial dermis was found. Due to the morphology and low expression of CD11c, these cells were classified as Langerhans cells. A modest increase in CD1a/CD11c double positive and CD11c single positive cells was found after PUVA, whereas the number of CD68/CD163 double positive macrophages remained unchanged (Fig. 32). It is very likely that the cells located at the most superficial sites in the tissue were directly affected by PUVA therapy. Additionally, a panel to look into subpopulation of T-cells with antibodies against CD4, CD8, CD69 and Foxp3 was used (Fig. 31). In this part of the analysis, the positivity of CD4 or CD8 was determined first, and then the expression of either CD69 or Foxp3 was evaluated. The results are shown in three categories of cells; CD8 and CD4 positive cells were grouped together for CD69 positivity or negativity (referred to as CD69+ or CD69-). CD4 positive cells positive for Foxp3 were referred to as Foxp3+. A discrete reduction of CD69- cells was observed while Foxp3+ and CD69+ numbers remained nearly unchanged after therapy. CD103 positive T-cells were reduced after PUVA.

To have a better understanding of which proportion each phenotype represents, the percentage of each population within the total immune cells that infiltrate lesional skin was calculated (Fig. 32B, 33B). CD4 cells were the main population of the skin, however they suffered a slight contraction from 46% to 37%. Macrophages were the second most frequent cells and although their total numbers didn’t change significantly, they increased up to 20% in the total infiltrate. CD8 T-cells did change insubstantially from 10% to 12%, however, B-cells (defined by CD20 positivity) decreased from 10% to 5%. CD1a/11c double positive cells increased from 4% to 10% in correlation with their absolute numbers. CD1a cells decreased almost by half from 13% to 7% while CD11c

went from 3% to 9%. In the distribution of T-cell subpopulations, the majority of T-cells were CD69- and they contracted from 81% down to 74%. CD69 positive cells increased from 10% up to 19% arguing in favour of an influx of new cells likely being recruited from the blood. CD103 positive cells decreased from 7% to 2% and Foxp3 cells increased from 2% to 5%. These results suggested that on top of the decreased cellularity of the skin after treatment, the remaining cells were still diverse in cell types, which implied a different cell-to-cell interaction that may have contributed to ease the severity of skin lesions.

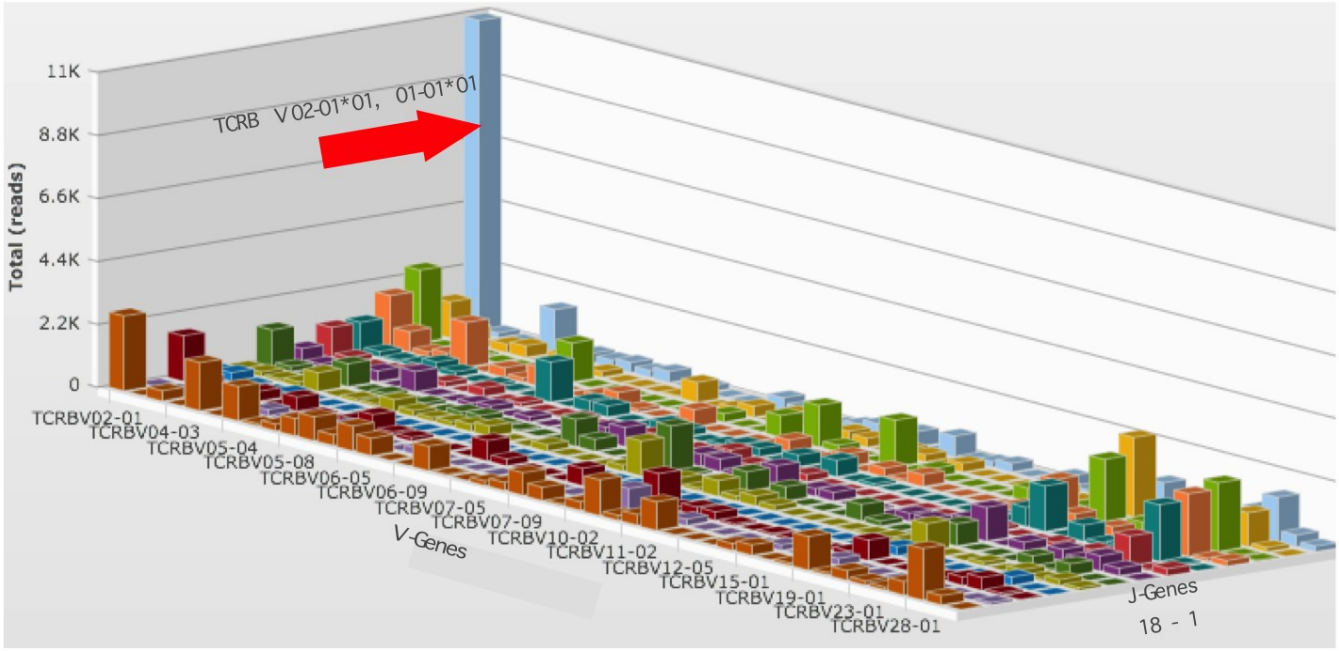

Figure 17: T-cell repertoire of early stage MF. Total DNA from lesional skin before and after treatment was used to carry out HTS of the CDR3 region in the beta chain of the TCR. The total number of sequence reads (y axis) was plotted in a 3D histogram (B) distributed by their constituent variable and joint regions (x and z axis). The malignant clone was identified by its outstanding frequency in the total T-cell repertoire (red arrow). The exact designation of the constituent V and J fragments are annotated above the arrow. These results are part of a recent publication (Vieyra-Garcia et al., 2016) and are included in this document under agreement with the publisher.

A

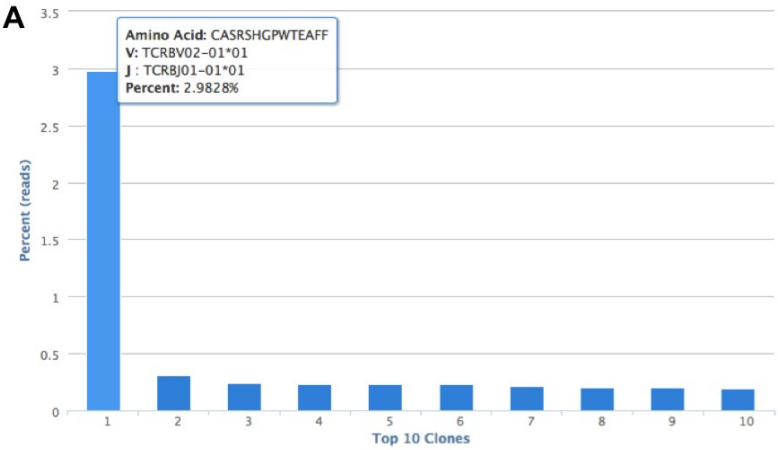

TCRβV02-01 (Vb22): 25,933 reads

TCRβV02-01*01
TCRβJ01-01*01
CASRHGPWTEAFF clone: 9,804 reads

Estimated clone freq: 37.80%

B

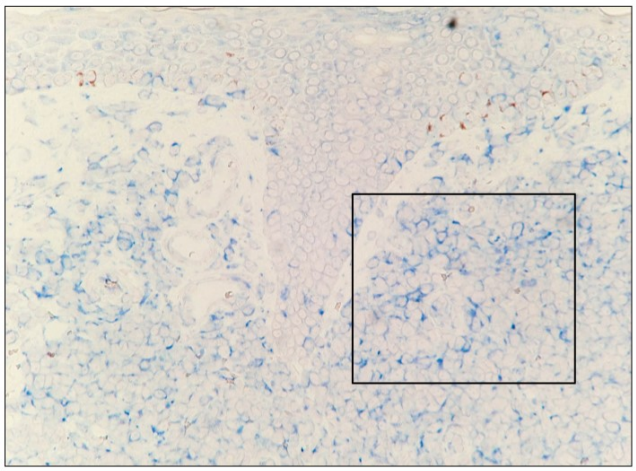

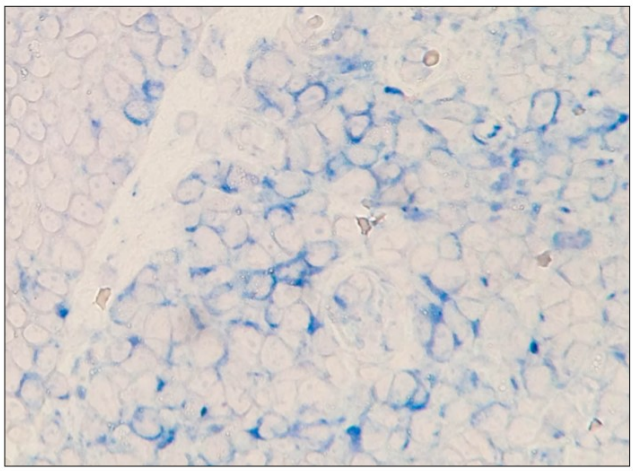

Vb22 /
Isotype

Figure 18: Malignant clones outnumber benign T-cells by several folds. A) Analysis of the top 10 Functional TCR sequences in lesional MF skin. The amino acid sequence of the CDR3 is shown (CASRHGPWTEAFF TCRBV02-01*01, TCRBJ01-01*01) and frequency of this clone was 3.5%. **B)** Immunohistochemical double stain; Vb22 (blue) and mouse isotype control (red). These results are part of a recent publication (Vieyra-Garcia et al., 2016) and are included in this document under agreement with the publisher.

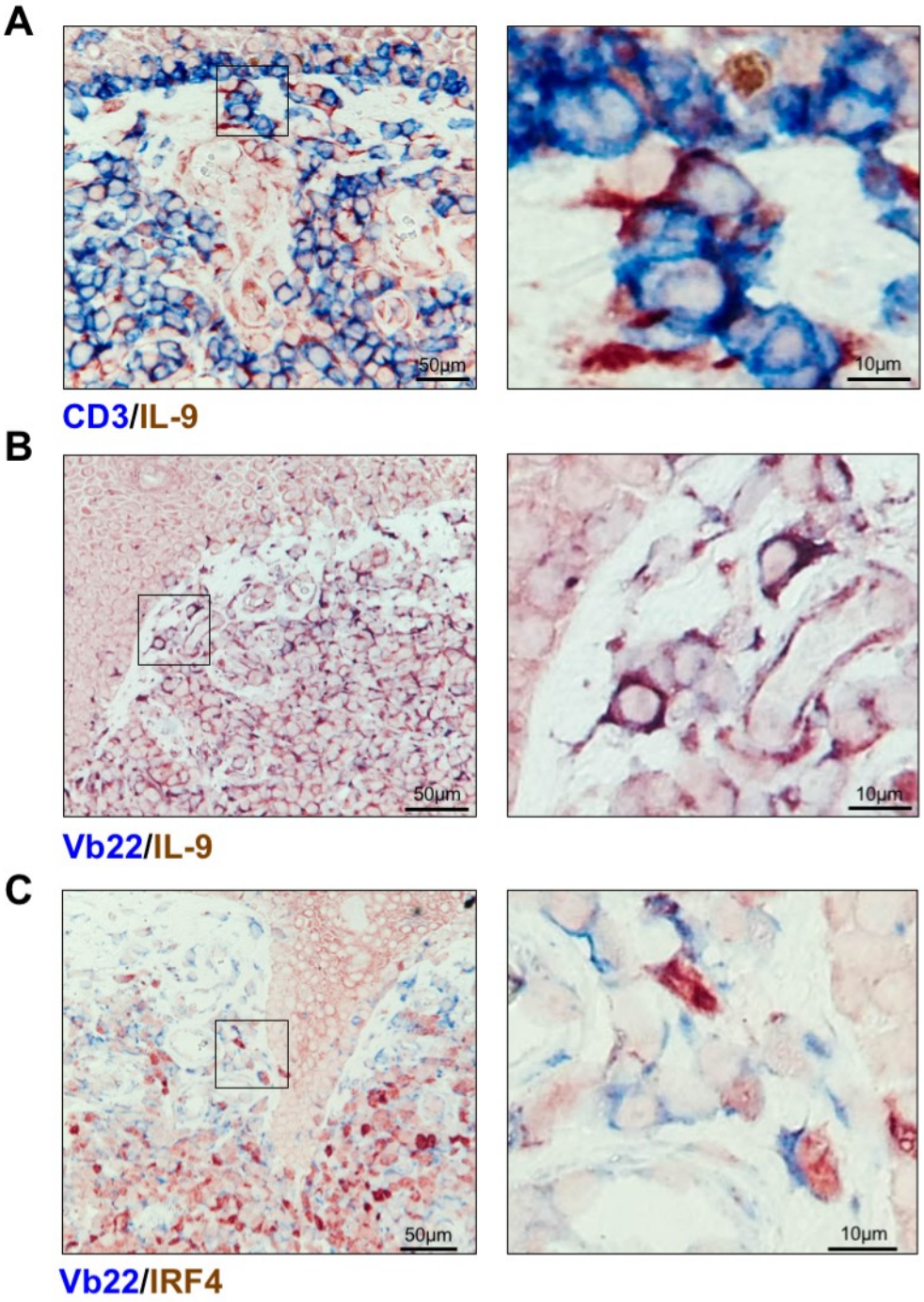

Figure 19: IL-9 is produced by benign and malignant T-cells. Paraffin-embedded skin biopsies from early stage MF patients were stained by two-colour immunohistochemistry (blue/red). **A)** Sections stained with CD3/IL-9, magnified areas are indicated (detailed scoring of double stains are shown in M&M table 4). **B-C)** Sections stain with the Vb22 antibody to identify the malignant clone by the expression of the TCRbV02-01 gene product (selected based on sequencing results), co-stained with IL-9 **(B)** or IRF4 **(C)** (patient A4 is shown). These results are part of a recent publication (Vieyra-Garcia et al., 2016) and are included in this document under agreement with the publisher.

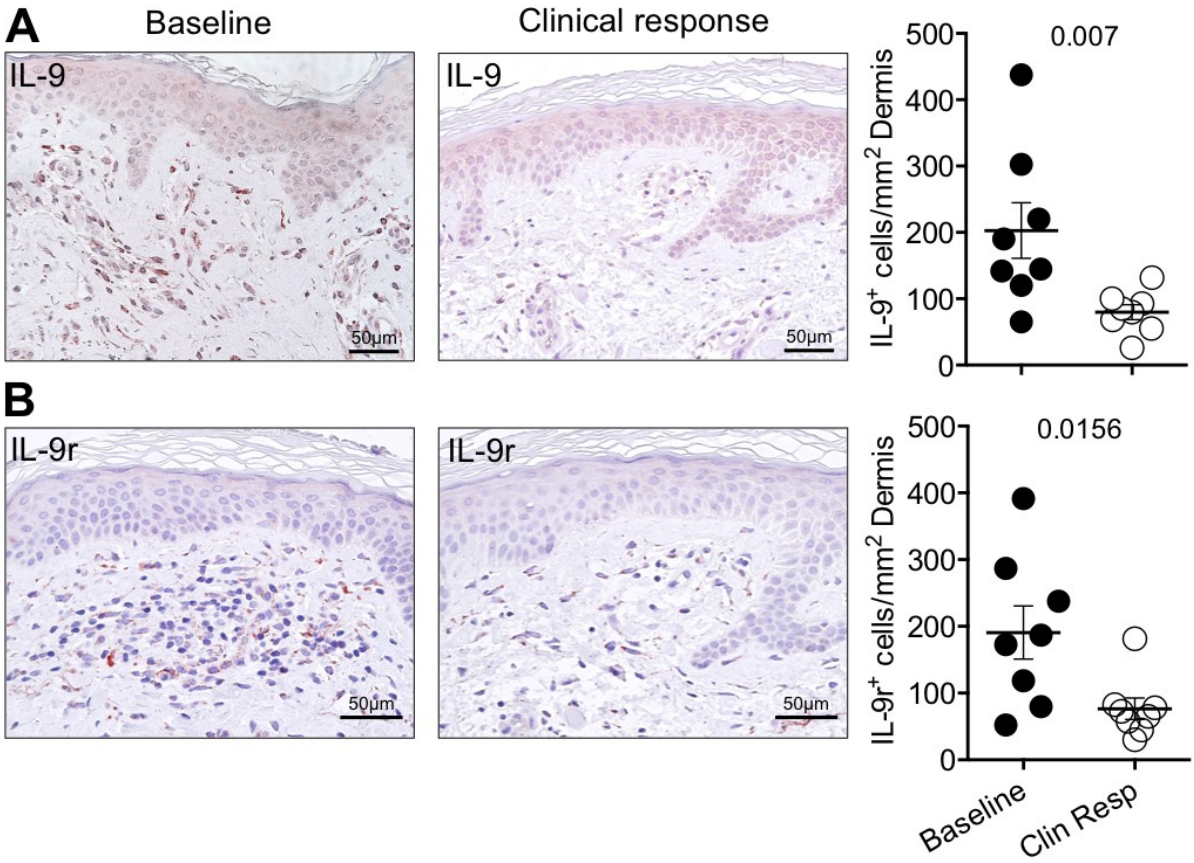

Figure 20: IL-9 production is reduced in MF patients treated with PUVA. Samples from MF patients before and after treatment (M&M table 4) were analysed for IL-9 **(A)** and IL-9r **(B)** expression (micrographs from patient A1 are shown). The average of positive cells in three 40x fields per sample is presented: adjusted to the unit of area (mm^2). Statistical significance was assessed by paired student t test. These results are part of a recent publication (Vieyra-Garcia et al., 2016) and are included in this document under agreement with the publisher.

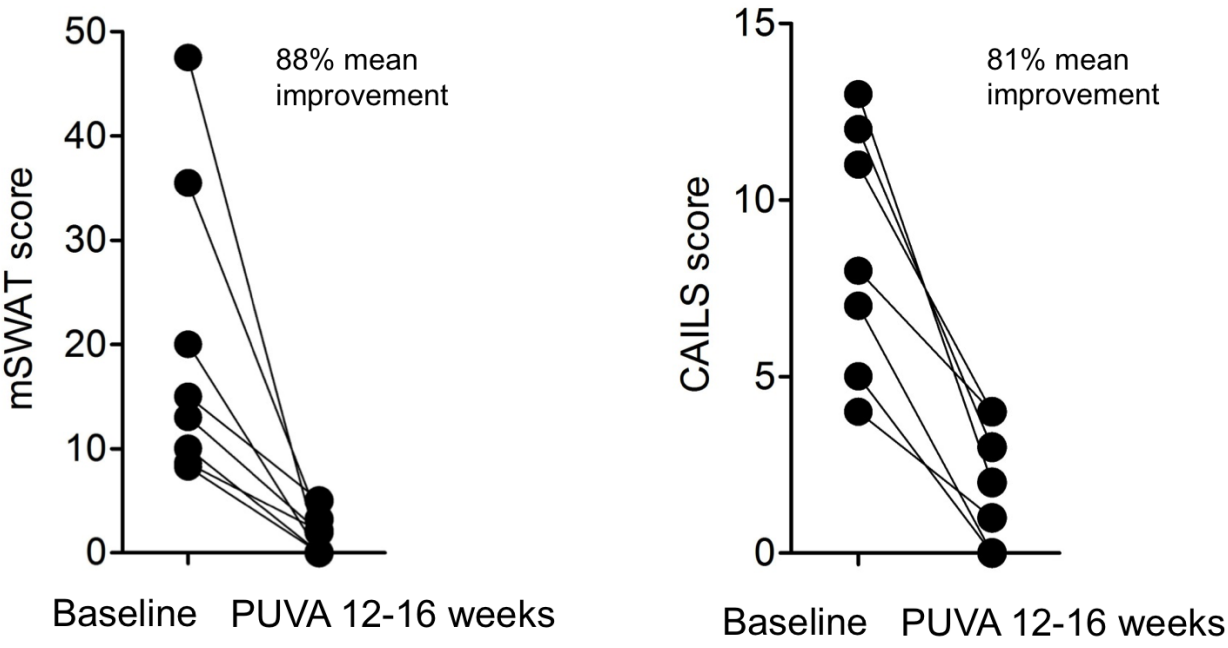

Figure 21: Clinical response of early stage MF patients to PUVA treatment. MF patients (n8, additional information of patients in M&M table 3) were treated with a standard regime of PUVA (described in materials and methods). Clinical response was evaluated systemically with mSWAT score. A marker lesion in a particular body site was selected to quantify response to therapy with the CAILS score. Both evaluations were done at baseline and after treatment (12-16 weeks). Overall percentage of improvement is shown.

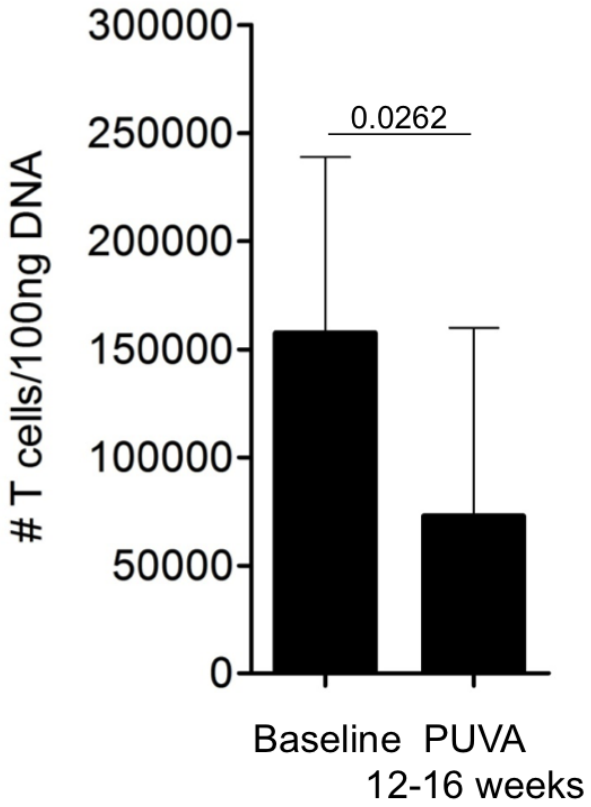

Figure 22: PUVA reduces the total T-cell infiltrate in MF lesions. Lesional skin was taken at baseline and after PUVA (12-16 weeks) to carry out HTS of the TCR. The total number of reads was adjusted to 100ng of DNA sequenced. Statistical significance was assessed by paired student t test.

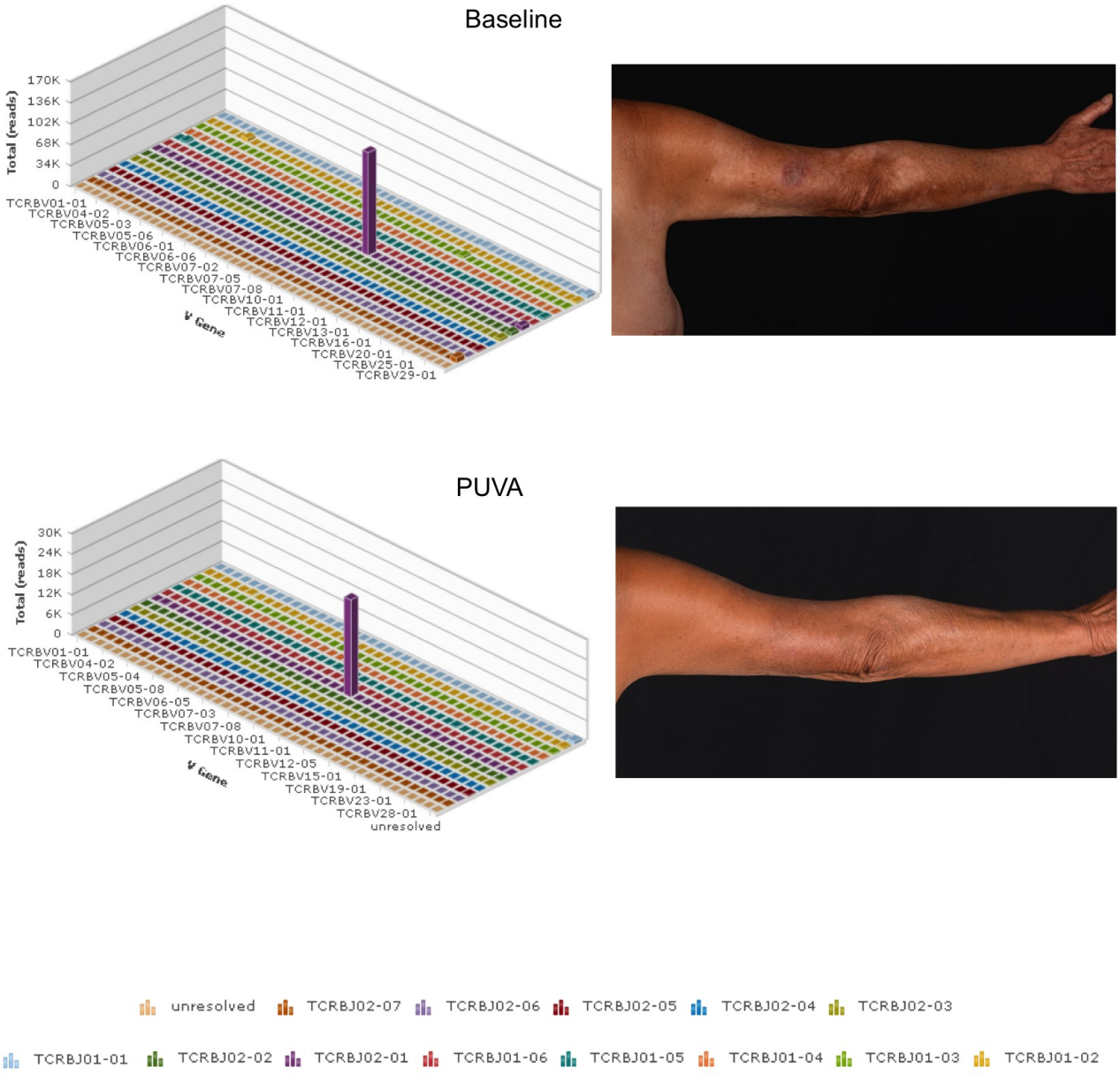

Figure 23: Clinical response does not eliminate malignant T-cell clones. 3D histogram of the T-cell repertoire at baseline (upper panel). The clinical photograph shows the body site biopsied and the degree of lesional skin at baseline. In the lower panel, the T-cell repertoire is shown after 12 weeks of PUVA. The patient showed clinical response (as seen in clinical photograph), however, the malignant clone was still present. A biopsy taken in a different body site with residual skin lesion showed the persistence of the same clone.

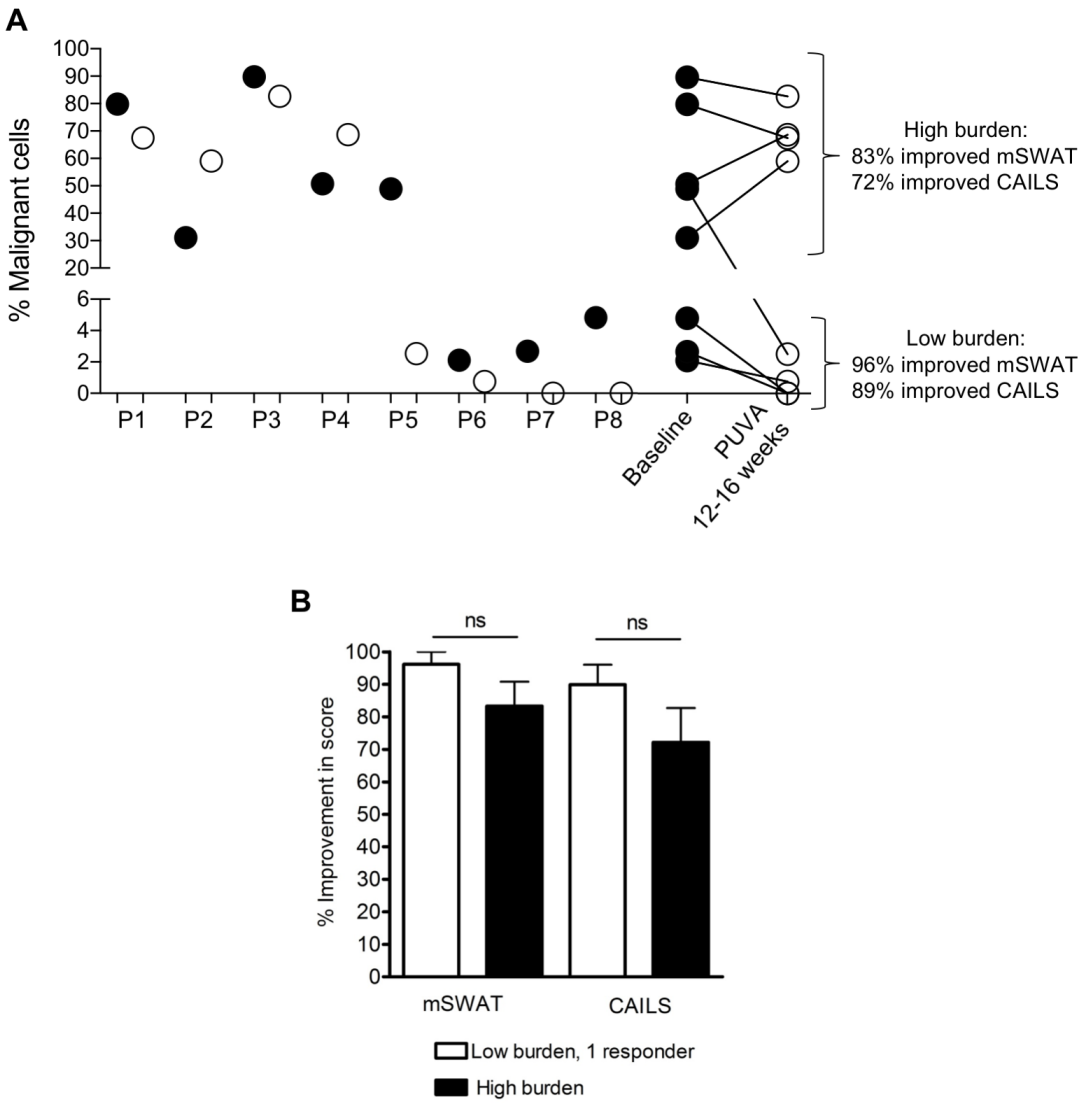

Figure 24: Malignant T-cell burden is not a prognostic marker for response to treatment. A) By using HTS data, the frequency of malignant clones in the total T-cell population was estimated at baseline and after PUVA. Patients were grouped in sets individuals having lesional skin with low (n3) or high (n5) burden of malignant cells. **B)** Percentage of clinical improvement in mSWAT and CAILS in the different sets of patients.

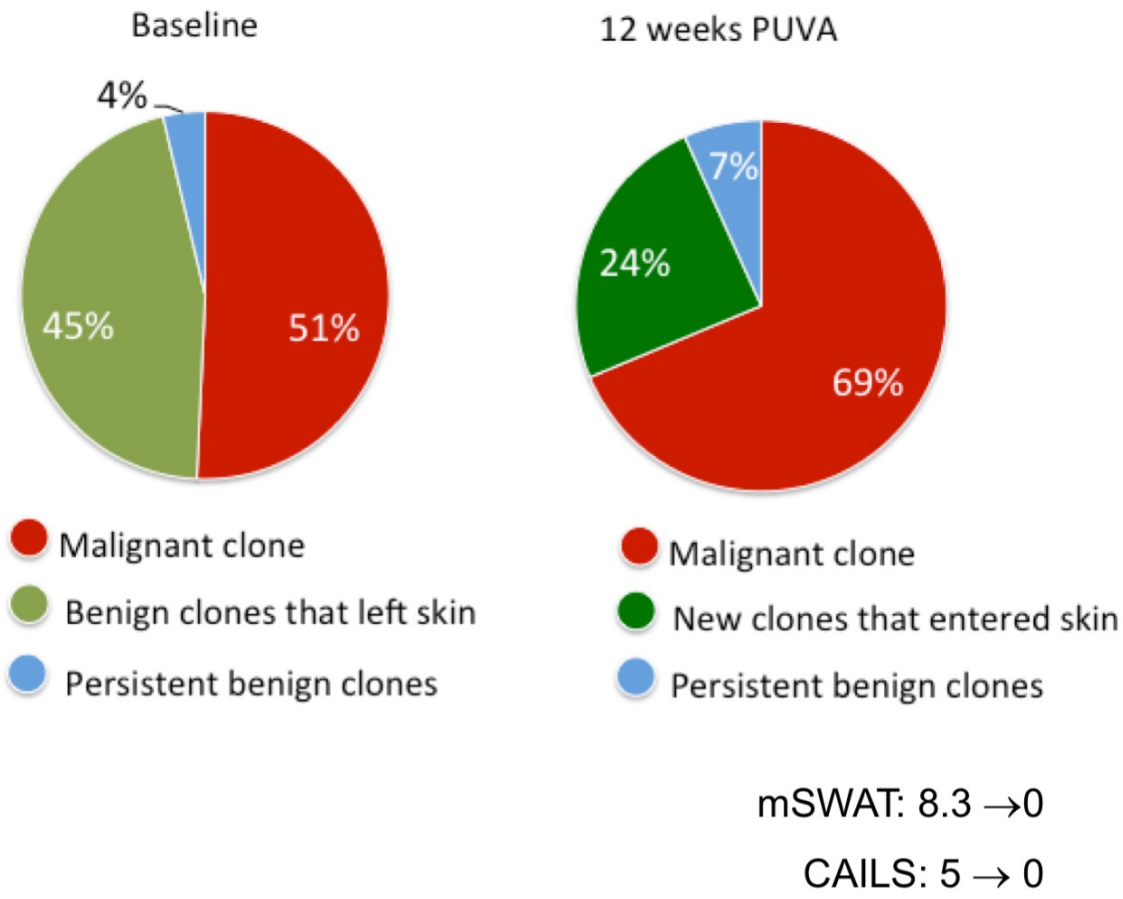

Figure 25: PUVA alters the T-cell repertoire in lesional MF skin by inducing benign T-cell turnover. Based on HTS data of lesional skin at baseline and after PUVA, the T-cell composition of the infiltrate was classified into four categories, according to their T-cell repertoire. Percentages of the different categories are shown: Malignant clone (red), persistent benign T-cells found in the tissue before and after treatment (blue), benign T-cells that left the skin (or were eliminated) after PUVA (light green) and benign T-cells recruited after PUVA (dark green). Results from a patient with complete response on mSWAT and CAILS are shown.

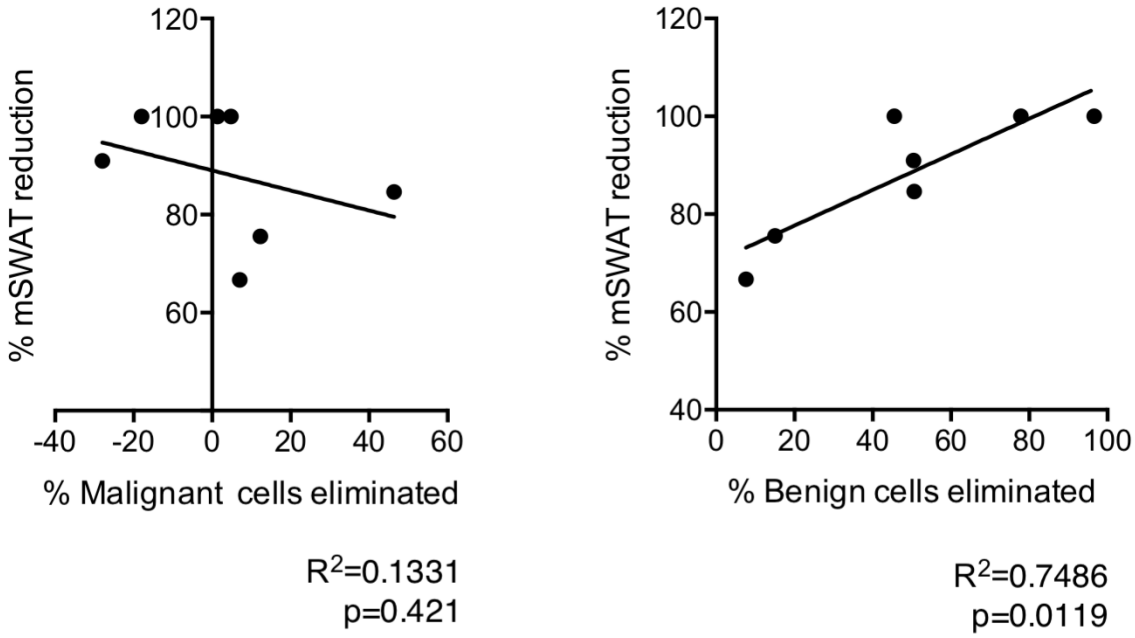

Figure 26: Clinical response correlates with benign T-cell turnover. The percentage of reduction in the severity of the mSWAT score was calculated. A correlation analysis was performed by linear regression of mSWAT to the percentage of malignant T-cell elimination (left panel) or to the percentage of benign T-cells eliminated (right panel). The p-value and R^2 score are shown.

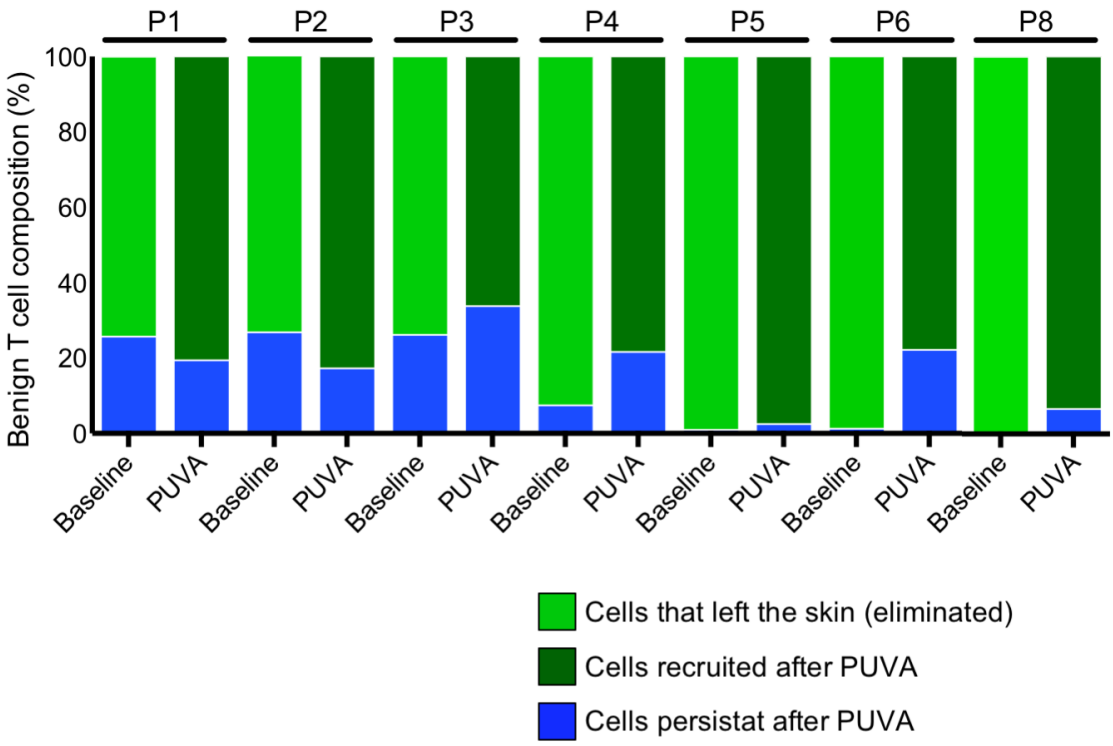

Figure 27: After PUVA newly recruited cells constitute the majority of the benign T-cell population. Composition of the benign T-cell population in each patient is depicted at baseline and after PUVA therapy. T-cells found in the tissue before and after treatment (blue), T-cells that left the skin (or were eliminated) after PUVA (light green) and benign T-cells recruited after therapy (dark green).

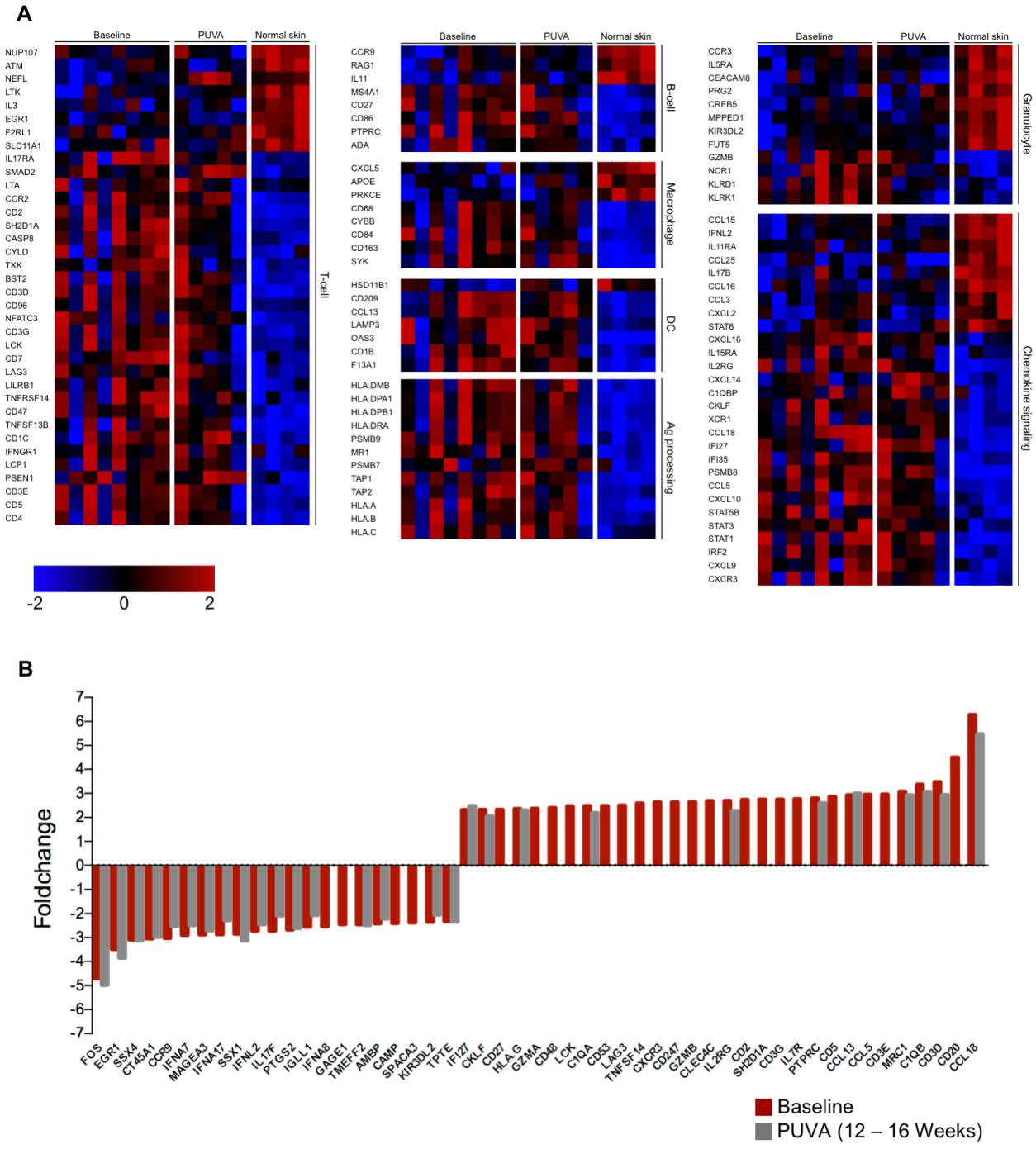

Figure 28: Transcriptional signature of early stage MF is partially normalized after PUVA. Frozen skin biopsies from lesional skin at baseline and after PUVA were used to extract RNA. The expression of inflammatory related genes, oncogenes and tumour suppressor genes was assessed by nanostring and compared to normal skin. **A)** Genes were grouped based on their biological function: T-cell activation, antigen processing, B-cell, macrophage, dendritic cell, chemokine signalling, and granulocytes. **B)** Waterfall plot (fold change) with down/up regulated genes at baseline (red) and after PUVA (grey) compared to normal skin. The cut-off value was +2.5, p value under 0.05 and FDR of 0.5.

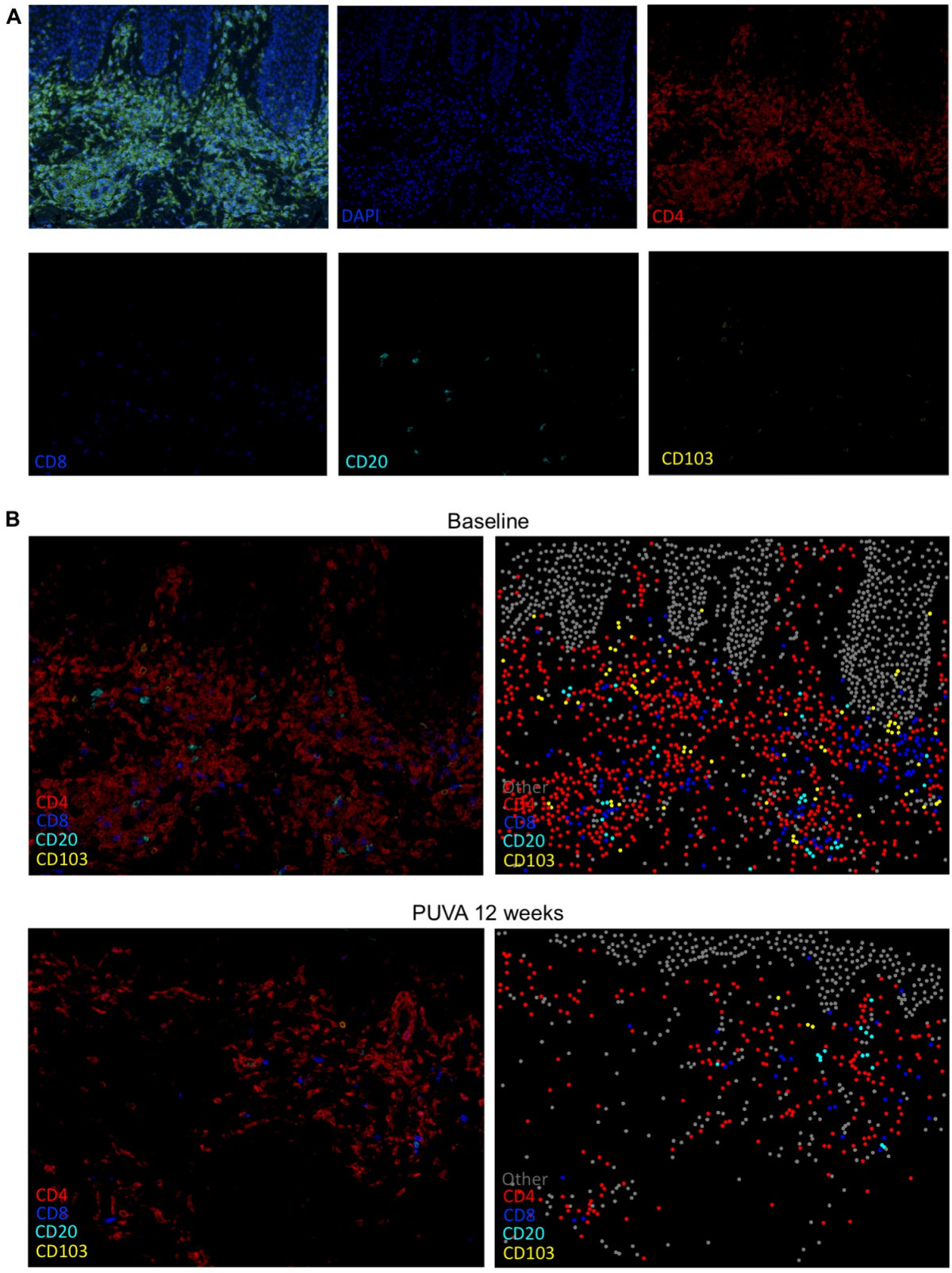

Figure 29: Adaptive immune infiltrate in lesional MF skin. Immunofluorescence imaging of lesional skin was done at baseline and after PUVA. **A)** Micrograph from all fluorophores (top left), DAPI, CD4, CD8, CD20 and CD103. **B)** Composite images from all markers except DAPI (left panel) and phenotyped image (right panel) were generated with inFrom software from baseline sections (upper panel) and after PUVA (lower panel).

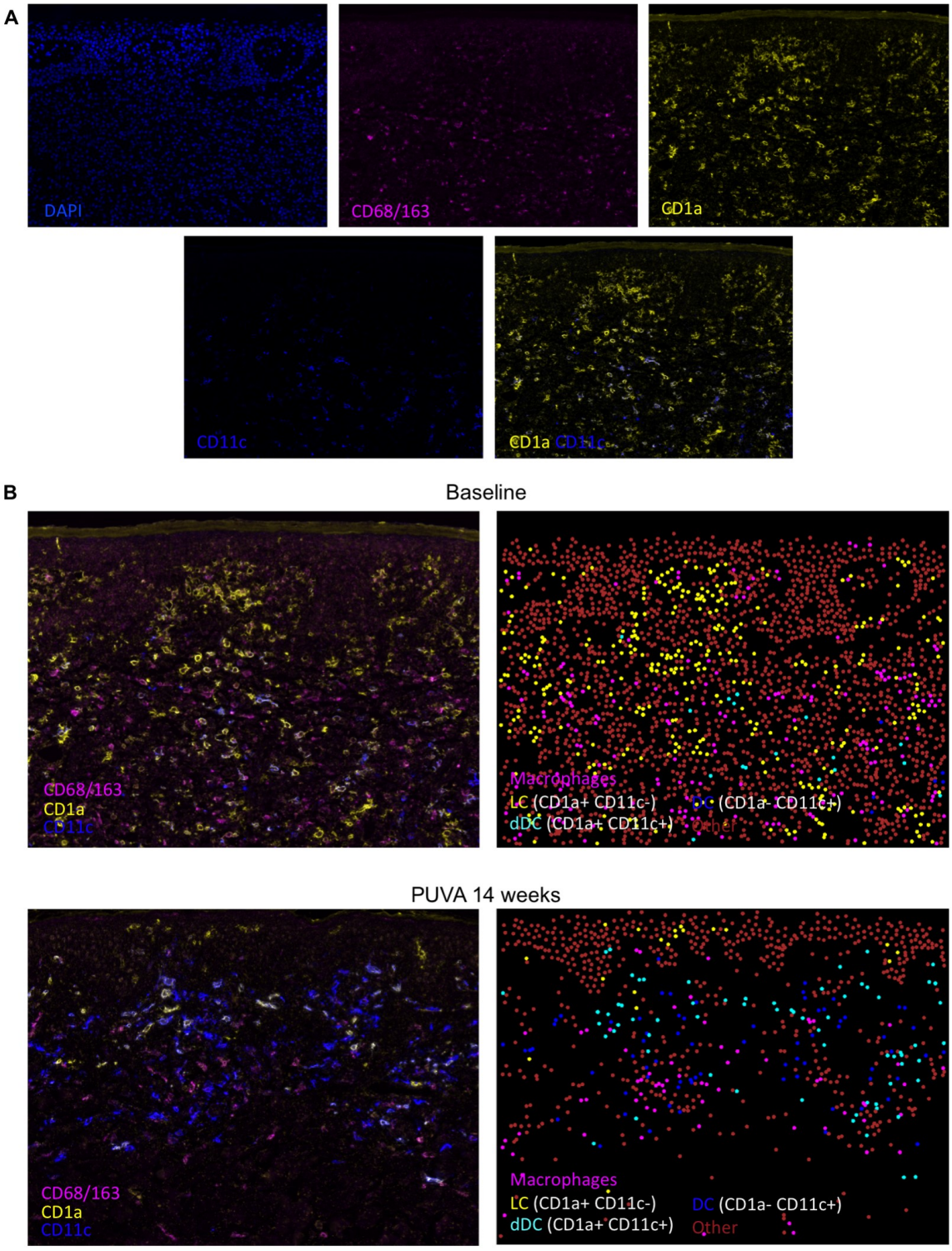

Figure 30: Innate immune infiltrate in lesional MF skin. A) Immunofluorescence stain of lesional skin at baseline and after PUVA. Nuclear staining of DAPI, CD68/163, CD1a, CD11c and CD1a/11c are shown. **B)** Composite images from all markers except DAPI (left panel) and phenotyped image (right panel) were generated with inFrom software from baseline sections (upper panel) and after PUVA (lower panel).

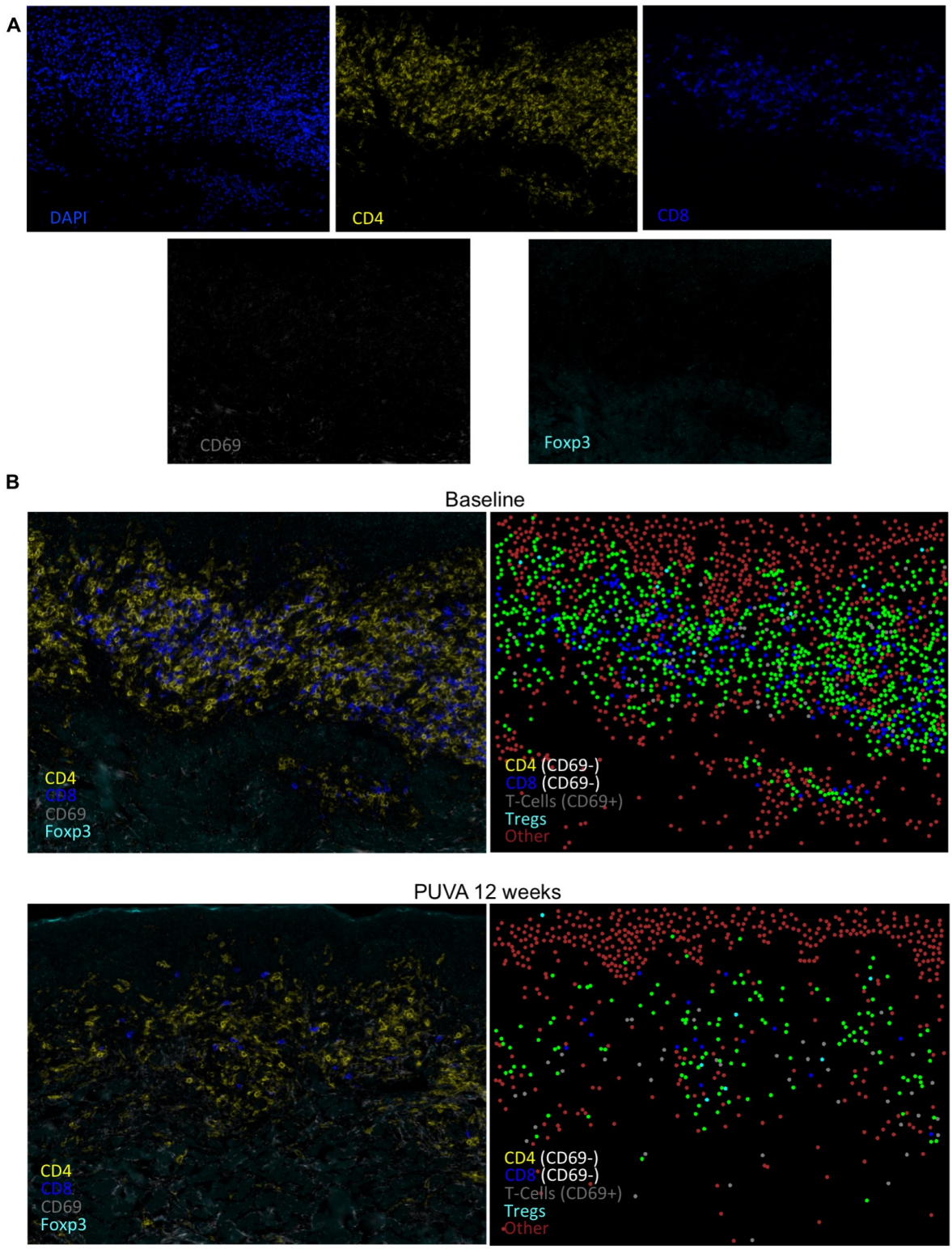

Figure 31: T-cell subpopulations infiltrate in lesional MF skin. Immunofluorescence stain of lesional skin was done at baseline and after PUVA. **A)** Nuclear staining with DAPI, CD4, CD8, CD69 and Foxp3. **B)** Composite images from all markers except DAPI (left panel) and phenotyped image (right panel) were generated with inFrom software from baseline sections (upper panel) and after PUVA (lower panel).

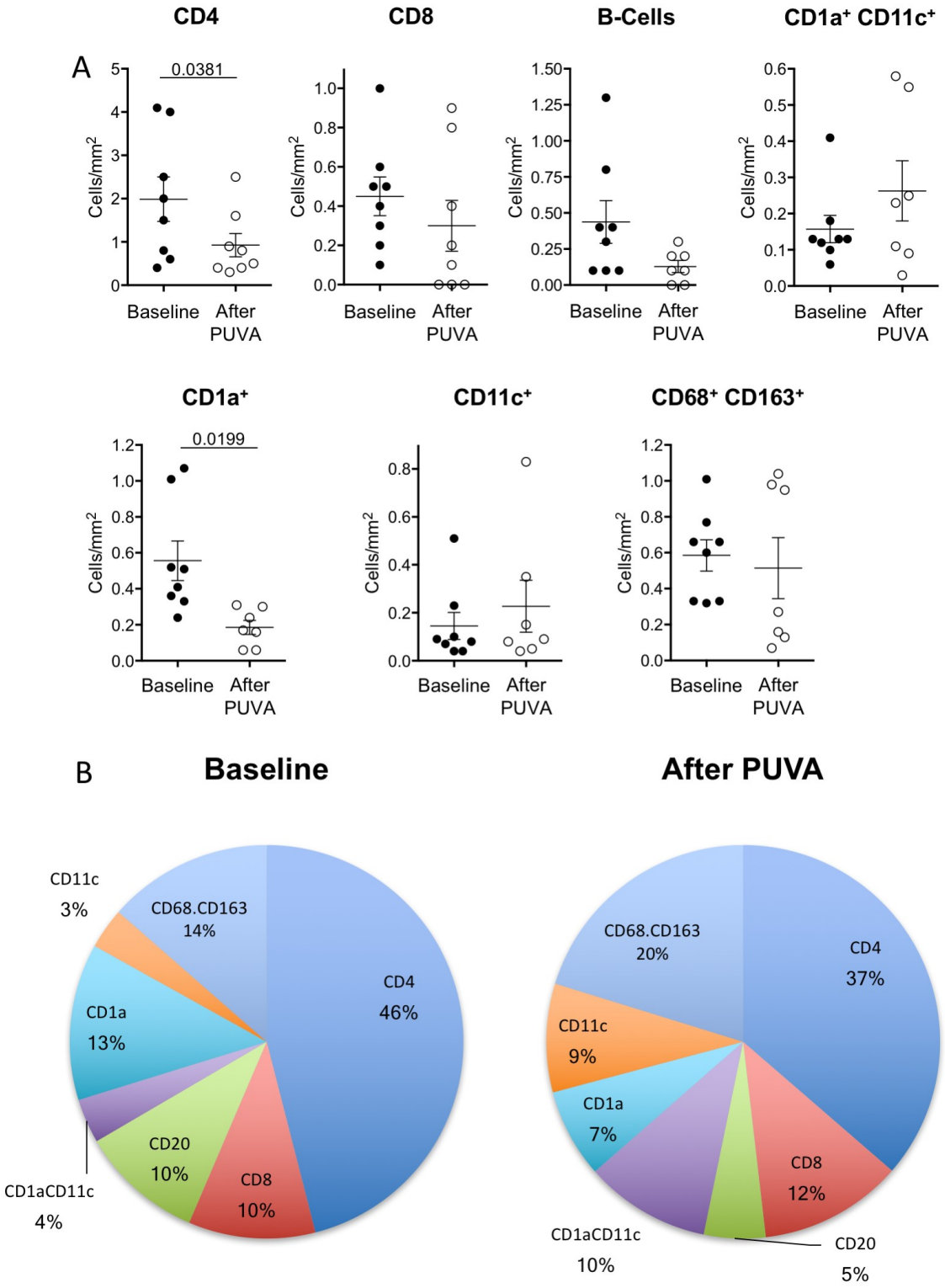

Figure 32: Quantitative analyses of cell infiltrate in lesional MF skin. A) Cell counts per mm^2 at baseline and after PUVA. Cells were phenotyped for CD4, CD8, CD20, CD1a, CD11c positivity and CD1a/CD11c or CD68/163 double positivity. **B)** Composition of infiltrating cell populations at baseline and after PUVA. Statistical significance was assessed by paired student t test.

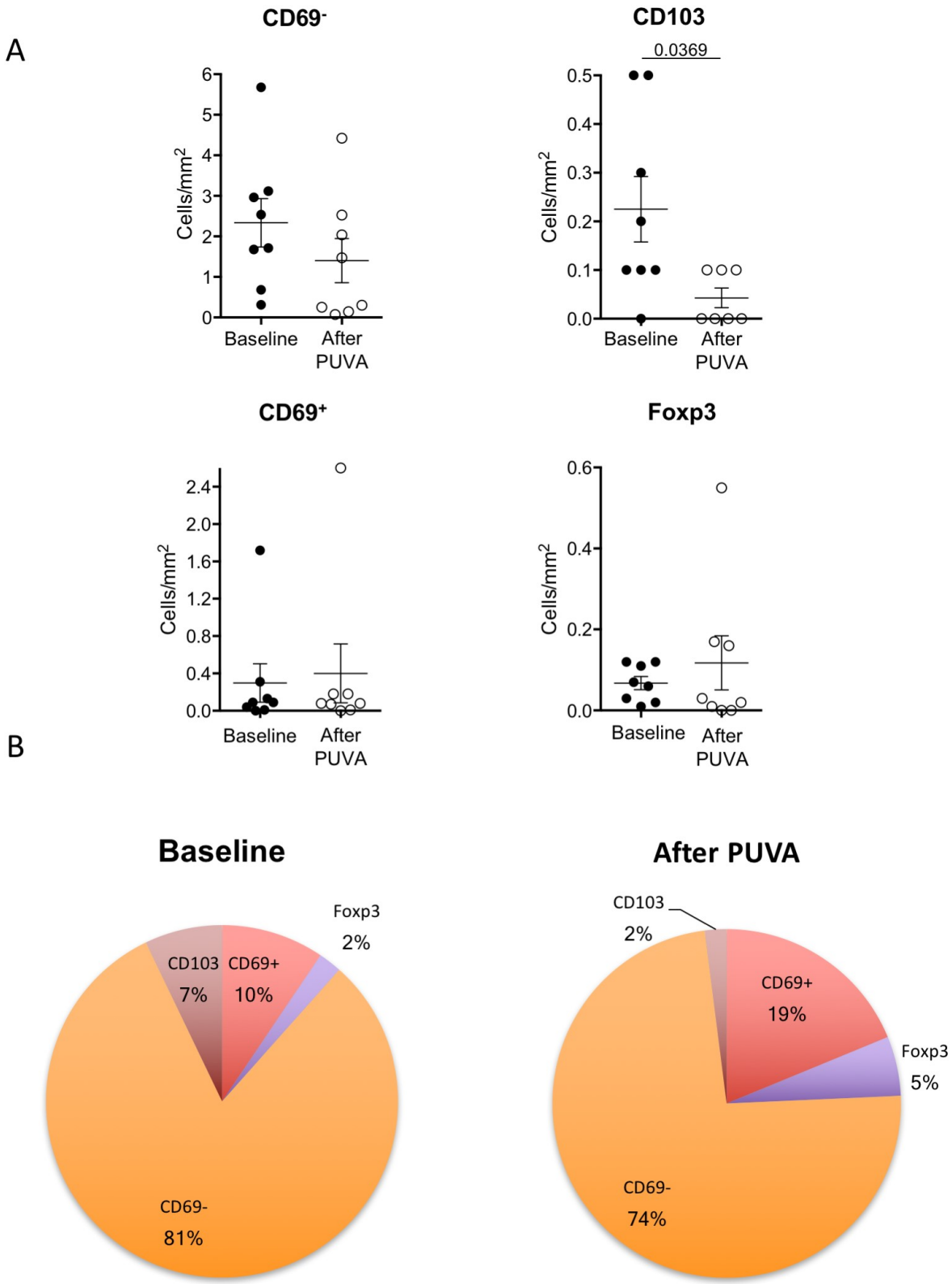

Figure 33: Quantitative analyses of T-cell subpopulations infiltrating lesional MF skin. A) Average cell counts per mm^2 at baseline and after PUVA is depicted for CD69 positive, CD69 negative, CD103 positive and Foxp3 positive cells. **B)** Composition of infiltrating T-cell sub-populations at baseline and after PUVA. Statistical significance was assessed by paired student t test.

Discussion

Recent advances in sequencing techniques and multiplex mRNA quantification have made the profound analyses of the imbalanced transcriptional landscape possible in a wide range of malignancies. Numerous reports on the genomic profile of MF and SS (Woollard et al., 2016, Ungewickell et al., 2015) coincide in the high heterogeneity of acquired mutations in these diseases, rising up the challenge of the discovery of genes to target in new therapies. However, alterations in p53, TNF family members and JAK/STAT signalling seem to be commonly shared among MF patients with a progressive malignant phenotype. Despite the advantage of having the genomic signature of malignant cells separated by cell sorting, as many of these studies do, the primary interest lays on alterations not only attributed to the neoplastic T-cells but their whole environment. This study aimed to have a better understanding of the pro-inflammatory microenvironment that the malignant clone is accompanied by; this has a particular relevance in the context of the alterations of basic functions of the skin, like losing skin barrier function that can lead to opportunistic infections (Mirvish et al., 2013). Alterations in p53 were not found in this analysis, most likely by the fact that the material analysed was total skin and the RNA of neoplastic cells was not predominant. However, the increase in TNF, TNFSF14 and TNFSF8 expression highlighted the relevance of TNF signalling. This result is also supported by previous findings (Cabal-Hierro and Lazo, 2012) which demonstrated recurrent activating mutations and genomic gains in TNFRSF1B leading to enhanced non canonical NFκB activation (Ungewickell et al., 2015). An up regulation of the NFκB mediator RelB (non-canonical) and RelA was found in MF patients (Fig. 2). Previous studies have linked CTSH with a metastatic phenotype in solid tumours (Nagai et al., 2003), consistent with the results here reported. CD154, a marker associated with chronic inflammation and autoimmune diseases, binds to CD40 and other integrins like αIIbβ3 and α5β1. After binding with the α5β1, Fas-mediated cell death is inhibited (Bachsais et al., 2016). This was particularly relevant to this study, since both CD154 and CD40 were up regulated in lesional skin. The search for common alterations in CTCL transcriptome has provided a small group of altered genes frequently seen in other lymphomas. MAPK, ERK, and

JAK/STAT activation have been recently described in MF (Woollard et al., 2016, Kiel et al., 2015), emphasising the role of pro-inflammatory signals fostering the malignant clones.

Various cytokines have been reported as important mediators of the pro-inflammatory microenvironment in MF. In this study, the cytokine panel showed an up regulation of TNF and the increased expression of IL-7R. This in context of previous findings of IL-7, as a proliferation-triggering factor in CTCL (Yamanaka et al., 2006b, Dalloul et al., 1992), suggests that targeting this cytokine might be a viable option for therapy to test in this disease.

The observed lower production of cytokines like IL-11, IL-4 and IL-15 in lesional skin compared to normal skin suggests that the microenvironment that keeps homeostasis (Hanel et al., 2013), builds on a diverse set of cytokines. It can be speculated that the malignant clones affect the microenvironment of the skin and in exchange, the secretion of cytokines like TNF is augmented.

LAG3, IDO and STAT5 as markers of T_{reg} cells were overexpressed in lesional skin. However, an up regulation of Foxp3 or IL-10 and TGF-β was not observed. Several studies have tried to assess the role of T_{reg} cells given that immune suppression is common in MF patients and may favour infections with opportunistic pathogens. Despite many efforts to uncover the role of T_{reg} cells in MF, the function of these cells in the context of this malignancy remains controversial. In a study looking at skin lesions of 44 MF patients, Foxp3 was only expressed by infiltrating benign lymphocytes and not malignant cells (Wada et al., 2010). Furthermore, another study showed that cells expressing Foxp3 also had a low expression of CD4, suggesting a phenotype of chronic effector T-cell activation rather than T-cells with regulatory function (Clark et al., 2011).

In this work STAT3 was found up regulated, supporting the notion of Th17 cell involvement in lesional skin contributing to the pro-inflammatory microenvironment. It has been shown that patients with progressive disease have a substantial increase of IL-17F secretion (Krejsgaard et al., 2013).

Although in this study IL-17 was not up regulated, the expression of IL-17r was increased, suggesting an important role of this cytokine in accordance with previous reports (Krejsgaard et al., 2013).

It has been shown that IL-9 is secreted in inflammatory skin diseases like psoriasis (Singh et al., 2013) (Schlapbach et al., 2014). More recently, the importance of this cytokine in infection models of *C. albicans* and other extracellular pathogens in the skin have been described (Schlapbach et al., 2014). IL-9 was expressed spontaneously in cells with an aberrant phenotype (Fig. 9), similarly to what is known in other malignancies like diffuse large B-cell lymphoma (Lv et al., 2013) and leukemia with HTLV-1 transformed T-cells (Kobayashi et al., 2012). IL-9's function as growth factor, angiogenesis promoter and anti-apoptotic mediator suggests a potential role of this cytokine in cell transformation and tumour development. Nevertheless, only MyLa2000 cells produced this cytokine while the other two cell lines tested did not. This may be inherited by the differential origin of the cells analysed (MF vs. SS) or may also indicate that SS cells produce this cytokine only after stimulation. This work did not elucidate the later condition in vitro but results from the serum of a SS patient indicated a considerable production of IL-9 with around 20pg/ml (data not shown).

By characterizing MyLa2000 cells, it was evident that these cells were positive for PU.1 and IRF4, two transcription factors strongly associated to IL-9 production. Controversially, PU.1 has been found as a tumour suppressor in B-cell lymphomas (Yuki et al., 2013) whereas IRF4 has been described as an oncogene under NFκB regulation in T-cell lymphomas (Boddicker et al., 2015). The phenotype found in cells from MF patients differed with regard of expression of PU.1 in MyLa2000 cells. In MF lesional skin, many PU.1 positive cells infiltrating the tissue were found. However, none of them were T-cells. In fact, PU.1 positive cells were CD1a positive (data not shown) suggesting a Langerhans phenotype. CD3 positive cells co-stained with IRF4, meaning that IL-9 was produced by the infiltrating T-cells, a finding that will be discussed further below.

The supernatant of MyLa2000 cells contained a substantial amount of IL-9, which triggered cell growth in other CTCL cell lines like SeAx and keratinocyte-originated HaCat cells (Fig. 10). Meanwhile, the stimulation with IL-9 increased proliferation of both SeAx and HaCat cells in a dose dependent manner (Fig. 11), highlighting the relevance of this cytokine in the amplification of visible inflammation in diseased skin. IL-9 increased the production of VEGF in keratinocytes (Wu et al., 2014) and activated the PI3K/Akt/mTOR signalling pathway on lymphoid cells (Kundu-Raychaudhuri et al., 2016). IL-9 blockade emphasized the role of this cytokine as a growth factor. The possibility of targeting this cytokine for therapeutic purpose is suggested as there are anti-IL-9 humanized antibodies in evaluation for treating inflammatory airway diseases like asthma (Antoniu, 2010).

The investigations carried out with MyLa2000 cells to test IL-9 targeting, showed how viable this strategy is. By using an anti-IL-9 antibody together with PUVA, an increase of cell death induction was found. These experiments had IFNα2b as standard adjuvant therapy, given its frequent use in patients with low response (Nikolaou et al., 2011) or low tolerance (Rupoli et al., 2005) to PUVA. A comparable response between IFNα2b and anti-IL-9 was found when cells were treated together with PUVA. Furthermore, anti-IL-9 treatment alone did not have a significant effect on cell viability (data not shown). This was perhaps due to exceeding production of IL-9, not matched by the limited availability of the antibody, which prompted us to use silencing RNA as different approach to block the signalling pathway of this cytokine both in vitro and in vivo (Fig. 14, 16).

The JAK1/2 inhibitor ruxolitinib reduced the production of IL-9 in MyLa2000 cells without a significant decrease in cell viability. Moreover, blockade of STAT3, STAT5 and IRF4 with siRNA further decreased IL-9 production, meaning that both the efferent and afferent branches of IL-9 signalling are good candidates for blocking the spontaneous production of this cytokine. It remains to be determined if any of the JAK/STAT activation mutations described for CTCL (da Silva Almeida et al., 2015, Wang et al., 2015) have been acquired by MyLa2000 cells.

The in vitro assay with EL-4 cells, suggested that IL-9 promotes proliferation mouse origin T-cells. Furthermore, the tumour mouse model had the key mycosis fungoides characteristic of being restricted only to the skin. It also offered a suitable time for tumour formation within two weeks with a relatively low number of injected tumour cells (10^4 cells). PUVA therapy was not powerful enough to entirely stop EL-4 cell growth but it had a systemic effect by inducing a higher percentage of T_{reg} cells in inguinal lymph nodes and spleen. This finding goes in line with previous observations in SS patients treated with ECP. After therapy, these patients had higher numbers of T_{reg} cells (Rao et al., 2009) with an augmented regulatory function, triggered by the conversion of ATP to adenosine by CD39 ectonucleotidase activity (Schmitt et al., 2009). Additionally, in a TGF-β transgenic mouse model of psoriasis in which animals treated with PUVA showed an increased number of skin tropic (CLA-positive) T_{reg} cells in lymph nodes (Singh et al., 2012).

This model was also useful to evaluate the role of IL-9 in tumour formation. In vivo depletion of IL-9 led to a slower tumour growth and higher number of T_{reg} cells in draining lymph nodes. A similar model with EL-4 cells has been validated in previous studies looking at the role of mast cells (Rabenhorst et al., 2012), tumour-associated macrophages with M2 phenotype (Wu et al., 2014), cytokine secretion and oncogenic pathways (Wu et al., 2011) in cutaneous lymphomas. Important to note, all of these investigations primarily focused on inflammatory mediators relevant in MF.

This work was developed in parallel to a clinical study, which offered the advantage to get freshly isolated biopsy material from MF patients. The follow up of these patients throughout treatment offered the means to analyse the therapeutic effect of PUVA with molecular biology methods. The usage of two different score systems to evaluate clinical status provided a clear readout of overall clinical response (mSWAT) and local marker lesions (CAILS). The HTS results showed a profound reduction of the total number of T-cells after therapy and allowed the identification of the malignant clones in every patient. The stratification of patients was done based on the relative individual proportion of

the malignant clone and its T-cell repertoire. Only few studies have looked at the tumour infiltrating lymphocytes with the major limitation that in patients with low number of neoplastic cells, the malignant clone is usually not detectable by current technology (Kirsch et al., 2015). Previous reports on a polyclonal response to super antigens of *S. aureus* showed that inflammatory mediators against *S. aureus* toxin fuels the rise of neoplastic clones, thus, spurring the debate on the pathophysiology of the disease at early stages (Willerslev-Olsen et al., 2013). With that in mind, a robust study is much needed to understand the role of benign T-cell infiltrate in MF. Moreover, this work is among the first studies that use sequencing data to conduct histological studies with antibodies that recognize the malignant clone, estimate the relative frequency of the neoplastic cell and visualize it in conjunction with other antibodies and scrutinize neoplastic cell production of inflammatory mediators like IL-9. This allowed the examination to attribute the high production of this cytokine to the malignant clone. However, it also showed that benign T-cells produced this cytokine, bringing support to the paradigm of an active benign population that feeds the malignant clone. A possible explanation of this is that malignant cells can reprogram benign T-cells in producing cytokines and other growth factors (Guenova et al., 2013). Nevertheless, the malignant cells had the distinct expression of IRF4, while only a handful of benign T-cells expressed this transcription factor. This is arguing on the distinct Th9 phenotype of the malignant cells and making IRF4 a possible marker of malignancy as seen in multiple myeloma. In this disease, IRF4 has an extensive network of targeted genes by a trans-activation of Myc (Shaffer et al., 2008).

Despite a significant reduction of the total TCR count as a measure of T-cell infiltration accompanied by clinical response to PUVA, a generalized pattern of predominance of the malignant clone over the rest of residual T cell population was observed (Fig. 24). This effect was accentuated in those patients with high burden of malignant cells. Nevertheless, both high and low burden patients had a substantial benign T-cell turnover and a low percentage of benign clones surviving after therapy (Fig. 26). This finding uncovers the underlying role of benign T-cell infiltration and brings up several questions: Are these patients cured? Is it necessary to kill all the malignant clones in order to get a sustained

response? Does malignant T-cell burden in clinical remission correlate with earlier relapse? The pragmatic point of view indicates that absolute depletion of the malignant clone is not necessary and many treatments like PUVA, ECP and immune modulatory therapy fall into a set of therapeutic alternatives that silence the disease while accomplishing a long lasting remission. PUVA may reach long-term disease free status in some patients after complete initial response (Herrmann et al., 1995b). ECP requires a long time of therapy to get the patient into remission, however, not enough evidence is available regarding the duration of clinical response (Geskin, 2007). The combination of immune modulatory regimes like IFNα and retinoids can achieve up to 6 years of remission in CTCL patients (Polansky et al., 2015). These data indicates that there are still many areas for improvement and studies like this one bring light into what can be expected from the therapies in current use and helps to understand their advantages and limitations. In fact, the data presented correlate benign T-cell turnover with clinical response (Fig. 26). PUVA offers the possibility to understand the general mechanism of anti CTCL treatments by elucidating the role of the cells that are depleted and those that repopulate the skin lesions. Early analyses showed that newly recruited cells have a high diversity (data not shown) and a lower degree of activation by lower expression of TCR signalling pathways like ZAP70, NFAT, LCK and SH2D1A (Fig. 28).

After therapy, changes in T-cell activation markers were not alone, MHC-II and B-cell and macrophage markers were down regulated, suggesting a decrease of non-T-cell infiltrate. Furthermore, many of the genes with high expression in diseased skin lost statistical significance after therapy and were normalized to levels as observed in healthy skin. Moreover, most genes down regulated in diseased skin compared to normal skin remained unchanged and only a few of them went back to normal levels after treatment (Fig. 28), suggesting that it is the exacerbated inflammation related to the genes up regulated in the untreated lesional skin that causes clinical signs of disease.

These findings opened a new avenue of research taking into account the role of immune cells other than T-cells in the onset of visible inflammation. A quantitative analyses regarding the kind of cells that infiltrate the skin in MF, an

estimation of the density and distribution of these cells and the fate of these cells after therapy were areas to address in this work. The significance of the analyses is that all these studies such as co-staining of the Vb22 segment of the T-cell receptor were done in situ, looking at the cells embedded in the microenvironment of the lesional skin. The ability to do immunofluorescence for several markers of inflammatory cells in sections of lesions had the advantage of looking at the spatial relations of cells to each other that provided more information rather than just looking at the absolute numbers.

As expected, CD4 positive cells were the most abundant cell type in lesional skin before and at much lower density after treatment. Cells intercalated in the infiltrate of lesional skin like CD8, CD20 (B-cells), CD1a and CD68/CD163 (macrophages) double positive cells were decreased (some of them significantly) after therapy compared to baseline. The majority of these cells were uniformly distributed in the dermis, although, many CD1a single positive cells allocated only in the epidermis (not unexpected since Langerhans cells harbour this marker) and its number was significantly reduced by PUVA.

The ratio of CD4 positive cells to macrophages was approximately 3.2:1 similar compared to the ratio of CD1a single positive cells to CD4 positive cells of 3.5:1 (Fig. 32). Importantly, the T-cell compartment only accounted for 46% of the total cellularity while the approximate other half was constituted by other inflammatory cell types. This may explain why the immune modulatory effect of PUVA plays an important role, by causing a reduction of the visible inflammation. This can be attributed also to the reduction of those cells not belonging to the T-cell compartment (Fig. 31). Previous reports explore this angle of infiltrating cells in CTCL, functioning as elements of tumour surveillance vs. tumour tolerance. M2 macrophages providing VEGF, CCL18 and IL-10 (Gunther et al., 2011, Wu et al., 2011), immature DC-SIGN+ DCs inducing tolerance (Schlapbach et al., 2010) (Ni and Duvic, 2011) and targeted B-cell have been proposed as means to re-establish immunologic tumour-control in early MF (Theurich et al., 2016). Additionally, in response to PUVA the T-cell composition of the infiltrate in MF skin was redistributed and a minor contraction of CD69 negative cells and an increase of Foxp3 cells and CD69

positive cells was observed in MF cases, findings going in line with previous reports of ECP in leukemic CTCL (Shiue et al., 2015). These results complemented the current discussion on the role of T_{RM} cells in CTCL. Although the expression of T_{RM} related markers was not observed directly in neoplastic T-cells, lesional skin had an abundance of T_{RM} when compared to normal tissue and the expression levels of ITGAE, CD96 and NFAT among others were reduced after therapy. These findings suggested that these cells are involved in the severity of MF, a question currently addressed by many research groups trying to identify players that may limit or contribute to this disease.

This work highlighted the role of the T-cell repertoire in the onset of early stage mycosis fungoides. Despite its limitations like the restricted number of patients analysed and an animal model in which the malignant clone used doesn't share all the characteristics of CTCL neoplastic cells it did show that that PUVA changes the composition of the infiltrating benign T-cells and that growth factors like IL-9 are produced by both benign and malignant T-cells.

Conclusions

We found a transcriptional signature of lesional skin in early stage MF enriched with expression of T-cell activation-related, antigen processing-presentation and JAK-STAT signalling genes. This signature was partially normalized after PUVA therapy.

MF patients had T-cells positive for IL-9, IL-9r, IRF4 and STAT3 in their skin lesions. By using HTS data the malignant clone was identified and IL-9 production was found to come from both malignant and benign T-cells. In vitro assays suggested a high expression of IL-9 driven by STAT3/5 and IRF4 activation.

Patients with both low and high burden of malignant cells responded well to PUVA as evident by a lower score of mSWAT and CAILS after treatment. Despite this, determination of the T-cell repertoire in the biopsies taken after PUVA from suspicious sites of residual MF showed that the malignant clone was still present in many cases and had the highest frequency in the T-cell infiltrate and clinical improvement correlated with benign T-cell turnover. After treatment, the total number of CD4 T-cells was reduced by 50%, a result confirmed by HTS and immunofluorescence. Langerhans cells (CD1a positive) and skin resident T-cells (CD103 positive) also had a substantial reduction in skin after therapy.

The EL-4 mouse model showed that PUVA triggered systemic immune suppression by induction of higher frequencies of T_{reg} cells, despite the fact, that the model failed to replicate in full the therapeutic effect of PUVA against tumour formation. IL-9 blockade in mice delayed tumour growth and increased the frequency of activated T-cells in spleen and lymph nodes, highlighting the role of IL-9 in tumour development.

Together, these results highlight the relevance of the inflammation that accompanies the growth of neoplastic T-cells in the tissue and suggest a close interaction between malignant T-cells and other immune cells in lesional skin

in MF. Benign T-cells may support the growth of malignant T-cells by feeding them with cytokines, chemokines and other inflammatory mediators. Interfering with those factors may pave the way for novel treatments.

Materials and methods

Patients

Human tissue samples from two sets of patients were available. Archived biopsies were tracked by computer-assisted search in the electronic patient documentation system of the Phototherapy Unit at the Department of Dermatology in the Medical University of Graz. Paraffin-embedded samples from eight patients with MF who had complete clinical and histological response to photo(chemo)therapy were identified. The patients had been treated with PUVA (n5) or 311-nm UVB (n3). The biopsies were taken before and after therapy in the period of 2002-2012. The second set of biopsies came from a clinical study (NCT01686594), where patients with MF clinical stage IA–IIB were treated in a standardized manner by oral PUVA (8-MOP, 10 mg per 20 kg of body weight; UVA 2x week). Biopsies were taken at baseline and after 12-16 weeks of therapy for histological analysis, high throughput TCR sequencing and nanostring. Normal lesion-adjacent skin samples were available from patients who had undergone surgery for skin lesions (i.e., melanocytic nevus or basal cell carcinoma) or cosmetic procedures. The ethics committee of the Medical University of Graz reviewed all procedures and gave their approval (protocols no. 25-294 ex 12/13; 24-169 ex 11/12; 21-080 ex 09/10; and 18-068 ex 06/07). This study was performed in compliance with the Declaration of Helsinki.

Cell lines

Cell lines derived from CTCL patients were used: MyLa2000 cells derived from a patient with MF, Hut78 and SeAx cells derived from patients with Sèzary syndrome were kindly provided by Professor Robert Gniadecki (Department of Dermatology, Bispebjerg Hospital, Copenhagen University, Denmark). MyLa2000 and SeAx cell lines were cultured in high glucose DMEM medium with 10% FBS, 50µM 2-mercaptoethanol and 50U/ml penicillin and 50µg/ml streptomycin. Hut78 cells were maintained in RPMI 1640 medium with 10% FBS, 2mM L-glutamine, 1mM sodium pyruvate, 10mM HEPES, 50U/ml penicillin and 50µg/ml streptomycin. HaCat cells were used for IL-9

supplementation experiments. The cells were cultivated in high glucose DMEM medium with 10% FBS, 50µM 2-mercaptoethanol and 50U/ml penicillin and 50µg/ml streptomycin.

For the animal lymphoma model the mouse T-cell lymphoma cell line EL-4 was used. EL-4 cells were purchased in ATCC and maintained in high glucose DMEM medium with 10% FBS, 50µM 2-mercaptoethanol and 50U/ml penicillin and 50µg/ml streptomycin.

Nanostring analysis

A robust gene expression analysis with nanostring technology was performed, using the PanCancer Immune Profiling Panel (Nanostring). The expression of 770 genes involved in immune responses and cancer driving genes together with 40 reference genes were examined. 100ng of RNA extracted from lesional skin (see methods below) was used after being checked on RNA quality by the bioanalyzer system (Agilent). The assay was performed by the molecular core facility of the Brigham and Woman's Hospital (Harvard Medical School, Boston, MA, USA). The results were analysed with the nCounter software (Nanostring) making a comparison between healthy skin, lesional skin at baseline and after PUVA therapy.

KEGG pathway analyses

The KEGG platform was used to analyse the biological interactions of the nanostring data. The fold change values of healthy skin compared to lesional biopsies were put into the KEGG algorithm to generate a graphical representation of enriched pathways in TCR and BCR signalling as well as cytokine-cytokine receptor interaction and signalling.

Enzyme linked immunoassay

The production of IL-9 by the cell lines MyLa2000 and Hut78 was quantified in the supernatant. The Human IL-9 ELISA kit (eBioscience, 88-7958-22) was used according to the manufacturer's instructions. The assay is a sandwich

version of a conventional ELISA with a capture antibody bound to the bottom of the wells. 50µl of sample to test and a HRP linked secondary antibody was used. After substrate addition, a spectrophotometer machine at an optical wavelength of 450 nm was used to quantify the colorimetric reaction.

Flow cytometry

0.25 - 0.5 x 10^6 cells were used to carry out flow cytometry analyses. To stain PU.1, MyLa2000 and Hut78 cell lines were fixed with Fixation/Permeabilization buffer (eBioscience, 00-5123) for 30 minutes. An isotype control antibody or an anti-IRF4-eFlour660 antibody (eBioscience, 50-9858-82) was added in permeabilization buffer (eBioscience, 00-8333) and incubated for 30 minutes. For analysis of mouse cells, lymph nodes were minced in PBS to make cell suspensions. Cells (0.5x10^6) were stained with an anti-CD3-BrilliantViolet421 (Biolegend, 100335), anti-CD4- PercP (eBioscience, 45-0042-82), anti-CD8-APC (Biolegend, 100711), anti-CD44-PE-eFlour610 (eBioscience, 61-0441), anti-CD62L-APC-Cy7 (Biolegend, 104428) and anti-CD25-Pe-Cy7 (eBioscience, 25-0251-82) antibody for 20 minutes. Intracellular staining of Foxp3 (eBioscience, 17-5773-82) was carried out as described above. All samples were examined in the FACS LSR-II (BD Biosciences) and analysed with FlowJo V9.3.2 (Tree Star).

Genetic material isolation and polymerase chain reaction

Total DNA and RNA were isolated from frozen material of lesional skin biopsies, healthy skin or cell suspensions using the AllPrep DNA/RNA Mini Kit (Qiagen 80204) in accordance with the manufacturer instructions. The samples were homogenized with the MagNa liser (Roche) and a column based DNA/RNA extraction was performed. The concentration of DNA/RNA obtained was quantified with a nanodrop (Thermo-Scientific). For cDNA synthesis, 0.5µg of RNA were used for reverse transcription (Applied Biosystems, 4368814). For quantitative expression analyses 5ng of cDNA were used to test for IL-9 (Forward 5'-CTCTGTTTGGGCATTCCCTCT-3', reverse 5'-GGGTATCTTGTTTGCATGGTGG-3') by qPCR with Power SYBR Green (Applied Biosystems, 4367659). Results were normalized by adjusting against

GAPDH with the ΔCt method to calculate relative expression. For in vitro silencing of STAT3/5 and IRF4, gene expression was quantified by purifying total RNA with RNeasy Mini Kit (Qiagen, 74104). 1µg of RNA was used to generate cDNA by RT-PCR (Applied Biosystems, 4368814) and TaqMan based qPCR was performed to test for IL-9 (Applied Biosystems, HS00914237-m1). IL-32 was used as control cytokine (Applied Biosystems,HS00992441-m1). Gene expression was normalized on the basis of GAPDH quantification (Applied Biosystems, HS02758991-g1). Relative units are reported.

Proliferation assay

Proliferation was determined by determined by measuring thymidine incorporation. 10^4 cells were seeded in supplemented RPMI medium and incubated for 48h. Thymidine was added 16h before harvesting and transferred the cells into 96-wells filtered plates (PerkinElmer, 6005174). As cells synthetize DNA, daughter cells are labelled with thymidine and non-incorporated thymidine flows through the membrane. The amount of ionizing radiation was measured with a scintillation counter (PerkinElmer, Wallac Oy 1450 Microbeta)

Supernatant supplementation

Cells were seeded with different ratios of supernatant from 96h-cultured MyLa2000 or Hut78. The ratios were 1:10, 3:10 5:10 supernatant:fresh medium without FBS and cells were incubated for 48h to measure proliferation.

In vitro IL-9 stimulation and inhibition

HaCat, Hut78 and SeAx cells were seeded in RPMI medium without FBS supplemented with increasing concentrations of recombinant human IL-9. For blocking experiments, the medium was supplemented with 100ng/ml of IL-9 and added anti IL-9 blocking antibody (R&D Systems, AB-209-NA) was added in increasing concentrations. After 48h of cell culture, proliferation was determined.

In vitro PUVA

MyLa2000 cells were treated with 1 mmol/l of 8-Methoxypsoralen (8-MOP) 2 hours before UVA irradiation. A sub-lethal dose of UVA light (0.4 or 0.8 J/cm^2) was given to the cells and which were then incubated in DMEM supplemented with 1,500 U/mL of IFNa2b (Merck-Millipore, GF417) and 20 mg/mL of goat polyclonal anti-human IL-9 antibody. For siRNA experiments, MyLa2000 cells were transfected with STAT5ab-siRNA or siCTRL and incubated for 24 hours before PUVA treatment. Forty-eight hours after UVA irradiation, the cells were stained with the apoptosis kit AnnexinV-FITC and PI (Beckman Coulter, PN-IM2375) and analysed by flow cytometry (Beckman Coulter, Cell-Lab-Quanta-SC-MPL).

In vitro JAK/STAT and IRF4 inhibition

MyLa2000 cells were treated with 180 nmol/L of the JAK1/2 inhibitor ruxolitinib (Selleck Chemicals, INCB018424), and cultured for up to 48h to test for IL-9 expression by qPCR with the TaqMan method described above.

MyLa2000 cells were transfected using the SMART pool ON-TARGETplus specific siRNA to STAT3, STAT5ab, or negative control siRNA (siCTRL; Thermo Scientific, L-003544-00-0005, L-005169-00- 000, and L-010539-00-0005; each at 0.041 nmol/10^6 cells), siRNA targeting IRF4 (Ambion, AM16708-145051), or siCTRL (Ambion, AM4611; 0.05 nmol/10^6 cells) with an Amaxa Nucleofector (Lonza). Silencing was confirmed by western blotting. Cells were lysed in a RIPA buffer (EDTA 1%). Protein quantification was done with a Pierce BCA Protein Assay kit (Thermo Scientific). A 4%–12% PAGE gel (Bio-Rad, 345-0125) was used to separate protein content and plotted on a 0.45-µm nitrocellulose membrane (Bio-Rad, 9004-70-0, 170-4071). Antibodies against IRF4 (Abcam, ab133590), STAT5, phospho-STAT5 (Y694), (Cell Signalling Technology; 9363 and 9356) or b-actin (Sigma, A5441) were used for labelling.

EL-4 lymphoma animal model

This model was based on previous publications (Wu et al., 2014) (Rabenhorst et al., 2012). C57BL/6 mice were purchased from Charles River (Boston, USA) and used to implant lymphoma cells. 6-8 weeks old female mice were used for

experiments. Animals were shaved on their backs and EL-4 cells were administered in a 100µl PBS solution ($1x10^5$ cell/ml) by intradermal injection. Mice were killed by cervical dislocation at the indicated time points or when tumour diameter exceeded 1cm. Tumours and draining lymph nodes were excised to carry out histological analyses and flow cytometry. All experimental animal procedures were done with the approval of the Federal Ministry of Science, Research and Economy of Austria (protocol number: BMWF-66.010/0022-II/3b/2013).

PUVA In vivo

Mice were treated with PUVA every 72h. After 24h of cell injection, the back of mice was treated with 60µl of 8-Methoxypsoralen 1% in oily vehicle. After 15 minutes to let the compound penetrate the skin, mice were irradiated with 1500 mJ/cm^2 of UVA, a dose below the minimal phototoxic dose (MPD). The MPD was determined in previous experiments by giving increasing doses of UVA and measuring skin swelling after 24 and 48h, being 2000 mJ/cm^2 the MPD established in two separate experiments.

Depletion of IL-9 in vivo

20µg of anti-IL-9 antibody (R&D Systems, ab-409-na) was administered 6 hours after tumour cell injection and subsequent doses were given every 48h for up to 2 weeks. A goat antibody was used as isotype control (R&D Systems, ab-108-c). Tumour growth was monitored daily by measuring lesion diameter in two opposite axes with a vernier calliper (Mitutoyo).

mSWAT and CAILS clinical assessment

The extent of skin involvement was assessed by the modified Severity Weighted Assessment Tool (mSWAT). This score is based on a system of 12 areas of the body and rates the involved body surface area adjusted by a weight factor (patch=1, plaque=2 and tumour=4). It is expressed as the sum of the total as shown in M&M table 1. Additionally, the Composite Assessment of Index Lesion Severity score (CAILS), takes into account erythema scaling, plaque

elevation, pigmentation and lesion size in a scale of 0-8 as shown in M&M table 2 was used to monitor marker lesions.

Materials & methods table 1: Modified Severity Weighted Assessment Tool

Body Region	% BSA in Body Region	Assessment of Involvement in Patient's Skin		
		Patch*	Plaque†	Tumor‡
Head	7			
Neck	2			
Anterior trunk	13			
Arms	8			
Forearms	6			
Hands	5			
Posterior trunk	13			
Buttocks	5			
Thighs	19			
Legs	14			
Feet	7			
Groin	1			
Subtotal of lesion BSA				
Weighting factor		×1	×2	×4
Subtotal lesion BSA × weighting factor				

NOTE. mSWAT score equals summation of each column line.
Abbreviations: BSA, body surface area; mSWAT, modified Severity Weighted Assessment Tool.
*Any size lesion without induration or significant elevation above the surrounding uninvolved skin; poikiloderma may be present.
†Any size lesion that is elevated or indurated; crusting, ulceration, or poikiloderma may be present.
‡Any solid or nodular lesion ≥ 1 cm in diameter with evidence of deep infiltration in the skin and/or vertical growth.

Taken from Olsen et al (Olsen et al., 2011)

Materials & methods table 2: Composite Assessment of Index Lesion Severity

Clinical Sign and Degree or Size (scale of 0-8)	Index Lesion				
	1	2	3	4	5
Erythema					
Scaling					
Plaque elevation					
Hypo- or hyperpigmentation					
Lesion size*					
Subtotal					
Total (sum of subtotals)					

NOTE. Cannot be used as skin assessment in global response score. Suggestions for improvement include using actual size of lesion versus categorical score for size and eliminating pigmentation as a clinical parameter.
*Lesion size (cm^2): 0: no measurable area; 1: > 0 to ≤ 4; 2: > 4 to ≤ 10; 3: > 10 to ≤ 16; 4: > 16 to ≤ 25; 5: > 25 to ≤ 35; 6: > 35 to ≤ 45; 7: > 45 to ≤ 55; 8: > 55 to ≤ 70; 9: > 70 to ≤ 90; 10: > 90 to ≤ 110; 11: > 110 to ≤ 130; 12: > 130 to ≤ 155; 13: > 155 to ≤ 180; 14: > 180 to ≤ 210; 15: > 210 to ≤ 240; 16: > 240 to ≤ 270; 17: > 270 to ≤ 300; 18: > 300.

Taken from Olsen et al (Olsen et al., 2011)

High throughput TCR sequencing

Sequencing of the beta chain of the TCR was performed using 400ng of DNA isolated from lesional skin. Amplicon libraries of 80-120 bp were generated with a set of primers on the variable (V) and joint (J) segments flanking the CDR3 region. The sequencing was carried out on the ImmunoSEQ platform (Adaptive Biotechnologies) with an approximate coverage of 20x. Sets of clustering algorithms were used to correct sequencing errors and amplicon alignment. Sequence reads were annotated in accordance to the ImmunoGeneTics collaboration to assemble the contributing V, D and J segments to every rearranged functional TCR (Ruiz et al., 2000).

Materials & methods table 3: Clinical examination and identification of malignant clones

Patient No.	Diagnosis (EORTC-ISCL classification)	Type of skin lesion biopsied	Type of treatment	mSWAT		CAILS		Clone found
				Basleine	After PUVA	Basleine	After PUVA	
P1	Ia	Patch	PUVA	8.6	2.1	12	3	TCRBV24
P2	Ib	Patch	PUVA	35.5	3.2	8	4	TCRBV20
P3	Ia	Patch	PUVA	15	5	11	4	TCRBV06
P4	Ia	Patch	PUVA	8.25	0	5	0	TCRBV10-03*01
P5	Ib	Patch	PUVA	13	2	13	2	TCRBV12
P6	Ib	Patch	PUVA	47.5	0	4	1	TCRBV02-01*01
P7	Ia	Patch	PUVA	10	0	5	0	TCRBV02-01*01
P8	Ia	Patch	PUVA	20	0	7	0	TCRBV05-06*01

Patients from the clinical PUVA trial (ClinicalTrials.gov no. NCT01686594) were treated with oral 8-MOP (10mg per 20kg of body weight) and UVA (PUVA) two times per week. The patients were started on treatment with 50% of the minimal phototoxic dose (MPD) and UVA dose was increased thereafter by 0-30% per week, depending on the individual preceding erythema response.

Histological examinations

Tissue sections of 3µm thickness from mouse or human FFPE blocks were used. For histological assessment, haematoxylin and eosin stainings were done. Sections from mouse skin having tumours were evaluated in 5 different fields per sample to determine the effect of PUVA. Image analyses were done to quantify tumour infiltration and epidermal alterations.

For human samples, FFPE sections were rehydrated by immersing them in xylene and increasing dilutions of ethanol. Antigen retrieval was performed in TRIS-EDTA buffer at pH 9 (Dako, S2367) or citrate buffer at pH 6 according to the particular antibody used. The following antibodies were used for chromogen stainings: IL-9 (Abcam, ab134434), IL-9r (Abcam, ab61196), IRF4 (Abcam, ab124691), STAT3 (Abcam, ab50761-100), CD3 (Novocastra, NCL-CD3-PS1) and PU.1 (Abcam, ab76543). The Peroxidase/AEC, rabbit/mouse REAL detection system (Dako, K5003) was used for detection in single stains. Briefly described: After overnight incubation with the primary antibody, the slides were covered with a secondary antibody for 10 minutes, followed by streptavidin-HRP binding incubation for 10 minutes, and addition of AEC/H2O2 substrate. Nuclei were counterstained with haematoxylin and cell quantification was performed by imaging with the 40x objective. Positive cells were counted in three different view fields and the mean number of cells per square millimetre

was calculated. Double stainings were prepared with the MultiVision polymer detection system (Thermo Scientific, TL-012-MARH). Two primary antibodies were added (one raised in rabbit and the other in mouse) and incubated overnight. Ultra V block solution was applied for 10 minutes followed by the MultiVision polymer cocktail (anti-rabbit/HRP and anti-mouse/AP) for 30 minutes. Then, LVBlue chromogen (reacting with anti-mouse/AP immunoglobulins) was added for 10 minutes, followed by the LVRed chromogen (reacting with anti-rabbit/HRP immunoglobulins) for 10 minutes. Four washes with TBS-Tween 20 (0.5%) were done in between every step. For visualization of the malignant clone, the TCR sequencing data was used to select the anti-TCRVb22 antibody (Beckman Coulter, IM1484) to co-stain with IL-9 and IRF4 by the MultiVision stain system. For immunofluorescence imaging, the Opal 6c kit (PerkinElmer, NEL796001KT) was used. After antigen retrieval the slides were covered with a primary antibody, incubated for 1h at 4ºC. The slides were incubated with a biotinylated secondary antibody and then with a streptavidin-HRP linked (Dako, Advance HRP K4069) for 10 minutes each. Then, the fluorescent opal dye was added and incubated for 10 minutes. This kit uses tyramide-HRP interactions to activate the fluorescence of the compound and amplify the signal. In order to use a second, third, etc. antibody, the slides were put in citrate buffer and heated at 70ºC in a steam cooker for 15 minutes. These steps destabilized the antigen-antibody interaction and caused the separation of the reaction complex. However, the florescent dye remained fixed to the surface of the slide. A second primary antibody was added and the same set of steps as previously described was followed to get fluorescent signals of each antibody at different wavelengths. The advantage of this technique over conventional immunofluorescence is the high degree of specific signal amplification, the possibility of usage of antibodies with different specificity on the same panel, regardless of species origin and the narrow spectrum of fluorescence emission by the synthetic opal compounds. The last step was the addition of the nuclear dye DAPI in the mount medium before imaging.

Materials & methods table 4: Set of samples from archived materials

Patient No.	Sex	Age (y) baseline biopsy	Diagnosis (EORTC-ISCL classification)	Type of skin lesion biopsied	**IHC** CD3/IL-9 (0-4)	**IHC** STAT3 (0-4)	**IHC** CD3/IRF4 (0-4)	**IHC** CD3/PU1 (0-4)	Type of treatment	Length of treatment (weeks)	Response
A1	M	95	Ib	Patch	DP, 2	3	DP 1	SP 3,2	311nm UVB	12	CR
A2	M	75	Ib	Patch	DP, 1	3	0	SP 3,2	PUVA, Bexarotene	18	CR
A3	M	60	Ib	Patch	DP, 2	3	DP, 2	SP 4,4	311nm UVB	2	CR
A4	M	47	Ib	Patch	DP, 3	2	DP, 2	SP 4,3	PUVA	48	CR
A5	M	90	III	Tumor	0	2	DP, 1	SP 4,2	PUVA, steroids	6	CR
A6	M	71	Ia	Patch	0	1	0	0	PUVA	45	CR
A7	M	69	Ia	Patch	DP, 1	3	DP, 1	SP 3,2	311nm UVB	6	CR
A8	F	59	Ia	Patch	DP, 1	1	0	SP 1,0	PUVA	6	CR

Patients were treated under daily life conditions with standard 311nm UVB phototherapy or photochemotherapy with 8- or 5-methoxypsoralen. Additional treatment with bexarotene or steroids was given as depicted. Single or double stains immunohistochemistry (IHC) were performed as indicated. The preparations were evaluated as containing single positive (SP) or double positive (DP) cells (mainly in the dermis) at baseline by a 0-4 score system of positivity with **0,** <10%; **1**, 10-25%; **2**, 25-50%; **3**, 50-75%; and **4**, 75-100%. No clinical signs of skin lesions and lack of infiltrate in histological examination were considered as complete response (CR).

Fluorescence imaging and analyses

The Mantra Quantitative Pathology Workstation (PerkinElmer) and the inForm software analysis tool (PerkinElmer) were used to analyse fluorescence preparations. The microscope was calibrated for panels of 5 fluorescent dyes as described in M&M table 5. A minimum of 3 different fields per slide (20x objective) was captured with a ratio of 90/10% of dermis/epidermis. The cellularity of each image was determined by the number of DAPI stained nuclei and a trained algorithm was used with a minimum of 150 user-curated positive cells for each phenotype based on the expression of each marker. The average number of cells positive for the respective marker in all samples was calculated for all samples.

Materials & methods table 5: Panels of antibodies used for multicolour immunofluorescence

Adaptive immune cells		
Antigen	Manufacturer	Catalog number
CD4	Novus Biologicals	NBP1-19371
CD8	Novus Biologicals	NBP2-29475
CD20	Santa Cruz	sc-58985
CD103	Novocastra	PA0374
Innate immune cells		
CD68	Dako	M0876
CD163	Acris	BM4041
CD1a	Acris	DB 071-0.1
CD11c	Abcam	Ab52632
T-cell subset panel		
CD4	Novus Biologicals	NBP1-19371
CD8	Novus Biologicals	NBP2-29475
CD69	Sigma	HPA050525
Foxp3	Abcam	Ab20034

Statistics

The data was analysed in two steps; first testing for normal distribution with Shapiro test on SPSS 22 (IBM) and based on these results, the most appropriate post-test analyses was chosen for each experiment as indicated in the figure legend. Charts were generated with GraphPad Prism 6 (GraphPad).

References

ABDALLAT, S. A., ALQAQAA, A. S., OBAIDAT, N. A. & ALNUEIMI, R. F. 2014. Efficacy and Side Effects of Narrowband-UVB in Early Stage Cutaneous T-Cell Lymphoma in Jordanian Patients. *ISRN Dermatol,* 2014**,** 951821.

AGAR, N. S., WEDGEWORTH, E., CRICHTON, S., MITCHELL, T. J., COX, M., FERREIRA, S., ROBSON, A., CALONJE, E., STEFANATO, C. M., WAIN, E. M., WILKINS, B., FIELDS, P. A., DEAN, A., WEBB, K., SCARISBRICK, J., MORRIS, S. & WHITTAKER, S. J. 2010. Survival outcomes and prognostic factors in mycosis fungoides/Sezary syndrome: validation of the revised International Society for Cutaneous Lymphomas/European Organisation for Research and Treatment of Cancer staging proposal. *J Clin Oncol,* 28**,** 4730-9.

AL HOTHALI, G. I. 2013. Review of the treatment of mycosis fungoides and Sezary syndrome: A stage-based approach. *Int J Health Sci (Qassim),* 7**,** 220-39.

ANTONIU, S. A. 2010. MEDI-528, an anti-IL-9 humanized antibody for the treatment of asthma. *Curr Opin Mol Ther,* 12**,** 233-9.

ARSTILA, T. P., CASROUGE, A., BARON, V., EVEN, J., KANELLOPOULOS, J. & KOURILSKY, P. 1999. A direct estimate of the human alphabeta T cell receptor diversity. *Science,* 286**,** 958-61.

ARULOGUN, S. O., PRINCE, H. M., NG, J., LADE, S., RYAN, G. F., BLEWITT, O. & MCCORMACK, C. 2008. Long-term outcomes of patients with advanced-stage cutaneous T-cell lymphoma and large cell transformation. *Blood,* 112**,** 3082-7.

AUBRY, F., SATIE, A. P., RIOUX-LECLERCQ, N., RAJPERT-DE MEYTS, E., SPAGNOLI, G. C., CHOMEZ, P., DE BACKER, O., JEGOU, B. & SAMSON, M. 2001. MAGE-A4, a germ cell specific marker, is expressed differentially in testicular tumors. *Cancer,* 92**,** 2778-85.

BACHSAIS, M., NADDAF, N., YACOUB, D., SALTI, S., ALAAEDDINE, N., AOUDJIT, F., HASSAN, G. S. & MOURAD, W. 2016. The Interaction of CD154 with the alpha5beta1 Integrin Inhibits Fas-Induced T Cell Death. *PLoS One,* 11**,** e0158987.

BATISTA, D. A., VONDERHEID, E. C., HAWKINS, A., MORSBERGER, L., LONG, P., MURPHY, K. M. & GRIFFIN, C. A. 2006. Multicolor fluorescence in situ hybridization (SKY) in mycosis fungoides and Sezary syndrome: search for recurrent chromosome abnormalities. *Genes Chromosomes Cancer,* 45**,** 383-91.

BERGER, C. L., HANLON, D., KANADA, D., DHODAPKAR, M., LOMBILLO, V., WANG, N., CHRISTENSEN, I., HOWE, G., CROUCH, J., EL-FISHAWY, P. & EDELSON, R. 2002. The growth of cutaneous T-cell lymphoma is stimulated by immature dendritic cells. *Blood,* 99**,** 2929-39.

BERGER, C. L., TIGELAAR, R., COHEN, J., MARIWALLA, K., TRINH, J., WANG, N. & EDELSON, R. L. 2005. Cutaneous T-cell lymphoma: malignant proliferation of T-regulatory cells. *Blood,* 105**,** 1640-7.

BLUME-PEYTAVI, U. & VOGT, A. 2015. Translational Positioning of Janus Kinase (JAK) Inhibitors in Alopecia Areata. *EBioMedicine,* 2**,** 282-3.

BODDICKER, R. L., KIP, N. S., XING, X., ZENG, Y., YANG, Z. Z., LEE, J. H., ALMADA, L. L., ELSAWA, S. F., KNUDSON, R. A., LAW, M. E.,

KETTERLING, R. P., CUNNINGHAM, J. M., WU, Y., MAURER, M. J., O'BYRNE, M. M., CERHAN, J. R., SLAGER, S. L., LINK, B. K., PORCHER, J. C., GROTE, D. M., JELINEK, D. F., DOGAN, A., ANSELL, S. M., FERNANDEZ-ZAPICO, M. E. & FELDMAN, A. L. 2015. The oncogenic transcription factor IRF4 is regulated by a novel CD30/NF-kappaB positive feedback loop in peripheral T-cell lymphoma. *Blood,* 125**,** 3118-27.

BRADFORD, P. T., DEVESA, S. S., ANDERSON, W. F. & TORO, J. R. 2009. Cutaneous lymphoma incidence patterns in the United States: a population-based study of 3884 cases. *Blood,* 113**,** 5064-73.

CABAL-HIERRO, L. & LAZO, P. S. 2012. Signal transduction by tumor necrosis factor receptors. *Cell Signal,* 24**,** 1297-305.

CAMPBELL, J. J., CLARK, R. A., WATANABE, R. & KUPPER, T. S. 2010. Sezary syndrome and mycosis fungoides arise from distinct T-cell subsets: a biologic rationale for their distinct clinical behaviors. *Blood,* 116**,** 767-71.

CAMPO, E., SWERDLOW, S. H., HARRIS, N. L., PILERI, S., STEIN, H. & JAFFE, E. S. 2011. The 2008 WHO classification of lymphoid neoplasms and beyond: evolving concepts and practical applications. *Blood,* 117**,** 5019-32.

CAPRINI, E., CRISTOFOLETTI, C., ARCELLI, D., FADDA, P., CITTERICH, M. H., SAMPOGNA, F., MAGRELLI, A., CENSI, F., TORRERI, P., FRONTANI, M., SCALA, E., PICCHIO, M. C., TEMPERANI, P., MONOPOLI, A., LOMBARDO, G. A., TARUSCIO, D., NARDUCCI, M. G. & RUSSO, G. 2009. Identification of key regions and genes important in the pathogenesis of sezary syndrome by combining genomic and expression microarrays. *Cancer Res,* 69**,** 8438-46.

CEDENO-LAURENT, F., SINGER, E. M., WYSOCKA, M., BENOIT, B. M., VITTORIO, C. C., KIM, E. J., YOSIPOVITCH, G. & ROOK, A. H. 2015. Improved pruritus correlates with lower levels of IL-31 in CTCL patients under different therapeutic modalities. *Clin Immunol,* 158**,** 1-7.

CELERIER, P., BUREAU, B., LITOUX, P. & DRENO, B. 1997. Keratinocyte-lymphocyte interaction in cutaneous T-cell lymphoma. Modulation of keratinocyte antigen My7 by a soluble factor produced by T lymphocytes. *Arch Dermatol,* 133**,** 837-40.

CHEN, N. & WANG, X. 2014. Role of IL-9 and STATs in hematological malignancies (Review). *Oncol Lett,* 7**,** 602-610.

CLARK, R. A., CHONG, B., MIRCHANDANI, N., BRINSTER, N. K., YAMANAKA, K., DOWGIERT, R. K. & KUPPER, T. S. 2006. The vast majority of CLA+ T cells are resident in normal skin. *J Immunol,* 176**,** 4431-9.

CLARK, R. A., SHACKELTON, J. B., WATANABE, R., CALARESE, A., YAMANAKA, K., CAMPBELL, J. J., TEAGUE, J. E., KUO, H. P., HIJNEN, D. & KUPPER, T. S. 2011. High-scatter T cells: a reliable biomarker for malignant T cells in cutaneous T-cell lymphoma. *Blood,* 117**,** 1966-76.

CLARK, R. A., WATANABE, R., TEAGUE, J. E., SCHLAPBACH, C., TAWA, M. C., ADAMS, N., DOROSARIO, A. A., CHANEY, K. S., CUTLER, C. S., LEBOEUF, N. R., CARTER, J. B., FISHER, D. C. & KUPPER, T. S. 2012. Skin effector memory T cells do not recirculate and provide

immune protection in alemtuzumab-treated CTCL patients. *Sci Transl Med,* 4**,** 117ra7.
CRISCIONE, V. D. & WEINSTOCK, M. A. 2007. Incidence of cutaneous T-cell lymphoma in the United States, 1973-2002. *Arch Dermatol,* 143**,** 854-9.
DA SILVA ALMEIDA, A. C., ABATE, F., KHIABANIAN, H., MARTINEZ-ESCALA, E., GUITART, J., TENSEN, C. P., VERMEER, M. H., RABADAN, R., FERRANDO, A. & PALOMERO, T. 2015. The mutational landscape of cutaneous T cell lymphoma and Sezary syndrome. *Nat Genet,* 47**,** 1465-70.
DALIANI, D., ULMER, R. A., JACKOW, C., PUGH, W., GANSBACHER, B., CABANILLAS, F., DUVIC, M. & SARRIS, A. H. 1998. Tumor necrosis factor-alpha and interferon-gamma, but not HTLV-I tax, are likely factors in the epidermotropism of cutaneous T-cell lymphoma via induction of interferon-inducible protein-10. *Leuk Lymphoma,* 29**,** 315-28.
DALLOUL, A., LAROCHE, L., BAGOT, M., MOSSALAYI, M. D., FOURCADE, C., THACKER, D. J., HOGGE, D. E., MERLE-BERAL, H., DEBRE, P. & SCHMITT, C. 1992. Interleukin-7 is a growth factor for Sezary lymphoma cells. *J Clin Invest,* 90**,** 1054-60.
DAVE, S. S., WRIGHT, G., TAN, B., ROSENWALD, A., GASCOYNE, R. D., CHAN, W. C., FISHER, R. I., BRAZIEL, R. M., RIMSZA, L. M., GROGAN, T. M., MILLER, T. P., LEBLANC, M., GREINER, T. C., WEISENBURGER, D. D., LYNCH, J. C., VOSE, J., ARMITAGE, J. O., SMELAND, E. B., KVALOY, S., HOLTE, H., DELABIE, J., CONNORS, J. M., LANSDORP, P. M., OUYANG, Q., LISTER, T. A., DAVIES, A. J., NORTON, A. J., MULLER-HERMELINK, H. K., OTT, G., CAMPO, E., MONTSERRAT, E., WILSON, W. H., JAFFE, E. S., SIMON, R., YANG, L., POWELL, J., ZHAO, H., GOLDSCHMIDT, N., CHIORAZZI, M. & STAUDT, L. M. 2004. Prediction of survival in follicular lymphoma based on molecular features of tumor-infiltrating immune cells. *N Engl J Med,* 351**,** 2159-69.
DEREURE, O., LEVI, E., VONDERHEID, E. C. & KADIN, M. E. 2002. Infrequent Fas mutations but no Bax or p53 mutations in early mycosis fungoides: a possible mechanism for the accumulation of malignant T lymphocytes in the skin. *J Invest Dermatol,* 118**,** 949-56.
DIAMANDIDOU, E., COLOME, M., FAYAD, L., DUVIC, M. & KURZROCK, R. 1999. Prognostic factor analysis in mycosis fungoides/Sezary syndrome. *J Am Acad Dermatol,* 40**,** 914-24.
DOBBELING, U., DUMMER, R., LAINE, E., POTOCZNA, N., QIN, J. Z. & BURG, G. 1998. Interleukin-15 is an autocrine/paracrine viability factor for cutaneous T-cell lymphoma cells. *Blood,* 92**,** 252-8.
DULMAGE, B. O. & GESKIN, L. J. 2013. Lessons learned from gene expression profiling of cutaneous T-cell lymphoma. *Br J Dermatol,* 169**,** 1188-97.
DUVIC, M., PINTER-BROWN, L. C., FOSS, F. M., SOKOL, L., JORGENSEN, J. L., CHALLAGUNDLA, P., DWYER, K. M., ZHANG, X., KURMAN, M. R., BALLERINI, R., LIU, L. & KIM, Y. H. 2015a. Phase 1/2 study of mogamulizumab, a defucosylated anti-CCR4 antibody, in previously treated patients with cutaneous T-cell lymphoma. *Blood,* 125**,** 1883-9.
DUVIC, M., TETZLAFF, M. T., GANGAR, P., CLOS, A. L., SUI, D. & TALPUR, R. 2015b. Results of a Phase II Trial of Brentuximab Vedotin for CD30+

Cutaneous T-Cell Lymphoma and Lymphomatoid Papulosis. *J Clin Oncol,* 33**,** 3759-65.
EDER, J., KERN, A., MOSER, J., KITZWOGERER, M., SEDIVY, R. & TRAUTINGER, F. 2015. Frequency of primary cutaneous lymphoma variants in Austria: retrospective data from a dermatology referral centre between 2006 and 2013. *J Eur Acad Dermatol Venereol,* 29**,** 1517-23.
EHRENTRAUT, S., SCHNEIDER, B., NAGEL, S., POMMERENKE, C., QUENTMEIER, H., GEFFERS, R., FEIST, M., KAUFMANN, M., MEYER, C., KADIN, M. E., DREXLER, H. G. & MACLEOD, R. A. 2016. Th17 cytokine differentiation and loss of plasticity after SOCS1 inactivation in a cutaneous T-cell lymphoma. *Oncotarget,* 7**,** 34201-16.
FIVENSON, D. P., HANSON, C. A. & NICKOLOFF, B. J. 1994. Localization of clonal T cells to the epidermis in cutaneous T-cell lymphoma. *J Am Acad Dermatol,* 31**,** 717-23.
FREDHOLM, S., LITVINOV, I. V., MONGAN, N. P., SCHIELE, S., WILLERSLEV-OLSEN, A., PETERSEN, D. L., KREJSGAARD, T., SIBBESEN, N., NASTASI, C., BONEFELD, C. M., PERSSON, J. L., STRATEN, P. T., ANDERSEN, M. H., KORALOV, S. B., WASIK, M. M., GEISLER, C., SASSEVILLE, D., WOETMANN, A. & ODUM, N. 2016. The Expression of IL-21 Is Promoted by MEKK4 in Malignant T Cells and Associated with Increased Progression Risk in Cutaneous T-Cell Lymphoma. *J Invest Dermatol,* 136**,** 866-9.
FRENCH, L. E., HUARD, B., WYSOCKA, M., SHANE, R., CONTASSOT, E., ARRIGHI, J. F., PIGUET, V., CALDERARA, S. & ROOK, A. H. 2005. Impaired CD40L signaling is a cause of defective IL-12 and TNF-alpha production in Sezary syndrome: circumvention by hexameric soluble CD40L. *Blood,* 105**,** 219-25.
FROST, E. L., KERSH, A. E., EVAVOLD, B. D. & LUKACHER, A. E. 2015. Cutting Edge: Resident Memory CD8 T Cells Express High-Affinity TCRs. *J Immunol,* 195**,** 3520-4.
GESKIN, L. 2007. ECP versus PUVA for the treatment of cutaneous T-cell lymphoma. *Skin Therapy Lett,* 12**,** 1-4.
GESKIN, L. J., VIRAGOVA, S., STOLZ, D. B. & FUSCHIOTTI, P. 2015. Interleukin-13 is overexpressed in cutaneous T-cell lymphoma cells and regulates their proliferation. *Blood,* 125**,** 2798-805.
GIRARDI, M., HEALD, P. W. & WILSON, L. D. 2004. The pathogenesis of mycosis fungoides. *N Engl J Med,* 350**,** 1978-88.
GUENOVA, E., WATANABE, R., TEAGUE, J. E., DESIMONE, J. A., JIANG, Y., DOWLATSHAHI, M., SCHLAPBACH, C., SCHAEKEL, K., ROOK, A. H., TAWA, M., FISHER, D. C., KUPPER, T. S. & CLARK, R. A. 2013. TH2 cytokines from malignant cells suppress TH1 responses and enforce a global TH2 bias in leukemic cutaneous T-cell lymphoma. *Clin Cancer Res,* 19**,** 3755-63.
GUNTHER, C., ZIMMERMANN, N., BERNDT, N., GROSSER, M., STEIN, A., KOCH, A. & MEURER, M. 2011. Up-regulation of the chemokine CCL18 by macrophages is a potential immunomodulatory pathway in cutaneous T-cell lymphoma. *Am J Pathol,* 179**,** 1434-42.
HANAHAN, D. & WEINBERG, R. A. 2011. Hallmarks of cancer: the next generation. *Cell,* 144**,** 646-74.

HANEL, K. H., CORNELISSEN, C., LUSCHER, B. & BARON, J. M. 2013. Cytokines and the skin barrier. *Int J Mol Sci,* 14**,** 6720-45.
HERRMANN, J. J., ROENIGK, H. H., JR. & HONIGSMANN, H. 1995a. Ultraviolet radiation for treatment of cutaneous T-cell lymphoma. *Hematol Oncol Clin North Am,* 9**,** 1077-88.
HERRMANN, J. J., ROENIGK, H. H., JR., HURRIA, A., KUZEL, T. M., SAMUELSON, E., RADEMAKER, A. W. & ROSEN, S. T. 1995b. Treatment of mycosis fungoides with photochemotherapy (PUVA): long-term follow-up. *J Am Acad Dermatol,* 33**,** 234-42.
HOPPE, R. T., MEDEIROS, L. J., WARNKE, R. A. & WOOD, G. S. 1995. CD8-positive tumor-infiltrating lymphocytes influence the long-term survival of patients with mycosis fungoides. *J Am Acad Dermatol,* 32**,** 448-53.
HRISTOV, A. C., VONDERHEID, E. C. & BOROWITZ, M. J. 2011. Simplified flow cytometric assessment in mycosis fungoides and Sezary syndrome. *Am J Clin Pathol,* 136**,** 944-53.
HSI, A. C., LEE, S. J., ROSMAN, I. S., CARSON, K. R., KELLEY, A., VIELE, V., PANG, X., MUSIEK, A. & SCHAFFER, A. 2015. Expression of helper T cell master regulators in inflammatory dermatoses and primary cutaneous T-cell lymphomas: diagnostic implications. *J Am Acad Dermatol,* 72**,** 159-67.
HSU, L. & ARMSTRONG, A. W. 2014. JAK inhibitors: treatment efficacy and safety profile in patients with psoriasis. *J Immunol Res,* 2014**,** 283617.
JACKOW, C. M., CATHER, J. C., HEARNE, V., ASANO, A. T., MUSSER, J. M. & DUVIC, M. 1997. Association of erythrodermic cutaneous T-cell lymphoma, superantigen-positive Staphylococcus aureus, and oligoclonal T-cell receptor V beta gene expansion. *Blood,* 89**,** 32-40.
JACOBY, E., CHIEN, C. D. & FRY, T. J. 2014. Murine models of acute leukemia: important tools in current pediatric leukemia research. *Front Oncol,* 4**,** 95.
JAHAN-TIGH, R. R., HUEN, A. O., LEE, G. L., POZADZIDES, J. V., LIU, P. & DUVIC, M. 2013. Hydrochlorothiazide and cutaneous T cell lymphoma: prospective analysis and case series. *Cancer,* 119**,** 825-31.
JOHNSTONE, R. W. 2002. Histone-deacetylase inhibitors: novel drugs for the treatment of cancer. *Nat Rev Drug Discov,* 1**,** 287-99.
JONES, D., DANG, N. H., DUVIC, M., WASHINGTON, L. T. & HUH, Y. O. 2001. Absence of CD26 expression is a useful marker for diagnosis of T-cell lymphoma in peripheral blood. *Am J Clin Pathol,* 115**,** 885-92.
KARENKO, L., SARNA, S., KAHKONEN, M. & RANKI, A. 2003. Chromosomal abnormalities in relation to clinical disease in patients with cutaneous T-cell lymphoma: a 5-year follow-up study. *Br J Dermatol,* 148**,** 55-64.
KASPRZYCKA, M., ZHANG, Q., WITKIEWICZ, A., MARZEC, M., POTOCZEK, M., LIU, X., WANG, H. Y., MILONE, M., BASU, S., MAUGER, J., CHOI, J. K., ABRAMS, J. T., HOU, J. S., ROOK, A. H., VONDERHEID, E., WOETMANN, A., ODUM, N. & WASIK, M. A. 2008. Gamma c-signaling cytokines induce a regulatory T cell phenotype in malignant CD4+ T lymphocytes. *J Immunol,* 181**,** 2506-12.
KAVANAUGH, S. M., WHITE, L. A. & KOLESAR, J. M. 2010. Vorinostat: A novel therapy for the treatment of cutaneous T-cell lymphoma. *Am J Health Syst Pharm,* 67**,** 793-7.

KIEL, M. J., SAHASRABUDDHE, A. A., ROLLAND, D. C., VELUSAMY, T., CHUNG, F., SCHALLER, M., BAILEY, N. G., BETZ, B. L., MIRANDA, R. N., PORCU, P., BYRD, J. C., JEFFREY MEDEIROS, L., KUNKEL, S. L., BAHLER, D. W., LIM, M. S. & ELENITOBA-JOHNSON, K. S. 2015. Genomic analyses reveal recurrent mutations in epigenetic modifiers and the JAK-STAT pathway in Sezary syndrome. *Nat Commun,* 6**,** 8470.

KIM, Y. H., TAVALLAEE, M., SUNDRAM, U., SALVA, K. A., WOOD, G. S., LI, S., ROZATI, S., NAGPAL, S., KRATHEN, M., REDDY, S., HOPPE, R. T., NGUYEN-LIN, A., WENG, W. K., ARMSTRONG, R., PULITZER, M., ADVANI, R. H. & HORWITZ, S. M. 2015. Phase II Investigator-Initiated Study of Brentuximab Vedotin in Mycosis Fungoides and Sezary Syndrome With Variable CD30 Expression Level: A Multi-Institution Collaborative Project. *J Clin Oncol,* 33**,** 3750-8.

KIRSCH, I. R., WATANABE, R., O'MALLEY, J. T., WILLIAMSON, D. W., SCOTT, L. L., ELCO, C. P., TEAGUE, J. E., GEHAD, A., LOWRY, E. L., LEBOEUF, N. R., KRUEGER, J. G., ROBINS, H. S., KUPPER, T. S. & CLARK, R. A. 2015. TCR sequencing facilitates diagnosis and identifies mature T cells as the cell of origin in CTCL. *Sci Transl Med,* 7**,** 308ra158.

KOBAYASHI, H., KUMAI, T., HAYASHI, S., MATSUDA, Y., AOKI, N., SATO, K., KIMURA, S. & CELIS, E. 2012. A naturally processed HLA-DR-bound peptide from the IL-9 receptor alpha of HTLV-1-transformed T cells serves as a T helper epitope. *Cancer Immunol Immunother,* 61**,** 2215-25.

KOPP, K. L., RALFKIAER, U., GJERDRUM, L. M., HELVAD, R., PEDERSEN, I. H., LITMAN, T., JONSON, L., HAGEDORN, P. H., KREJSGAARD, T., GNIADECKI, R., BONEFELD, C. M., SKOV, L., GEISLER, C., WASIK, M. A., RALFKIAER, E., ODUM, N. & WOETMANN, A. 2013. STAT5-mediated expression of oncogenic miR-155 in cutaneous T-cell lymphoma. *Cell Cycle,* 12**,** 1939-47.

KREJSGAARD, T., GJERDRUM, L. M., RALFKIAER, E., LAUENBORG, B., ERIKSEN, K. W., MATHIESEN, A. M., BOVIN, L. F., GNIADECKI, R., GEISLER, C., RYDER, L. P., ZHANG, Q., WASIK, M. A., ODUM, N. & WOETMANN, A. 2008. Malignant Tregs express low molecular splice forms of FOXP3 in Sezary syndrome. *Leukemia,* 22**,** 2230-9.

KREJSGAARD, T., LITVINOV, I. V., WANG, Y., XIA, L., WILLERSLEV-OLSEN, A., KORALOV, S. B., KOPP, K. L., BONEFELD, C. M., WASIK, M. A., GEISLER, C., WOETMANN, A., ZHOU, Y., SASSEVILLE, D. & ODUM, N. 2013. Elucidating the role of interleukin-17F in cutaneous T-cell lymphoma. *Blood,* 122**,** 943-50.

KREJSGAARD, T., RALFKIAER, U., CLASEN-LINDE, E., ERIKSEN, K. W., KOPP, K. L., BONEFELD, C. M., GEISLER, C., DABELSTEEN, S., WASIK, M. A., RALFKIAER, E., WOETMANN, A. & ODUM, N. 2011. Malignant cutaneous T-cell lymphoma cells express IL-17 utilizing the Jak3/Stat3 signaling pathway. *J Invest Dermatol,* 131**,** 1331-8.

KUNDU-RAYCHAUDHURI, S., ABRIA, C. & RAYCHAUDHURI, S. P. 2016. IL-9, a local growth factor for synovial T cells in inflammatory arthritis. *Cytokine,* 79**,** 45-51.

LAHARANNE, E., CHEVRET, E., IDRISSI, Y., GENTIL, C., LONGY, M., FERRER, J., DUBUS, P., JOUARY, T., VERGIER, B., BEYLOT-BARRY, M. & MERLIO, J. P. 2010a. CDKN2A-CDKN2B deletion defines

an aggressive subset of cutaneous T-cell lymphoma. *Mod Pathol,* 23**,** 547-58.

LAHARANNE, E., OUMOUHOU, N., BONNET, F., CARLOTTI, M., GENTIL, C., CHEVRET, E., JOUARY, T., LONGY, M., VERGIER, B., BEYLOT-BARRY, M. & MERLIO, J. P. 2010b. Genome-wide analysis of cutaneous T-cell lymphomas identifies three clinically relevant classes. *J Invest Dermatol,* 130**,** 1707-18.

LANSIGAN, F. & FOSS, F. M. 2010. Current and emerging treatment strategies for cutaneous T-cell lymphoma. *Drugs,* 70**,** 273-86.

LI, J. Y., HORWITZ, S., MOSKOWITZ, A., MYSKOWSKI, P. L., PULITZER, M. & QUERFELD, C. 2012. Management of cutaneous T cell lymphoma: new and emerging targets and treatment options. *Cancer Manag Res,* 4**,** 75-89.

LINDAHL, L. M., FREDHOLM, S., JOSEPH, C., NIELSEN, B. S., JONSON, L., WILLERSLEV-OLSEN, A., GLUUD, M., BLUMEL, E., PETERSEN, D. L., SIBBESEN, N., HU, T., NASTASI, C., KREJSGAARD, T., JAEHGER, D., PERSSON, J. L., MONGAN, N., WASIK, M. A., LITVINOV, I. V., SASSEVILLE, D., KORALOV, S. B., BONEFELD, C. M., GEISLER, C., WOETMANN, A., RALFKIAER, E., IVERSEN, L. & ODUM, N. 2016. STAT5 induces miR-21 expression in cutaneous T cell lymphoma. *Oncotarget*.

LITVINOV, I. V., CORDEIRO, B., FREDHOLM, S., ODUM, N., ZARGHAM, H., HUANG, Y., ZHOU, Y., PEHR, K., KUPPER, T. S., WOETMANN, A. & SASSEVILLE, D. 2014. Analysis of STAT4 expression in cutaneous T-cell lymphoma (CTCL) patients and patient-derived cell lines. *Cell Cycle,* 13**,** 2975-82.

LITVINOV, I. V., JONES, D. A., SASSEVILLE, D. & KUPPER, T. S. 2010. Transcriptional profiles predict disease outcome in patients with cutaneous T-cell lymphoma. *Clin Cancer Res,* 16**,** 2106-14.

LUNDIN, J., HAGBERG, H., REPP, R., CAVALLIN-STAHL, E., FREDEN, S., JULIUSSON, G., ROSENBLAD, E., TJONNFJORD, G., WIKLUND, T. & OSTERBORG, A. 2003. Phase 2 study of alemtuzumab (anti-CD52 monoclonal antibody) in patients with advanced mycosis fungoides/Sezary syndrome. *Blood,* 101**,** 4267-72.

LV, X., FENG, L., FANG, X., JIANG, Y. & WANG, X. 2013. Overexpression of IL-9 receptor in diffuse large B-cell lymphoma. *Int J Clin Exp Pathol,* 6**,** 911-6.

MACKAY, L. K., RAHIMPOUR, A., MA, J. Z., COLLINS, N., STOCK, A. T., HAFON, M. L., VEGA-RAMOS, J., LAUZURICA, P., MUELLER, S. N., STEFANOVIC, T., TSCHARKE, D. C., HEATH, W. R., INOUYE, M., CARBONE, F. R. & GEBHARDT, T. 2013. The developmental pathway for CD103(+)CD8+ tissue-resident memory T cells of skin. *Nat Immunol,* 14**,** 1294-301.

MAIER, E., WERNER, D., DUSCHL, A., BOHLE, B. & HOREJS-HOECK, J. 2014. Human Th2 but not Th9 cells release IL-31 in a STAT6/NF-kappaB-dependent way. *J Immunol,* 193**,** 645-54.

MAO, X., LILLINGTON, D., CHILD, F., RUSSELL-JONES, R., YOUNG, B. & WHITTAKER, S. 2002. Comparative genomic hybridization analysis of primary cutaneous B-cell lymphomas: identification of common genomic

alterations in disease pathogenesis. *Genes Chromosomes Cancer,* 35**,** 144-55.

MAO, X., ORCHARD, G., VONDERHEID, E. C., NOWELL, P. C., BAGOT, M., BENSUSSAN, A., RUSSELL-JONES, R., YOUNG, B. D. & WHITTAKER, S. J. 2006. Heterogeneous abnormalities of CCND1 and RB1 in primary cutaneous T-Cell lymphomas suggesting impaired cell cycle control in disease pathogenesis. *J Invest Dermatol,* 126**,** 1388-95.

MARCUS MUCHE, J., KARENKO, L., GELLRICH, S., KARHU, R., KYTOLA, S., KAHKONEN, M., LUKOWSKY, A., STERRY, W. & RANKI, A. 2004. Cellular coincidence of clonal T cell receptor rearrangements and complex clonal chromosomal aberrations-a hallmark of malignancy in cutaneous T cell lymphoma. *J Invest Dermatol,* 122**,** 574-8.

MARGOLSKEE, E., JOBANPUTRA, V., JAIN, P., CHEN, J., GANAPATHI, K., NAHUM, O., LEVY, B., MORSCIO, J., MURTY, V., TOUSSEYN, T., ALOBEID, B., MANSUKHANI, M. & BHAGAT, G. 2016. Genetic landscape of T- and NK-cell post-transplant lymphoproliferative disorders. *Oncotarget*.

MARZEC, M., HALASA, K., KASPRZYCKA, M., WYSOCKA, M., LIU, X., TOBIAS, J. W., BALDWIN, D., ZHANG, Q., ODUM, N., ROOK, A. H. & WASIK, M. A. 2008. Differential effects of interleukin-2 and interleukin-15 versus interleukin-21 on CD4+ cutaneous T-cell lymphoma cells. *Cancer Res,* 68**,** 1083-91.

MASCARENHAS, J. & HOFFMAN, R. 2013. A comprehensive review and analysis of the effect of ruxolitinib therapy on the survival of patients with myelofibrosis. *Blood,* 121**,** 4832-7.

MCCUSKER, M. E., GARIFALLOU, M. & BOGEN, S. A. 1997. Sezary lineage cells can be induced to proliferate via CD28-mediated costimulation. *J Immunol,* 158**,** 4984-91.

MCKENNA, K. E., WHITTAKER, S., RHODES, L. E., TAYLOR, P., LLOYD, J., IBBOTSON, S., RUSSELL-JONES, R., BRITISH PHOTODERMATOLOGY, G. & GROUP, U. K. S. L. 2006. Evidence-based practice of photopheresis 1987-2001: a report of a workshop of the British Photodermatology Group and the U.K. Skin Lymphoma Group. *Br J Dermatol,* 154**,** 7-20.

MEISSNER, K., MICHAELIS, K., REHPENNING, W. & LONING, T. 1990. Epidermal Langerhans' cell densities influence survival in mycosis fungoides and Sezary syndrome. *Cancer,* 65**,** 2069-73.

MIRVISH, J. J., POMERANTZ, R. G., FALO, L. D., JR. & GESKIN, L. J. 2013. Role of infectious agents in cutaneous T-cell lymphoma: facts and controversies. *Clin Dermatol,* 31**,** 423-31.

NAGAI, A., TERASHIMA, M., HARADA, T., SHIMODE, K., TAKEUCHI, H., MURAKAWA, Y., NAGASAKI, M., NAKANO, A. & KOBAYASHI, S. 2003. Cathepsin B and H activities and cystatin C concentrations in cerebrospinal fluid from patients with leptomeningeal metastasis. *Clin Chim Acta,* 329**,** 53-60.

NATTKEMPER, L. A., MARTINEZ-ESCALA, M. E., GELMAN, A. B., SINGER, E. M., ROOK, A. H., GUITART, J. & YOSIPOVITCH, G. 2016. Cutaneous T-Cell Lymphoma and Pruritus: the Expression of IL-31 and its Receptors in the Skin. *Acta Derm Venereol*.

NAVI, D., RIAZ, N., LEVIN, Y. S., SULLIVAN, N. C., KIM, Y. H. & HOPPE, R. T. 2011. The Stanford University experience with conventional-dose, total skin electron-beam therapy in the treatment of generalized patch or plaque (T2) and tumor (T3) mycosis fungoides. *Arch Dermatol,* 147**,** 561-7.

NI, X. & DUVIC, M. 2011. Dendritic cells and cutaneous T-cell lymphomas. *G Ital Dermatol Venereol,* 146**,** 103-13.

NIELSEN, M., KALTOFT, K., NORDAHL, M., ROPKE, C., GEISLER, C., MUSTELIN, T., DOBSON, P., SVEJGAARD, A. & ODUM, N. 1997. Constitutive activation of a slowly migrating isoform of Stat3 in mycosis fungoides: tyrphostin AG490 inhibits Stat3 activation and growth of mycosis fungoides tumor cell lines. *Proc Natl Acad Sci U S A,* 94**,** 6764-9.

NIELSEN, M., NISSEN, M. H., GERWIEN, J., ZOCCA, M. B., RASMUSSEN, H. M., NAKAJIMA, K., ROPKE, C., GEISLER, C., KALTOFT, K. & ODUM, N. 2002. Spontaneous interleukin-5 production in cutaneous T-cell lymphoma lines is mediated by constitutively activated Stat3. *Blood,* 99**,** 973-7.

NIKOLAOU, V., SIAKANTARIS, M. P., VASSILAKOPOULOS, T. P., PAPADAVID, E., STRATIGOS, A., ECONOMIDI, A., MARINOS, L., PAPADAKI, T. & ANTONIOU, C. 2011. PUVA plus interferon alpha2b in the treatment of advanced or refractory to PUVA early stage mycosis fungoides: a case series. *J Eur Acad Dermatol Venereol,* 25**,** 354-7.

NOBLE, W. S. 2009. How does multiple testing correction work? *Nat Biotechnol,* 27**,** 1135-7.

OCHSENBEIN, A. F., KLENERMAN, P., KARRER, U., LUDEWIG, B., PERICIN, M., HENGARTNER, H. & ZINKERNAGEL, R. M. 1999. Immune surveillance against a solid tumor fails because of immunological ignorance. *Proc Natl Acad Sci U S A,* 96**,** 2233-8.

OLSEN, E. A., WHITTAKER, S., KIM, Y. H., DUVIC, M., PRINCE, H. M., LESSIN, S. R., WOOD, G. S., WILLEMZE, R., DEMIERRE, M. F., PIMPINELLI, N., BERNENGO, M. G., ORTIZ-ROMERO, P. L., BAGOT, M., ESTRACH, T., GUITART, J., KNOBLER, R., SANCHES, J. A., IWATSUKI, K., SUGAYA, M., DUMMER, R., PITTELKOW, M., HOPPE, R., PARKER, S., GESKIN, L., PINTER-BROWN, L., GIRARDI, M., BURG, G., RANKI, A., VERMEER, M., HORWITZ, S., HEALD, P., ROSEN, S., CERRONI, L., DRENO, B., VONDERHEID, E. C., INTERNATIONAL SOCIETY FOR CUTANEOUS, L., UNITED STATES CUTANEOUS LYMPHOMA, C., CUTANEOUS LYMPHOMA TASK FORCE OF THE EUROPEAN ORGANISATION FOR, R. & TREATMENT OF, C. 2011. Clinical end points and response criteria in mycosis fungoides and Sezary syndrome: a consensus statement of the International Society for Cutaneous Lymphomas, the United States Cutaneous Lymphoma Consortium, and the Cutaneous Lymphoma Task Force of the European Organisation for Research and Treatment of Cancer. *J Clin Oncol,* 29**,** 2598-607.

PHAM-LEDARD, A., PROCHAZKOVA-CARLOTTI, M., LAHARANNE, E., VERGIER, B., JOUARY, T., BEYLOT-BARRY, M. & MERLIO, J. P. 2010. IRF4 gene rearrangements define a subgroup of CD30-positive

cutaneous T-cell lymphoma: a study of 54 cases. *J Invest Dermatol,* 130**,** 816-25.

PIERSON, D. M., JONES, D., MUZZAFAR, T., KERSH, M. J., CHALLAGUNDLA, P., MEDEIROS, L. J. & JORGENSEN, J. L. 2008. Utility of CD26 in flow cytometric immunophenotyping of T-cell lymphomas in tissue and body fluid specimens. *Cytometry B Clin Cytom,* 74**,** 341-8.

POLANSKY, M., TALPUR, R., DAULAT, S., HOSING, C., DABAJA, B. & DUVIC, M. 2015. Long-Term Complete Responses to Combination Therapies and Allogeneic Stem Cell Transplants in Patients With Sezary Syndrome. *Clin Lymphoma Myeloma Leuk,* 15**,** e83-93.

PONTI, R., FIERRO, M. T., QUAGLINO, P., LISA, B., PAOLA, F., MICHELA, O., PAOLO, F., COMESSATTI, A., NOVELLI, M. & BERNENGO, M. G. 2008. TCRgamma-chain gene rearrangement by PCR-based GeneScan: diagnostic accuracy improvement and clonal heterogeneity analysis in multiple cutaneous T-cell lymphoma samples. *J Invest Dermatol,* 128**,** 1030-8.

QUERFELD, C., ROSEN, S. T., KUZEL, T. M., KIRBY, K. A., ROENIGK, H. H., JR., PRINZ, B. M. & GUITART, J. 2005. Long-term follow-up of patients with early-stage cutaneous T-cell lymphoma who achieved complete remission with psoralen plus UV-A monotherapy. *Arch Dermatol,* 141**,** 305-11.

RABENHORST, A., SCHLAAK, M., HEUKAMP, L. C., FORSTER, A., THEURICH, S., VON BERGWELT-BAILDON, M., BUTTNER, R., KURSCHAT, P., MAUCH, C., ROERS, A. & HARTMANN, K. 2012. Mast cells play a protumorigenic role in primary cutaneous lymphoma. *Blood,* 120**,** 2042-54.

RAO, V., SAUNES, M., JORSTAD, S. & MOEN, T. 2009. Cutaneous T cell lymphoma and graft-versus-host disease: a comparison of in vivo effects of extracorporeal photochemotherapy on Foxp3+ regulatory T cells. *Clin Immunol,* 133**,** 303-13.

REISS, Y., PROUDFOOT, A. E., POWER, C. A., CAMPBELL, J. J. & BUTCHER, E. C. 2001. CC chemokine receptor (CCR)4 and the CCR10 ligand cutaneous T cell-attracting chemokine (CTACK) in lymphocyte trafficking to inflamed skin. *J Exp Med,* 194**,** 1541-7.

ROBINS, H. S., CAMPREGHER, P. V., SRIVASTAVA, S. K., WACHER, A., TURTLE, C. J., KAHSAI, O., RIDDELL, S. R., WARREN, E. H. & CARLSON, C. S. 2009. Comprehensive assessment of T-cell receptor beta-chain diversity in alphabeta T cells. *Blood,* 114**,** 4099-107.

ROOK, A. H., GOTTLIEB, S. L., WOLFE, J. T., VOWELS, B. R., SOOD, S. S., NIU, Z., LESSIN, S. R. & FOX, F. E. 1997. Pathogenesis of cutaneous T-cell lymphoma: implications for the use of recombinant cytokines and photopheresis. *Clin Exp Immunol,* 107 Suppl 1**,** 16-20.

RUIZ, M., GIUDICELLI, V., GINESTOUX, C., STOEHR, P., ROBINSON, J., BODMER, J., MARSH, S. G., BONTROP, R., LEMAITRE, M., LEFRANC, G., CHAUME, D. & LEFRANC, M. P. 2000. IMGT, the international ImMunoGeneTics database. *Nucleic Acids Res,* 28**,** 219-21.

RUPOLI, S., GOTERI, G., PULINI, S., FILOSA, A., TASSETTI, A., OFFIDANI, M., FILOSA, G., MOZZICAFREDDO, G., GIACCHETTI, A.,

BRANDOZZI, G., CATALDI, I., BARULLI, S., RANALDI, R., SCORTECHINI, A. R., CAPRETTI, R., FABRIS, G., LEONI, P. & MARCHE REGIONAL MULTICENTRIC STUDY GROUP OF CUTANEOUS, L. 2005. Long-term experience with low-dose interferon-alpha and PUVA in the management of early mycosis fungoides. *Eur J Haematol,* 75**,** 136-45.

SALGADO, R., SERVITJE, O., GALLARDO, F., VERMEER, M. H., ORTIZ-ROMERO, P. L., KARPOVA, M. B., ZIPSER, M. C., MUNIESA, C., GARCIA-MURET, M. P., ESTRACH, T., SALIDO, M., SANCHEZ-SCHMIDT, J., HERRERA, M., ROMAGOSA, V., SUELA, J., FERREIRA, B. I., CIGUDOSA, J. C., BARRANCO, C., SERRANO, S., DUMMER, R., TENSEN, C. P., SOLE, F., PUJOL, R. M. & ESPINET, B. 2010. Oligonucleotide array-CGH identifies genomic subgroups and prognostic markers for tumor stage mycosis fungoides. *J Invest Dermatol,* 130**,** 1126-35.

SCARISBRICK, J. J., MITCHELL, T. J., CALONJE, E., ORCHARD, G., RUSSELL-JONES, R. & WHITTAKER, S. J. 2003. Microsatellite instability is associated with hypermethylation of the hMLH1 gene and reduced gene expression in mycosis fungoides. *J Invest Dermatol,* 121**,** 894-901.

SCARISBRICK, J. J., WOOLFORD, A. J., RUSSELL-JONES, R. & WHITTAKER, S. J. 2000. Loss of heterozygosity on 10q and microsatellite instability in advanced stages of primary cutaneous T-cell lymphoma and possible association with homozygous deletion of PTEN. *Blood,* 95**,** 2937-42.

SCHLAPBACH, C., GEHAD, A., YANG, C., WATANABE, R., GUENOVA, E., TEAGUE, J. E., CAMPBELL, L., YAWALKAR, N., KUPPER, T. S. & CLARK, R. A. 2014. Human TH9 cells are skin-tropic and have autocrine and paracrine proinflammatory capacity. *Sci Transl Med,* 6**,** 219ra8.

SCHLAPBACH, C., OCHSENBEIN, A., KAELIN, U., HASSAN, A. S., HUNGER, R. E. & YAWALKAR, N. 2010. High numbers of DC-SIGN+ dendritic cells in lesional skin of cutaneous T-cell lymphoma. *J Am Acad Dermatol,* 62**,** 995-1004.

SCHMITT, S., JOHNSON, T. S., KARAKHANOVA, S., NAHER, H., MAHNKE, K. & ENK, A. H. 2009. Extracorporeal photophoresis augments function of CD4+CD25+FoxP3+ regulatory T cells by triggering adenosine production. *Transplantation,* 88**,** 411-6.

SHAFFER, A. L., EMRE, N. C., LAMY, L., NGO, V. N., WRIGHT, G., XIAO, W., POWELL, J., DAVE, S., YU, X., ZHAO, H., ZENG, Y., CHEN, B., EPSTEIN, J. & STAUDT, L. M. 2008. IRF4 addiction in multiple myeloma. *Nature,* 454**,** 226-31.

SHERWOOD, A. M., DESMARAIS, C., LIVINGSTON, R. J., ANDRIESEN, J., HAUSSLER, M., CARLSON, C. S. & ROBINS, H. 2011. Deep sequencing of the human TCRgamma and TCRbeta repertoires suggests that TCRbeta rearranges after alphabeta and gammadelta T cell commitment. *Sci Transl Med,* 3**,** 90ra61.

SHIN, J., MONTI, S., AIRES, D. J., DUVIC, M., GOLUB, T., JONES, D. A. & KUPPER, T. S. 2007. Lesional gene expression profiling in cutaneous T-cell lymphoma reveals natural clusters associated with disease outcome. *Blood,* 110**,** 3015-27.

SHIUE, L. H., COUTURIER, J., LEWIS, D. E., WEI, C., NI, X. & DUVIC, M. 2015. The effect of extracorporeal photopheresis alone or in combination therapy on circulating CD4(+) Foxp3(+) CD25(-) T cells in patients with leukemic cutaneous T-cell lymphoma. *Photodermatol Photoimmunol Photomed,* 31**,** 184-94.

SINGH, T. P., SCHON, M. P., WALLBRECHT, K., GRUBER-WACKERNAGEL, A., WANG, X. J. & WOLF, P. 2013. Involvement of IL-9 in Th17-associated inflammation and angiogenesis of psoriasis. *PLoS One,* 8**,** e51752.

SINGH, T. P., SCHON, M. P., WALLBRECHT, K. & WOLF, P. 2012. 8-Methoxypsoralen plus UVA treatment increases the proportion of CLA+ CD25+ CD4+ T cells in lymph nodes of K5.hTGFbeta1 transgenic mice. *Exp Dermatol,* 21**,** 228-30.

SISMANOPOULOS, N., DELIVANIS, D. A., ALYSANDRATOS, K. D., ANGELIDOU, A., VASIADI, M., THERIANOU, A. & THEOHARIDES, T. C. 2012. IL-9 induces VEGF secretion from human mast cells and IL-9/IL-9 receptor genes are overexpressed in atopic dermatitis. *PLoS One,* 7**,** e33271.

SORS, A., JEAN-LOUIS, F., PELLET, C., LAROCHE, L., DUBERTRET, L., COURTOIS, G., BACHELEZ, H. & MICHEL, L. 2006. Down-regulating constitutive activation of the NF-kappaB canonical pathway overcomes the resistance of cutaneous T-cell lymphoma to apoptosis. *Blood,* 107**,** 2354-63.

STEIDL, C., LEE, T., SHAH, S. P., FARINHA, P., HAN, G., NAYAR, T., DELANEY, A., JONES, S. J., IQBAL, J., WEISENBURGER, D. D., BAST, M. A., ROSENWALD, A., MULLER-HERMELINK, H. K., RIMSZA, L. M., CAMPO, E., DELABIE, J., BRAZIEL, R. M., COOK, J. R., TUBBS, R. R., JAFFE, E. S., LENZ, G., CONNORS, J. M., STAUDT, L. M., CHAN, W. C. & GASCOYNE, R. D. 2010. Tumor-associated macrophages and survival in classic Hodgkin's lymphoma. *N Engl J Med,* 362**,** 875-85.

THEURICH, S., SCHLAAK, M., STEGUWEIT, H., HEUKAMP, L. C., WENNHOLD, K., KURSCHAT, P., RABENHORST, A., HARTMANN, K., SCHLOSSER, H., SHIMABUKURO-VORNHAGEN, A., HOLTICK, U., HALLEK, M., STADLER, R. & VON BERGWELT-BAILDON, M. 2016. Targeting Tumor-Infiltrating B Cells in Cutaneous T-Cell Lymphoma. *J Clin Oncol,* 34**,** e110-6.

TRAUTINGER, F. 2011. Phototherapy of mycosis fungoides. *Photodermatol Photoimmunol Photomed,* 27**,** 68-74.

TRAUTINGER, F., KNOBLER, R., WILLEMZE, R., PERIS, K., STADLER, R., LAROCHE, L., D'INCAN, M., RANKI, A., PIMPINELLI, N., ORTIZ-ROMERO, P., DUMMER, R., ESTRACH, T. & WHITTAKER, S. 2006. EORTC consensus recommendations for the treatment of mycosis fungoides/Sezary syndrome. *Eur J Cancer,* 42**,** 1014-30.

UNGEWICKELL, A., BHADURI, A., RIOS, E., REUTER, J., LEE, C. S., MAH, A., ZEHNDER, A., OHGAMI, R., KULKARNI, S., ARMSTRONG, R., WENG, W. K., GRATZINGER, D., TAVALLAEE, M., ROOK, A., SNYDER, M., KIM, Y. & KHAVARI, P. A. 2015. Genomic analysis of mycosis fungoides and Sezary syndrome identifies recurrent alterations in TNFR2. *Nat Genet,* 47**,** 1056-60.

VAN DER FITS, L., OUT-LUITING, J. J., VAN LEEUWEN, M. A., SAMSOM, J. N., WILLEMZE, R., TENSEN, C. P. & VERMEER, M. H. 2012a. Autocrine IL-21 stimulation is involved in the maintenance of constitutive STAT3 activation in Sezary syndrome. *J Invest Dermatol,* 132**,** 440-7.

VAN DER FITS, L., REBEL, H. G., OUT-LUITING, J. J., POUW, S. M., SMIT, F., VERMEER, K. G., VAN ZIJL, L., TENSEN, C. P., WEIJER, K. & VERMEER, M. H. 2012b. A novel mouse model for Sezary syndrome using xenotransplantation of Sezary cells into immunodeficient RAG2(-/-) gammac(-/-) mice. *Exp Dermatol,* 21**,** 706-9.

VAN DOORN, R., VAN HASELEN, C. W., VAN VOORST VADER, P. C., GEERTS, M. L., HEULE, F., DE RIE, M., STEIJLEN, P. M., DEKKER, S. K., VAN VLOTEN, W. A. & WILLEMZE, R. 2000. Mycosis fungoides: disease evolution and prognosis of 309 Dutch patients. *Arch Dermatol,* 136**,** 504-10.

VAN DOORN, R., VAN KESTER, M. S., DIJKMAN, R., VERMEER, M. H., MULDER, A. A., SZUHAI, K., KNIJNENBURG, J., BOER, J. M., WILLEMZE, R. & TENSEN, C. P. 2009. Oncogenomic analysis of mycosis fungoides reveals major differences with Sezary syndrome. *Blood,* 113**,** 127-36.

VAQUE, J. P., GOMEZ-LOPEZ, G., MONSALVEZ, V., VARELA, I., MARTINEZ, N., PEREZ, C., DOMINGUEZ, O., GRANA, O., RODRIGUEZ-PERALTO, J. L., RODRIGUEZ-PINILLA, S. M., GONZALEZ-VELA, C., RUBIO-CAMARILLO, M., MARTIN-SANCHEZ, E., PISANO, D. G., PAPADAVID, E., PAPADAKI, T., REQUENA, L., GARCIA-MARCO, J. A., MENDEZ, M., PROVENCIO, M., HOSPITAL, M., SUAREZ-MASSA, D., POSTIGO, C., SAN SEGUNDO, D., LOPEZ-HOYOS, M., ORTIZ-ROMERO, P. L., PIRIS, M. A. & SANCHEZ-BEATO, M. 2014. PLCG1 mutations in cutaneous T-cell lymphomas. *Blood,* 123**,** 2034-43.

VERMA, N. K., DAVIES, A. M., LONG, A., KELLEHER, D. & VOLKOV, Y. 2010. STAT3 knockdown by siRNA induces apoptosis in human cutaneous T-cell lymphoma line Hut78 via downregulation of Bcl-xL. *Cell Mol Biol Lett,* 15**,** 342-55.

VIEYRA-GARCIA, P. A., WEI, T., NAYM, D. G., FREDHOLM, S., FINK-PUCHES, R., CERRONI, L., ODUM, N., O'MALLEY, J. T., GNIADECKI, R. & WOLF, P. 2016. STAT3/5-Dependent IL9 Overexpression Contributes to Neoplastic Cell Survival in Mycosis Fungoides. *Clin Cancer Res,* 22**,** 3328-39.

VOWELS, B. R., LESSIN, S. R., CASSIN, M., JAWORSKY, C., BENOIT, B., WOLFE, J. T. & ROOK, A. H. 1994. Th2 cytokine mRNA expression in skin in cutaneous T-cell lymphoma. *J Invest Dermatol,* 103**,** 669-73.

WADA, D. A., WILCOX, R. A., WEENIG, R. H. & GIBSON, L. E. 2010. Paucity of intraepidermal FoxP3-positive T cells in cutaneous T-cell lymphoma in contrast with spongiotic and lichenoid dermatitis. *J Cutan Pathol,* 37**,** 535-41.

WANG, L., NI, X., COVINGTON, K. R., YANG, B. Y., SHIU, J., ZHANG, X., XI, L., MENG, Q., LANGRIDGE, T., DRUMMOND, J., DONEHOWER, L. A., DODDAPANENI, H., MUZNY, D. M., GIBBS, R. A., WHEELER, D. A. & DUVIC, M. 2015. Genomic profiling of Sezary syndrome identifies

alterations of key T cell signaling and differentiation genes. *Nat Genet,* 47**,** 1426-34.
WANG, T., FELDMAN, A. L., WADA, D. A., LU, Y., POLK, A., BRISKI, R., RISTOW, K., HABERMANN, T. M., THOMAS, D., ZIESMER, S. C., WELLIK, L. E., LANIGAN, T. M., WITZIG, T. E., PITTELKOW, M. R., BAILEY, N. G., HRISTOV, A. C., LIM, M. S., ANSELL, S. M. & WILCOX, R. A. 2014. GATA-3 expression identifies a high-risk subset of PTCL, NOS with distinct molecular and clinical features. *Blood,* 123**,** 3007-15.
WATANABE, R., GEHAD, A., YANG, C., SCOTT, L. L., TEAGUE, J. E., SCHLAPBACH, C., ELCO, C. P., HUANG, V., MATOS, T. R., KUPPER, T. S. & CLARK, R. A. 2015. Human skin is protected by four functionally and phenotypically discrete populations of resident and recirculating memory T cells. *Sci Transl Med,* 7**,** 279ra39.
WEINSTOCK, M. A. & GARDSTEIN, B. 1999. Twenty-year trends in the reported incidence of mycosis fungoides and associated mortality. *Am J Public Health,* 89**,** 1240-4.
WHITTAKER, S. J., DEMIERRE, M. F., KIM, E. J., ROOK, A. H., LERNER, A., DUVIC, M., SCARISBRICK, J., REDDY, S., ROBAK, T., BECKER, J. C., SAMTSOV, A., MCCULLOCH, W. & KIM, Y. H. 2010. Final results from a multicenter, international, pivotal study of romidepsin in refractory cutaneous T-cell lymphoma. *J Clin Oncol,* 28**,** 4485-91.
WHITTEMORE, A. S., HOLLY, E. A., LEE, I. M., ABEL, E. A., ADAMS, R. M., NICKOLOFF, B. J., BLEY, L., PETERS, J. M. & GIBNEY, C. 1989. Mycosis fungoides in relation to environmental exposures and immune response: a case-control study. *J Natl Cancer Inst,* 81**,** 1560-7.
WILCOX, R. A. 2010. Cancer-associated myeloproliferation: old association, new therapeutic target. *Mayo Clin Proc,* 85**,** 656-63.
WILCOX, R. A. 2016. Cutaneous T-cell lymphoma: 2016 update on diagnosis, risk-stratification, and management. *Am J Hematol,* 91**,** 151-65.
WILCOX, R. A., WADA, D. A., ZIESMER, S. C., ELSAWA, S. F., COMFERE, N. I., DIETZ, A. B., NOVAK, A. J., WITZIG, T. E., FELDMAN, A. L., PITTELKOW, M. R. & ANSELL, S. M. 2009. Monocytes promote tumor cell survival in T-cell lymphoproliferative disorders and are impaired in their ability to differentiate into mature dendritic cells. *Blood,* 114**,** 2936-44.
WILLEMZE, R., JAFFE, E. S., BURG, G., CERRONI, L., BERTI, E., SWERDLOW, S. H., RALFKIAER, E., CHIMENTI, S., DIAZ-PEREZ, J. L., DUNCAN, L. M., GRANGE, F., HARRIS, N. L., KEMPF, W., KERL, H., KURRER, M., KNOBLER, R., PIMPINELLI, N., SANDER, C., SANTUCCI, M., STERRY, W., VERMEER, M. H., WECHSLER, J., WHITTAKER, S. & MEIJER, C. J. 2005. WHO-EORTC classification for cutaneous lymphomas. *Blood,* 105**,** 3768-85.
WILLERSLEV-OLSEN, A., KREJSGAARD, T., LINDAHL, L. M., BONEFELD, C. M., WASIK, M. A., KORALOV, S. B., GEISLER, C., KILIAN, M., IVERSEN, L., WOETMANN, A. & ODUM, N. 2013. Bacterial toxins fuel disease progression in cutaneous T-cell lymphoma. *Toxins (Basel),* 5**,** 1402-21.
WILLERSLEV-OLSEN, A., KREJSGAARD, T., LINDAHL, L. M., LITVINOV, I. V., FREDHOLM, S., PETERSEN, D. L., NASTASI, C., GNIADECKI, R., MONGAN, N. P., SASSEVILLE, D., WASIK, M. A., BONEFELD, C. M.,

GEISLER, C., WOETMANN, A., IVERSEN, L., KILIAN, M., KORALOV, S. B. & ODUM, N. 2016. Staphylococcal enterotoxin A (SEA) stimulates STAT3 activation and IL-17 expression in cutaneous T-cell lymphoma. *Blood,* 127**,** 1287-96.

WOOLLARD, W. J., PULLABHATLA, V., LORENC, A., PATEL, V. M., BUTLER, R. M., BAYEGA, A., BEGUM, N., BAKR, F., DEDHIA, K., FISHER, J., AGUILAR-DURAN, S., FLANAGAN, C., GHASEMI, A. A., HOFFMANN, R. M., CASTILLO-MOSQUERA, N., NUTTALL, E. A., PAUL, A., ROBERTS, C. A., SOLOMONIDIS, E. G., TARRANT, R., YOXALL, A., BEYERS, C. Z., FERREIRA, S., TOSI, I., SIMPSON, M. A., DE RINALDIS, E., MITCHELL, T. J. & WHITTAKER, S. J. 2016. Candidate driver genes involved in genome maintenance and DNA repair in Sezary syndrome. *Blood,* 127**,** 3387-97.

WU, J., NIHAL, M., SIDDIQUI, J., VONDERHEID, E. C. & WOOD, G. S. 2009. Low FAS/CD95 expression by CTCL correlates with reduced sensitivity to apoptosis that can be restored by FAS upregulation. *J Invest Dermatol,* 129**,** 1165-73.

WU, J. & WOOD, G. S. 2011. Reduction of Fas/CD95 promoter methylation, upregulation of Fas protein, and enhancement of sensitivity to apoptosis in cutaneous T-cell lymphoma. *Arch Dermatol,* 147**,** 443-9.

WU, X., SCHULTE, B. C., ZHOU, Y., HARIBHAI, D., MACKINNON, A. C., PLAZA, J. A., WILLIAMS, C. B. & HWANG, S. T. 2014. Depletion of M2-like tumor-associated macrophages delays cutaneous T-cell lymphoma development in vivo. *J Invest Dermatol,* 134**,** 2814-22.

WU, X., SELLS, R. E. & HWANG, S. T. 2011. Upregulation of inflammatory cytokines and oncogenic signal pathways preceding tumor formation in a murine model of T-cell lymphoma in skin. *J Invest Dermatol,* 131**,** 1727-34.

XU, C., WAN, C., WANG, L., YANG, H. J., TANG, Y. & LIU, W. P. 2011. Diagnostic significance of TCR gene clonal rearrangement analysis in early mycosis fungoides. *Chin J Cancer,* 30**,** 264-72.

YAMANAKA, K., CLARK, R., DOWGIERT, R., HURWITZ, D., SHIBATA, M., RICH, B. E., HIRAHARA, K., JONES, D. A., EAPEN, S., MIZUTANI, H. & KUPPER, T. S. 2006a. Expression of interleukin-18 and caspase-1 in cutaneous T-cell lymphoma. *Clin Cancer Res,* 12**,** 376-82.

YAMANAKA, K., CLARK, R., RICH, B., DOWGIERT, R., HIRAHARA, K., HURWITZ, D., SHIBATA, M., MIRCHANDANI, N., JONES, D. A., GODDARD, D. S., EAPEN, S., MIZUTANI, H. & KUPPER, T. S. 2006b. Skin-derived interleukin-7 contributes to the proliferation of lymphocytes in cutaneous T-cell lymphoma. *Blood,* 107**,** 2440-5.

YAMASHITA, T., ABBADE, L. P., MARQUES, M. E. & MARQUES, S. A. 2012. Mycosis fungoides and Sezary syndrome: clinical, histopathological and immunohistochemical review and update. *An Bras Dermatol,* 87**,** 817-28; quiz 829-30.

YUKI, H., UENO, S., TATETSU, H., NIIRO, H., IINO, T., ENDO, S., KAWANO, Y., KOMOHARA, Y., TAKEYA, M., HATA, H., OKADA, S., WATANABE, T., AKASHI, K., MITSUYA, H. & OKUNO, Y. 2013. PU.1 is a potent tumor suppressor in classical Hodgkin lymphoma cells. *Blood,* 121**,** 962-70.

ZACK, T. I., SCHUMACHER, S. E., CARTER, S. L., CHERNIACK, A. D., SAKSENA, G., TABAK, B., LAWRENCE, M. S., ZHSNG, C. Z., WALA, J., MERMEL, C. H., SOUGNEZ, C., GABRIEL, S. B., HERNANDEZ, B., SHEN, H., LAIRD, P. W., GETZ, G., MEYERSON, M. & BEROUKHIM, R. 2013. Pan-cancer patterns of somatic copy number alteration. *Nat Genet,* 45**,** 1134-40.

ZACKHEIM, H. S. 1999. Cutaneous T cell lymphoma: update of treatment. *Dermatology,* 199**,** 102-5.

ZACKHEIM, H. S. 2003. Treatment of patch-stage mycosis fungoides with topical corticosteroids. *Dermatol Ther,* 16**,** 283-7.

ZACKHEIM, H. S., KASHANI-SABET, M. & AMIN, S. 1998. Topical corticosteroids for mycosis fungoides. Experience in 79 patients. *Arch Dermatol,* 134**,** 949-54.

ZHANG, Q., WANG, H. Y., WOETMANN, A., RAGHUNATH, P. N., ODUM, N. & WASIK, M. A. 2006. STAT3 induces transcription of the DNA methyltransferase 1 gene (DNMT1) in malignant T lymphocytes. *Blood,* 108**,** 1058-64.

Appendices

Abbreviations

AKT	Protein kinase (also PKB)
ATP	Adenosine triphosphate
Bax	BCL2-associated X protein
Bcl-2	B-cell lymphoma 2
BCR	B-cell Receptor
c-MYD	c-Myelocytomatosis Viral Oncogene (also MYC)
CAILS	Composite Assessment of Index Lesion Severity
CCL	Chemokine ligand
CCR	Chemokine receptor
CD	Cluster differentiation
CDKN	Cyclin-dependent kinase inhibitor
CDR3	Complementarity-determining region
CLA	Cutaneous lymphocyte-associated antigen
CRABPs	Cellular retinoic acid-binding protein
CTCL	Cutaneous T-cell lymphoma
CTSH	Cathepsin H
CXCL	Chemokine (C-X-C motif) ligand
CXCR	Chemokine (C-X-C motif) receptor
DC	Dendritic cell
DC-SIGN	Cluster of Differentiation 209
DNA	Deoxyribonucleic acid
DNMT1	DNA (cytosine-5)-methyltransferase 1
ECP	Extracorporeal photophoresis
ELISA	Enzyme-Linked Immunosorbent Assay
EORTC	European Organization for Research and Treatment of Cancer
ERK	Extracellular regulated kinase
FAS	Apoptosis antigen 1 (also APO-1)
FOXP3	Fork head box P3
GATA3	GATA binding protein 3
HLA	Human leukocyte antigen
HRP	Enzyme horseradish peroxidase
HTLV-1	Human T-lymphotropic virus 1
HTS	High throughput sequencing
IDO	Indoleamine-pyrrole 2,3-dioxygenase
IFNγ	Interferon gamma
IRF4	Interferon regulatory factor 4
ITGAE	Integrin Subunit Alpha E
ITK	IL2 Inducible T-Cell Kinase
JAK	Janus kinase
KEGG	Kyoto Encyclopedia of Genes and Genomes
L-CTCL	Leukemic-CTCL
LAMP1	Lysosomal Associated Membrane Protein 1

LCK	Lymphocyte specific protein tyrosine kinase
LCP1	Lymphocyte Cytosolic Protein 1
LDH	Lactate dehydrogenase
LEU13	Interferon-induced trans-membrane protein 1 (also IFITM1)
LYN	Lck/Yes novel tyrosine kinase
MAPK	Mitogen-activated protein kinase
MEKK4	Mitogen-activated protein kinase 4 (also MAP3K4)
MF	Mycosis fungoides
miR-	Micro-RNA
MR1	Myofibrillogenesis regulator 1
MRC	OX-2 membrane glycoprotein (also CD200)
mSWAT	Modified Severity Weight Assessment Tool
mTOR	Mechanistic target of rapamycin
NFAT	Nuclear factor of activated T-cells
NFκB	Nuclear factor kappa-light-chain-enhancer of activated B cells
PAGE	Polyacrylamide gel electrophoresis
PI3K	Phosphatidylinositol-4,5-biphosphate 3-kinase
PLCG1	Phospholipase C, gamma 1
PU.1	Transcription factor PU.1 (also SPI1)
PUVA	psoralen + UVA
qPCR	Quantitative polymerase chain reaction
RAG	Recombination-activating gene
RB1	Retinoblastoma protein 1
RELA	p65 subunit NFκB
RNA	Ribonucleic acid
RORγT	RAR-related orphan receptor gamma
SEER	Surveillance, Epidemiology, and End Results
SH2D1A	SH2 domain–containing protein 1A
SHIP	Inositol Polyphosphate-5-Phosphatase D (also INPP5D)
siCTRL	Silencing RNA control
siRNA	Silencing RNA
SS	Sèzary syndrome
STAT	Signal transducer and activator of transcription
t-BET	T-box transcription factor TBX21 (also TBX21)
TAP	Transporter associated with Antigen Processing
T_{CM}	Central memory T-cell
TCR	T-cell receptor
TGF-β	Transforming growth factor beta
T_{MM}	Migrant memory T-cell
TNF	Tumor necrosis factor
TRAF	TNF receptor-associated factor
T_{RM}	Resident memory T-cell
TSA	Tyramide Signal Amplification
UVB	Ultraviolet light B
VEGF	Vascular endothelial growth factor A
ZAP70	Zeta-chain-associated protein kinase 70

Conference presentations

1. **Vieyra-Garcia PA,** O'Malley JT, Teague J, Lowry EL, Gehad A, Clark RO and Wolf P. *Understanding benign T-cell infiltration in mycosis fungoides: Malignant clones are not alone.* ESDR Annual meeting 2016 (Munich, 2016). [**Poster**]

2. **Vieyra PA,** O'Malley JT, Teague J, Lowry EL, Gehad A, Wolf P and Clark R. *PUVA therapy fails to deplete malignant T cells in CTCL and instead exerts its clinical effect by modulating benign T cell populations.* Society of Investigative Dermatology Annual meeting 2016 (Arizona, USA). [**Oral** presentation, Plenary session]

3. O'Malley JT, Lowry EL, Gehad A, Teague J, Elco CP, **Vieyra PA**, LeBoeuf N, Devlin P, Kupper TS and Clark R. *Low-dose radiation preferentially kills malignant T cells, recruits benign T cells and normalizes the immune milieu in mycosis fungoides.* Society of Investigative Dermatology Annual meeting 2016 (Arizona, USA). [**Poster**]

4. **Vieyra-Garcia PA**, Mayer G, Pressl H, Reginato E, Schweintzger N, Bambach I, Legat F, Hofer A, Gruber-Wackernagel A, Cerroni L, Fink-Puches R and Wolf P.
   Higher frequencies but impaired suppressive capacity of regulatory T cells after PUVA in cutaneous T-cell lymphoma. Inflammatory Skin Disease Summit 2014 (Vienna, Austria). [**Poster**]

5. **Vieyra-Garcia PA**, Mayer G, Pressl H, Reginato E, Schweintzger NA, Bambach I, Hofer A, Gruber-Wackernagel A, Cerroni L and Wolf P.
   Increased frequency of regulatory T cells with impaired suppressive capacity after PUVA in cutaneous T-cell lymphoma. ESDR Annual meeting 2014 (Copenhagen, Denmark). [**Poster**]

Awards

Non-Melanoma Skin Cancer award 2016. Austrian Society of Dermatology and Venereology Annual meeting, Vienna (AT). November 2016.

Michael Hornstein Award. EADV Annual meeting, Vienna (AT). October 2016.

Best poster award, 2nd DK-MOLIN Retreat. Schloss Seggau (AT), October 2014.

Best presentation, 2nd place, Doctoral Day 2013. Graz (AT), December 2013.

Publications

1. **Vieyra-Garcia, P**; Wei, T; Gram Naym, D; Fredholm, S; Fink-Puches, R; Cerroni, L; Odum, N; T. O'Malley, J; Gniadecki, R; and Wolf, P.
   STAT3/5 dependent IL-9 overexpression contributes to neoplastic cell survival in mycosis fungoides.
   Clinical Cancer Research. 2016: Jul 1;22(13):3328-39.

2. Tenorio, EP; Olguín, JE; Fernández, J; **Vieyra, P**; Saavedra, R
   Reduction of Foxp3+ cells by depletion with the PC61 mAb induces mortality in resistant BALB/c mice infected with Toxoplasma gondii.
   Journal Biomedicine Biotechnology. 2010; 2010:786078-786078 [OPEN ACCESS]

Light up the darkness

Acknowledgements:

I'm in one of the happiest times of my life, there is a long list of people I had the fortune to meet that intentionally or by accident have had an important role to get me to this point.

Mom, Dad, Gero and Tania, with no question you have been the core of my life and as new people get close to us, I realize that a new chapter has opened in our lives with the coming of Victoria. I have trust and I smile by just imagining the things to come.

Rebecca, you are the closest person to me, I cherish every second with you. Where are the oceans, the clouds and the mountains without gravity?

I want to thank Professor Wolf for the opportunity and all the freedom he gave me to educate myself. He supported me to explore every idea I had, even some of the bad ones. He guided me and listened to me when I much needed it and above all, he trusted me.

I want to thank Rachael Clark for opening the door of her lab, for her mentorship, support, and enthusiasm and for being fundamental in realizing the potential of a bold idea.

I want to thank the help and guidance from Gerlinde, Isabella, Nitesh, Vijay, Jessica, Lizzy and Beatrice on both sides of the Atlantic. Their friendship and constant input have been essential for the accomplishments in these PhD years.

I want to thank our collaborators in Denmark and the US, together we have done things that I thought were much more difficult to achieve.

I want to thank Akos Heinemann, Miriam Sedej and everyone in the DK-MOLIN especially to Mina, Angela and Ana. The opportunities, guidance and laughter I got from them helped in a great deal to make Austria my home in these years. In that line I also want to thank people in Mexico and the US: Abraham, Jose Manuel and Laura.